THE UNIVERSITY OF OKLAHOMA

GRADUATE COLLEGE

PRESTACK SEISMIC ANALYSIS OF A MISSISSIPPI LIME RESOURCE PLAY

IN THE MIDCONTINENT, U.S.A.

A THESIS

SUBMITTED TO THE GRADUATE FACULTY

in partial fulfillment of the requirements for the

Degree of

MASTER OF SCIENCE

By

BENJAMIN LEWIS DOWDELL
Norman, Oklahoma
2013

PRESTACK SEISMIC ANALYSIS OF A MISSISSIPPI LIME RESOURCE PLAY
IN THE MIDCONTINENT, U.S.A.

A THESIS APPROVED FOR THE
CONOCOPHILLIPS SCHOOL OF GEOLOGY AND GEOPHYSICS

BY

_____
Dr. Kurt J. Marfurt, Chair

_____
Dr. John D. Pigott

_____
Dr. J. Tim Kwiatkowski

For my family, and my ever-patient dog, Jack

ACKNOWLEDGEMENTS

TABLE OF CONTENTS

LIST OF TABLES

LIST OF FIGURES

Figure 8: Generalized stratigraphic column for Osage County. "Osage A" is as a silicified limestone with high diagenetic susceptibility, and is where tripolite most commonly occurs. "Osage B" contains interbedded tight, fractured limestone and chert and has low diagenetic susceptibility.   The St. Joe

ABSTRACT

With the advent of horizontal drilling and hydraulic fracturing in the Midcontinent, U.S.A., fields once thought to be exhausted are now experiencing renewed exploitation. However, traditional Midcontinent seismic analysis techniques no longer provide satisfactory reservoir characterization for these plays; new seismic analysis methods are needed to properly characterize these radically innovative play concepts. Prestack impedance inversion correlated with surface seismic attributes and well log measurements from within the bounds of the 3D seismic survey maps tripolitic high-porosity chert sweet spots within a highly fractured Mississippian limestone reservoir.

A raw 3D prestack seismic survey from Osage County, Oklahoma, U.S.A., is reprocessed with the goal of performing a prestack time migration. Time processing and filtering is applied, paying careful attention to velocity analysis and coherent noise filtering. The use of a robust prestack structure-oriented filter and spectral whitening greatly enhances the results. Prestack time migration is applied using an azimuthally binned Kirchhoff algorithm, which allows for better imaging of subtle discontinuities in an otherwise mostly flat terrain. Migration stretch is then corrected by removing the normal moveout, picking new velocities, applying a new normal moveout correction, followed by a final prestack structure-oriented filter and spectral whitening.

Using the reprocessed and prestack time-migrated seismic data along with a well from within the survey bounds, P- and S-Impedance, density, P- and S-wave, Lambda-Rho ($\lambda\rho$), Mu-Rho ($\lambda\rho$), and V_P/V_S ratio volumes are

generated using simultaneous prestack inversion. Additionally, surface seismic attributes are generated to aid interpretation of the seismic data. Seismic attributes such as prestack impedance inversion are sensitive to lithology while coherence and curvature are sensitive to lateral changes in waveform and structure. These attributes are used in conjunction with interpreted horizontal image logs to identify zones of high porosity and high fracture density. Calibrating the results to well logs helps improve the understanding of the seismic behavior of highly porous tripolitic chert, aiding the proper characterization of this complex Mississippian carbonate reservoir play.

CHAPTER 1: INTRODUCTION

Osage County (Figure 1) is home to the Osage Indian Reservation and is located in northeastern Oklahoma, sharing a northern border with the Oklahoma-Kansas state line. Osage County has an extensive history of hydrocarbon exploration and production. In 1896, Osage County's first well was drilled with oil discovery occurring a year and two wells later (Bass, 1942). There are currently over 17,000 vertical wells in place from decades of conventional exploration and production (Walton, 2011). The fractured and highly porous Osagean tripolitic chert is the formation of interest with a target depth of 2,900-5,000 ft (880-1500 m). Recently, interest in the Mississippian Lime play has renewed with the utilization of horizontal drilling and hydraulic fracturing techniques, making it a "hot" resource play.
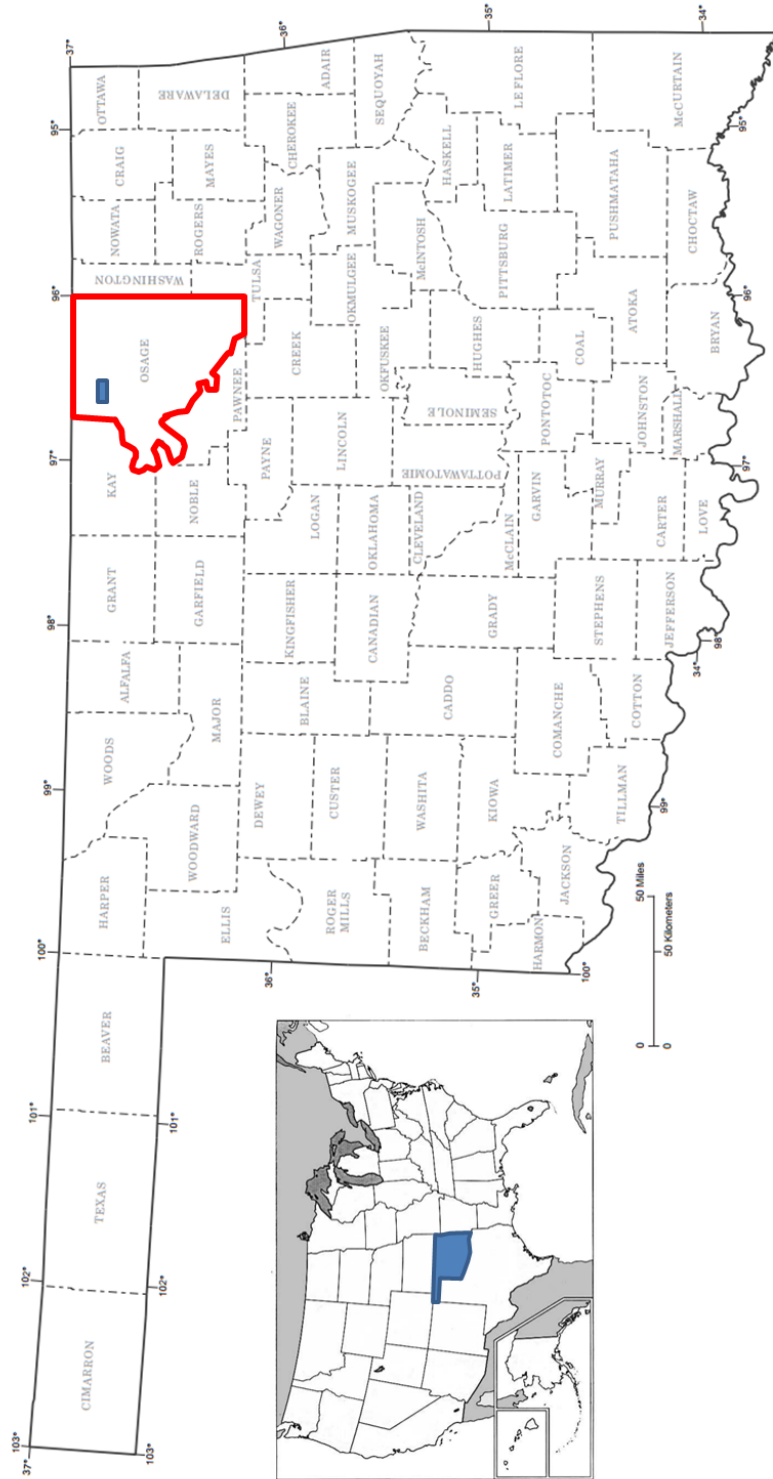
Figure 1: Map showing location of Osage County, Oklahoma, outlined in red. The blue box in the northwestern portion of the county shows the study area's approximate bounds (modified from OGS OK counties map and University of Texas Libraries PCL map collection).

The Mississippian Lime of northern Oklahoma consists of a tight highly fractured limestone, fractured nonporous chert, and a highly porous (20-50%) diagenetically altered chert called tripolite. The tripolite itself is discontinuous and occurs in pockets with varying thickness, making the tripolite a challenge to map.

The play concept is to drill horizontal wells perpendicular to the fractures in the lime and nonporous chert and then increase the number of migration pathways by hydraulically fracturing and/or acidizing the formation in order to produce from multiple tripolitic chert "sweet spots".

Seismic imaging of Mississippi Lime presents several challenges. First, the target in Osage County is shallow (t=530 ms, z=2900 ft) giving rise to significant acquisition footprint. Second, the tripolite is a diagenetic product and may not exhibit the same lateral continuity as the unaltered limestones. Third, natural fractures and joints are critical to the orientation of horizontal wells, requiring azimuthal velocity (VVAz) or amplitude (AVAz) analysis. Finally, optimal placement of horizontal wells requires high vertical resolution and the lateral resolution of potential geohazards.

Relatively little has been published on the Mississippian Lime play. Rogers (1996, 2001) presents a study and model for the diagenesis and deposition of the Mississippian chert in Kay County, Oklahoma, directly to the west of Osage County. Watney et al. (2001) characterize the Mississippian chert in south-central Kansas and describe the paleo-shelf carbonate system that existed during the Mississippian. Nissen et al. (2006) describe the

application of seismic attributes for fracture trend detection to Mississippian carbonate reservoirs in Kansas. Angelo (2010) uses Gray Level Co-Occurrence Matrix (GLCM) seismic texture attributes and self-organizing maps (SOM) to map subtle, thin-bed channels using seismic data from Osage County, Oklahoma. Yenugu et al. (2010, 2011) present a study of Osage County Mississippian chert reservoir property prediction using GLCM seismic texture analysis and AVO inversion correlated with observed well log properties. Yenugu and Marfurt (2011) present a correlation of seismic curvature with fractures observed on borehole image logs. Elebiju et al. (2011) study the basement structures of Osage County using seismic attributes and gravimetric data, concluding that basement deformation trends may control Mississippian chert deposition. Matos et al. (2011) use GLCM seismic texture analysis and Kohonen SOM to map chert facies in an Osage County study area. Zhao (2011) studies the petrologic and petrophysical characteristics of Mississippian chert and limestone using core and well logs from a well in Osage County and in Pawnee county just south of Osage County. Dowdell et al. (2012) present a study of a Mississippian tripolitic chert reservoir in Osage County using poststack acoustic impedance inversion, surface seismic attributes, well logs, and supervised and unsupervised 3D seismic facies analysis. Farzaneh (2012) presents an integrated paleomagnetic and diagenetic study to determine the origin and timing of diagenetic events for Mississippian limestones in northern Oklahoma. White et al. (2012) interprets natural fractures observed on horizontal borehole image logs and correlates the fractures to surface seismic

4

attributes to study the stresses and deformation of Osage County Mississippian limestones. Roy et al. (2012) uses supervised and unsupervised 3D seismic facies analysis to classify petrofacies within a Mississippi Lime reservoir located in Osage County.

I hypothesize that prestack impedance inversion of a 3D seismic prestack survey will allow me to successfully map zones of varying lithology. Due to the different petrophysical nature of the tripolite in comparison to the other carbonate and chert facies present in the study area, I believe that pockets of tripolitic chert can be identified using prestack impedance inversion. Additionally, I assert that when coupled with post stack seismic attributes such as coherence and curvature and with interpreted horizontal borehole image logs I will be able to map potential tripolitic chert "sweet spots" consisting of high porosity (low impedance values) and high fracture density.

I begin with an overview of the geology of the play in Chapter 2. Next, in Chapter 3, I discuss processing a 3D prestack seismic data to improve the spectral content and suppress groundroll. In Chapter 4 I discuss the petrophysical properties of the various facies encountered in the Mississippian Lime and show the results of simultaneous prestack impedance inversion and Lambda-Rho/Mu-Rho (LMR) inversion. I then use the inversion attributes and surface seismic attributes to map lithology and porosity, focused primarily on mapping tripolite. In Chapter 5 I present my conclusions, which I then follow with an in-depth discussion of my prestack time processing in Appendix A. Figure 2 summarizes my workflow for this thesis.
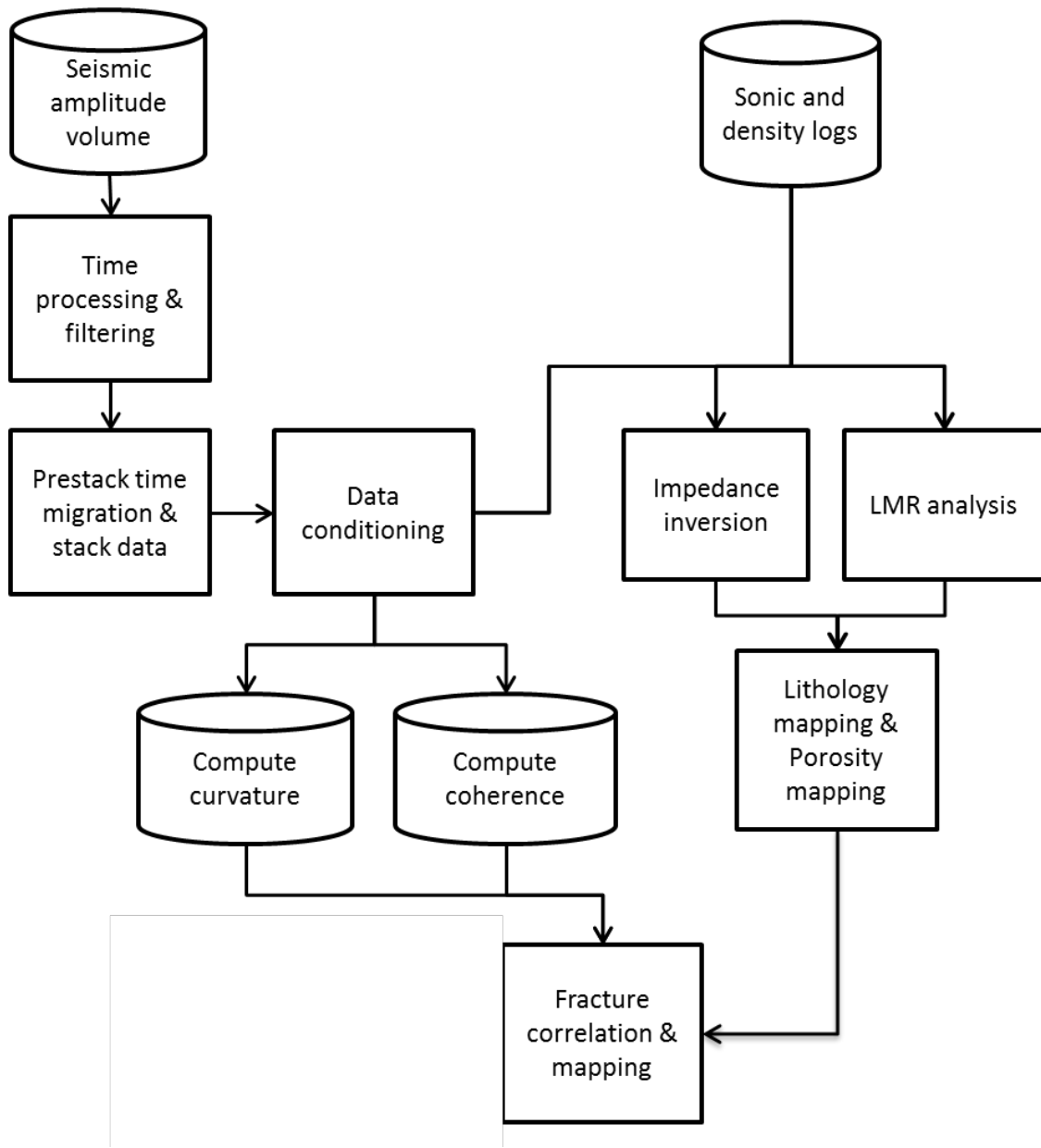
Figure 2: Summary of the thesis workflow.

CHAPTER 2: GEOLOGIC BACKGROUND

REGIONAL

Oklahoma's sedimentary rocks are mostly marine in origin, with thickness ranging between 6,000-12,000 m (20,000-40,000 ft) in the major basins and 0-3,000 m (0-10,000 ft) over the uplifts (Johnson and Cardott, 1992). Precambrian granites and rhyolites make up the majority of Oklahoma's basement rocks (Johnson and Cardott, 1992). Thick sequences of marine carbonates, typically deposited in warm, aerated, and shallow waters, are characteristic of Upper Cambrian through Mississippian strata, interbedded with thin sandstones and shales (Johnson and Cardott, 1992). Shales such as the Upper Devonian-Lower Mississippian Woodford Shale were deposited in anaerobic marine environments, where conditions were favorable for preservation of organic matter (Johnson and Cardott, 1992). Pennsylvanian strata consist of marine and nonmarine shale, sandstone, conglomerate, and limestone, while Permian and post-Permian sediments consist largely of red bed and evaporite deposits and terrestrial sediments (Johnson and Cardott, 1992).

Three major tectonic/depositional provinces existed in Oklahoma at the onset of the early Paleozoic (Johnson and Cardott, 1992). Figure 3 shows the extent of the Oklahoma Basin, the southern Oklahoma aulacogen, and the Ouachita trough.
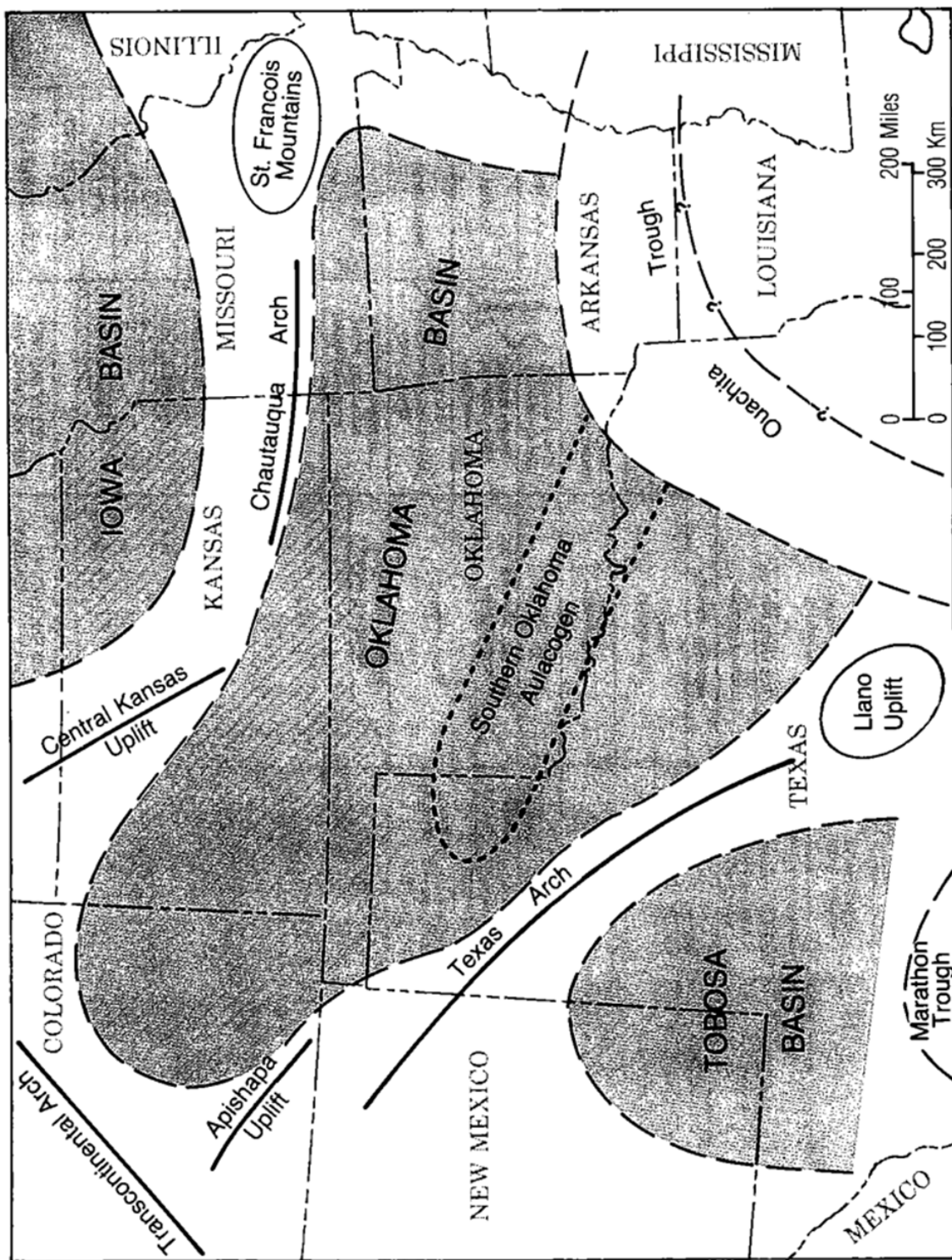
Figure 3: Major Oklahoma tectonic/depositional structures present during the early Paleozoic (Johnson and Cardott, 1992).

The Oklahoma Basin was a broad, shelf-like area where thick and extensive shallow-marine carbonates were deposited along with interbedded marine shales and sandstones (Johnson and Cardott, 1992). The southern Oklahoma aulacogen was a west-northwest trending trough and was the depocenter for the Oklahoma Basin (Johnson and Cardott, 1992). The Ouachita trough formed as a rift at the southern margin of the North American craton and was host to deep-water sediments (Johnson and Cardott, 1992).

During the Pennsylvanian, sharply uplifted crustal blocks divided the Oklahoma Basin and southern Oklahoma aulacogen into several well-defined marine basins (Johnson and Cardott, 1992). A Late Mississippian-Early Pennsylvanian epeirogenic uplift and erosion resulted in a widespread pre-Pennsylvanian unconformity (Johnson and Cardott, 1992). Continued orogenic pulses in the aulacogen and the Ouachita trough resulted in the Ouachita fold belt, the Wichita, Nemaha, Arbuckle, Ozark, and Criner uplifts, and intense downwarping of the Anadarko, Ardmore, Arkoma, Hollis, and Marietta basins (Johnson and Cardott, 1992). Figure 4 shows the major geologic provinces of Oklahoma that resulted from this series of orogenic events. Except for in the Ouachita province, early and middle Paleozoic sediments are quite laterally extensive throughout the state. Figure 5 shows a generalized rock unit correlation chart, while Figure 6 shows a generalized correlation chart for Mississippian stratigraphic units (Johnson and Cardott, 1992; Northcutt et al., 2001).

Figure 4: Major geologic provinces of Oklahoma, with Osage County outlined in red and the study area represented by a blue box (modified from Johnson and Cardott, 1992).

SYSTEM	SERIES	ANADARKO BASIN, SW OKLAHOMA	ARBUCKLE MOUNTAINS, ARDMORE BASIN	ARKOMA BASIN, NE OKLAHOMA	OUACHITA MOUNTAINS
QUATERNARY		Alluvium	and	Terrace	Deposits
TERTIARY		Ogallala Formation			
CRETACEOUS		Dakota Group			
JURASSIC		Morrison Formation			
TRIASSIC		Dockum Group			
PERMIAN	Ochoan	Elk City Sandstone / Doxey Shale			
PERMIAN	Guadalupian	Cloud Chief Formation / Whitehorse Group / El Reno Group			
PERMIAN	Leonardian	Hennessey Shale / Garber Sandstone / Wellington Formation	Garber Sandstone / Wellington Formation		
PERMIAN	Wolfcampian	Chase Group / Council Grove Group / Admire Group	Pontotoc Group	Pontotoc Group	Chase Group / Council Grove Group / Admire Group
PENNSYLVANIAN	Virgilian	Wabaunsee Group / Shawnee Group / Douglas Group	Ada Formation / Vamoosa Formation	Ada Fm. / Vamoosa	Waubunsee / Shawnee / Douglas
PENNSYLVANIAN	Missourian	Ochelata Group / Skiatook Group	Hoxbar Group	Hilltop Fm. / Skiatook Group	Ochelata Group
PENNSYLVANIAN	Desmoinesian	Marmaton Group / Cherokee Group	Deese Group	Marmaton Group / Cabaniss Group / Krebs Group	
PENNSYLVANIAN	Atokan	Atoka Group	Dornick Hills Group	Atoka Formation / Wapanucka / McCully	Atoka Formation / Johns Valley Shale
PENNSYLVANIAN	Morrowan	Morrow Group ?	Springer Formation ?	Union Valley / Sausbee	Jackfork Group
MISSISSIPPIAN	Chesterian	Springer Formation ? / Chester Group	Goddard Formation / Delaware Creek Shale ?	Pitkin Limestone / Fayetteville Shale / Hindsville Formation	Stanley Group
MISSISSIPPIAN	Meramecian	"Meramec Lime"	Sycamore Limestone	Moorefield Formation	
MISSISSIPPIAN	Osagean	"Osage Lime"		Boone Group / St. Joe Group	
MISSISSIPPIAN	Kinderhookian				
DEVONIAN	Upper	Woodford Shale / Misener Sandstone	Woodford Shale	Chattanooga Shale / Sylamore Sandstone	
DEVONIAN	Middle				Arkansas Novaculite
DEVONIAN	Lower	Haragan Fm. / Henryhouse Fm.	Frisco Formation / Haragan-Bois d'Arc Formation / Henryhouse Formation	Sallisaw Fm. / Frisco Fm.	Pinetop Chert
SILURIAN	Upper		Clarita Formation	Quarry Mtn. Fm.	
SILURIAN	Lower	Chimney Hill Subgroup	Cochrane Formation / Keel Formation	Tenkiller Fm. / Blackgum Fm. / Pettit Oolite	Missouri Mountain Shale / Blaylock Sandstone / Polk Creek Shale
ORDOVICIAN	Upper	Sylvan Shale / Viola Group	Sylvan Shale / Viola Group	Sylvan Shale / Viola Group / Fite Formation	Bigfork Chert
ORDOVICIAN	Middle	Simpson Group	Bromide Formation / Tulip Creek Formation / McLish Formation / Oil Creek Formation / Joins Formation	Tyner Formation / Burgen Sandstone	Womble Shale / Blakely Sandstone
ORDOVICIAN	Lower	Arbuckle Group	West Spring Creek Formation / Kindblade Formation / Cool Creek Formation / McKenzie Hill Formation / Butterly Dolomite	Arbuckle Group	Mazarn Shale / Crystal Mountain Sandstone
CAMBRIAN	Upper	Timbered Hills Group	Signal Mountain Formation / Royer Dolomite / Fort Sill Limestone / Honey Creek Limestone / Reagan Sandstone	Timbered Hills Group	Collier Shale ?
CAMBRIAN	Middle	Granite, Rhyolite, and Gabbro ?	Rhyolite		
CAMBRIAN	Lower				
PRECAMBRIAN		Granite, Rhyolite, and Metasediments	Granite and Gneiss	Granite and Rhyolite	

Figure 5: Generalized correlation of rock units in Oklahoma (Johnson and Cardott, 1992).

11

Figure 6: Correlation of Mississippian stratigraphic units in the southern Midcontinent. Osage County is located on the Cherokee Platform (Northcutt et al., 2001).

LOCALE

Osage County is located on the Cherokee Platform, bounded by the Nemaha uplift to the west and the Ozark uplift to the east (Johnson, 2008). The county is an area of low relief with exposures of Pennsylvanian shale, sandstone, and limestone throughout, dipping regionally to the west by 1°-2° (Thorman and Hibpshman, 1979). Figure 7a is a paleogeographic map showing the location of Oklahoma during the Mississippian (Blakey, 2011). The Mississippian occurred approximately 359 to 318 Ma and comprises approximately the lower two-thirds of the Carboniferous. A warm, shallow sea with plentiful marine life covered most of Oklahoma during the Mississippian (Rogers, 2001). Carbonate deposition occurred primarily during the Osagean, Meramecian, and Chesterian intervals of the Mississippian as slope and ramp margin banks with an extensive shelf margin, shown in Figure 7b, trending east-west along the Oklahoma-Kansas border (Watney et al., 2001).
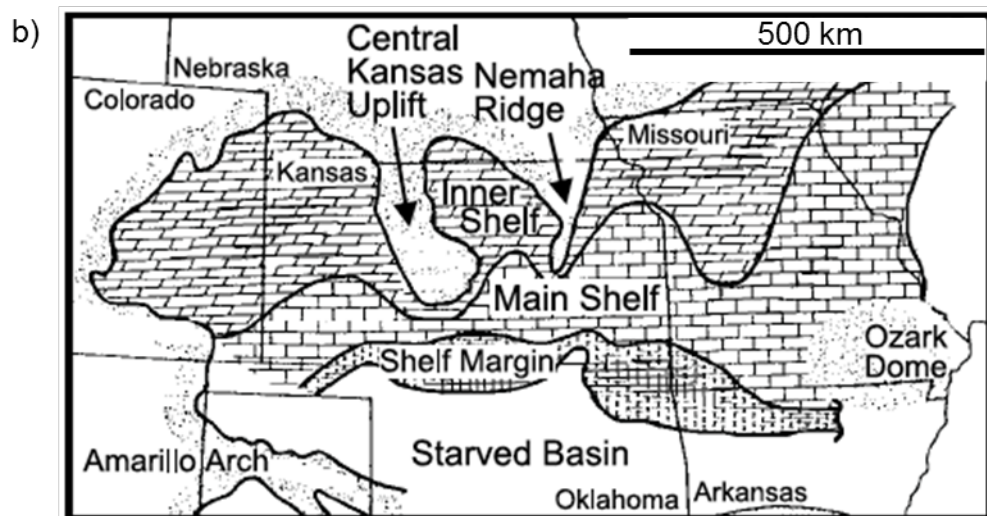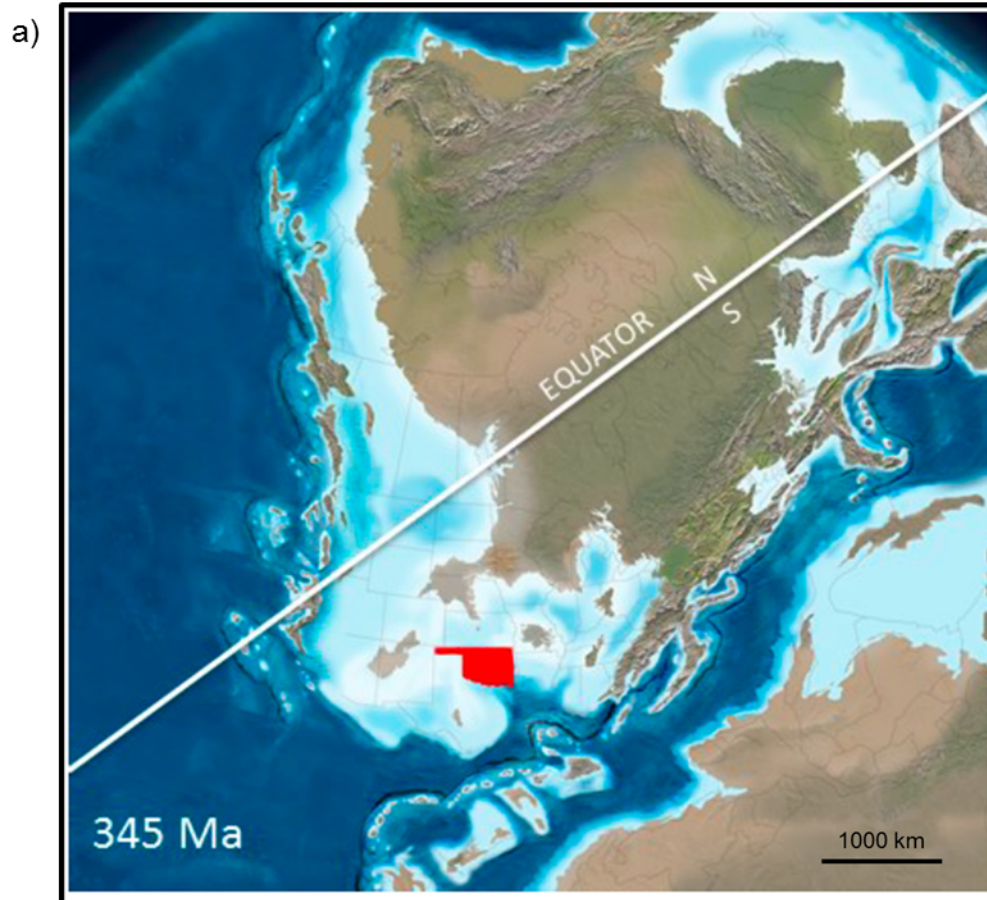
Figure 7: (a) Paleogeographic map showing the location of Oklahoma (red) during the middle Mississippian (modified from Blakey, 2011). (b) Extent of the Burlington shelf in Oklahoma during the Mississippian (Watney et al., 2001).

Figure 8 presents a generalized stratigraphic column for Osage County from Elebiju et al., (2011) based on the work of Zeller (1968), Thorman and Hibpshman (1979), and Franseen et al. (2004). Precambrian basement rocks underlie the entirety of Osage County and include the Washington County volcanic group, Spavinaw granite group, Osage County microgranite, and the Central Oklahoma granite group (Thorman and Hibpshman, 1979). The Precambrian basement surface is an irregular erosional feature with a broad westerly slope and a northwest trending series of domes extending from Tulsa across the county (Thorman and Hibpshman, 1979).

Paleozoic sediments overlie the Precambrian basement, recording four marine transgressions and regressions across the region from south to north, and there is almost no record of Mesozoic or Cenozoic deposition, save a few late Cenozoic deposits related to Pleistocene glaciation (Thorman and Hibpshman, 1979). Regional unconformities mark times of widespread non-deposition and/or erosion between each of these marine transgression/regression sequences (Thorman and Hibpshman, 1979). In this manner, it is possible to have relatively young rocks deposited on much older rocks with no record between (Thorman and Hibpshman, 1979).

Cambrian granite wash and the Reagan Sandstone were deposited unconformably on top of the Precambrian basement. While the granite wash is local in distribution and likely the result of reworked lag gravel deposits, the Reagan Sandstone represents a more continuous basal Paleozoic layer and is

15

a fine, well-sorted rock ranging in age from Late Cambrian to Early Ordovician (Thorman and Hibpshman, 1979).

The Arbuckle Group, consisting of interbedded siliceous limestone, dolomite, and sandstone units, ranges in age from Late Cambrian to Early Ordovician and lies unconformably on the Reagan Sandstone (Thorman and Hibpshman, 1979). Precambrian highs were not completely covered by Arbuckle Group strata until the Lower Ordovician, and subsequent post-Arbuckle erosion uncovered some of the Precambrian highs (Thorman and Hibpshman, 1979).

The Simpson Group is Middle Ordovician in age and is the only unit of Middle Ordovician-Lower Devonian age present in Osage County (Thorman and Hibpshman 1979). The group is composed of a basal sandstone (Burgen Sand), a middle green shale and sandstone with local dolomite (Tyner Formation), and an upper sandstone (Wilcox Sand; Thorman and Hibpshman, 1979). During this period, the Simpson sea transgressed and regressed, depositing this group; Late Devonian erosion removed any Upper Ordovician, Silurian, and Lower Devonian units that may have been deposited (Thorman and Hibpshman, 1979).

During the Middle Devonian, the Misener Sandstone was deposited from reworked Simpson sands; however, the Misener rarely exceeds 6 m (20 ft) in thickness and is only present in the southwestern part of the county as well as a small patch northwest of Bartlesville (Thorman and Hibpshman, 1979). The Late Devonian Woodford Shale, which is a black carbonaceous fissile rock,

16

overlies the Misener and is present throughout most of the county, but the thickness of Woodford rarely exceeds 15-20 m (50-75 ft) and is commonly absent over pre-Late Devonian topographic highs (Thorman and Hibpshman, 1979).

The Mississippi Lime, Lower Mississippian in age, overlies the Woodford Shale, although in places where the Woodford is absent, the lime overlies the Simpson and Arbuckle groups (Thorman and Hibpshman, 1979). The lime is present throughout the county with thickness ranging from 30-120 m (100-400 ft) and is composed of limestone, dolomite, and cherty limestone (Thorman and Hibpshman, 1979). The unconformity between the Mississippian and the Pennsylvanian resulted in an erosional, irregular surface at the top of the Mississippian with local relief in excess of 30 m (100 ft; Thorman and Hibpshman, 1979).

Following the orogenic events of Early and Middle Pennsylvanian, Middle and Late Pennsylvanian seas moved across the county interacting with major drainage systems, resulting in marine-delta deposition of sandstones and limestones (Thorman and Hibpshman, 1979). The base of the Pennsylvanian is the Mississippian Chert, a conglomerate derived from the underlying Mississippian Lime and deposited in an irregular channel system (Thorman and Hibpshman, 1979). Pennsylvanian units deposited on top of the chert include the Red Fork, Pink, Skinner, and Verdigris sandstones and the Oswego limestone.
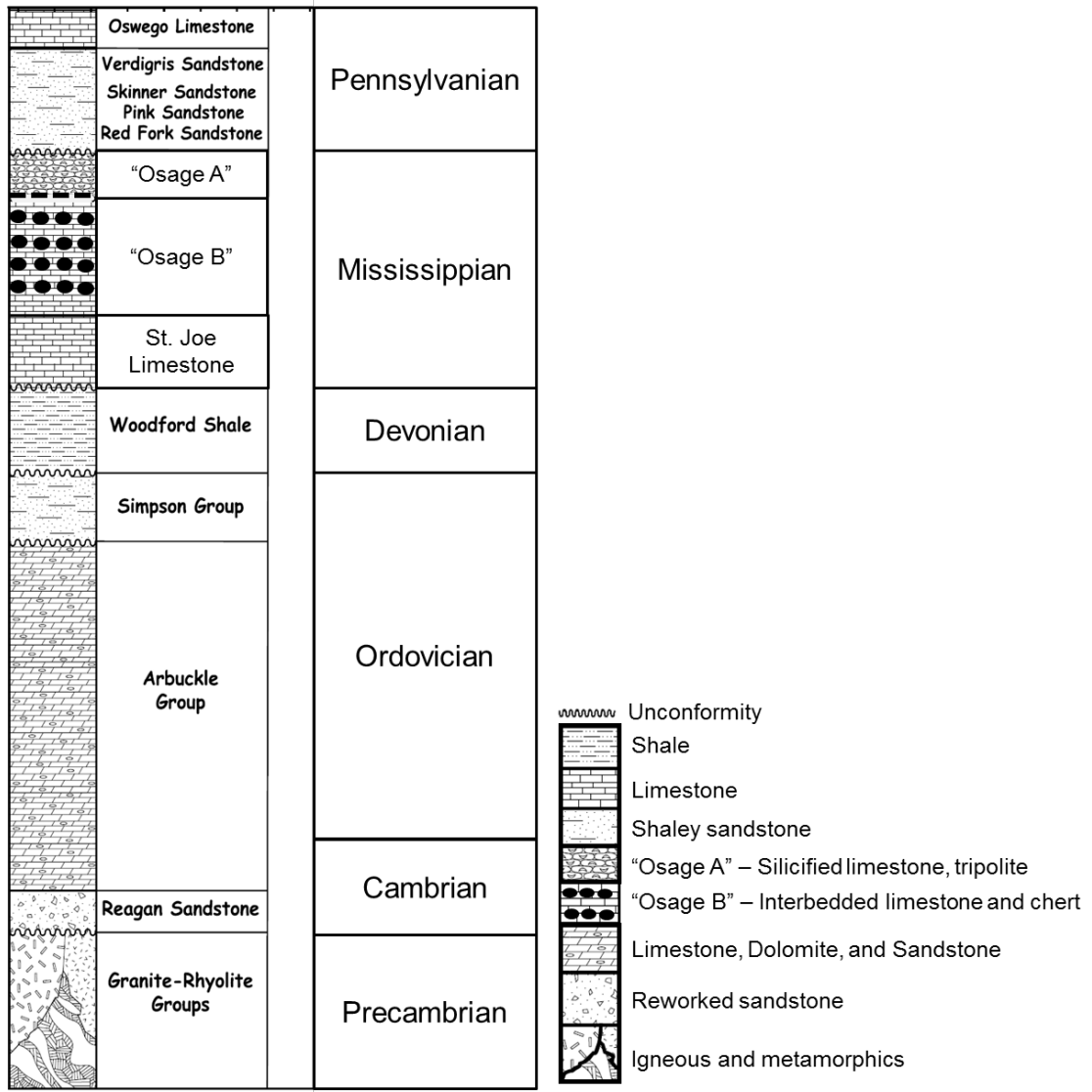
Figure 8: Generalized stratigraphic column for Osage County. "Osage A" is as a silicified limestone with high diagenetic susceptibility, and is where tripolite most commonly occurs. "Osage B" contains interbedded tight, fractured limestone and chert and has low diagenetic susceptibility. The St. Joe Limestone is the basal unit of the Mississippian in Osage County and contains no chert (Matson, 2013; Elebiju et al., 2011).

Figure 9 is Rogers' (1996, 2001) model for the diagenesis and deposition of both Mississippian chert lithologies. Rogers' (2001) model for the formation of the Mississippian chert describes two contemporaneous processes in two different settings. The first setting is along the shelf edge as illustrated in Figure 9a, 9c, and 9e, while the second setting is a subaerially exposed area as illustrated in Figure 9b, 9d, and 9f. Both settings involve dual-stage diagenesis (Rogers, 2001).

In the first setting along the shelf edge, cherty limestone erodes from the fore-reef and/or the shelf and is redeposited downslope in a mud matrix, as shown in Figure 9a (Rogers 2001). Stage one diagenesis begins with silica replacement of calcite, shown in Figure 9c. Stage two diagenesis follows with the dissolution of remaining calcite, possibly by leaching from infiltrated meteoric water, seen in Figure 9e (Rogers, 2001). Setting one is Rogers' (2001) model for the deposition of the hard, tight chert.

Rogers' (2001) second setting is subaerially exposed paleohighs, illustrated in Figure 9b, where deposition occurs from in situ weathering, resulting in vug and karst development, collapse breccia deposits, and the development of porous chert. Again, stage one diagenesis is the replacement of calcite with silica, shown in Figure 9d. Stage two diagenesis follows with the infiltration of meteoric water dissolving any remaining calcite (Rogers, 2001). Setting two is Rogers' (2001) model for the deposition of the porous, tripolitic chert.

19
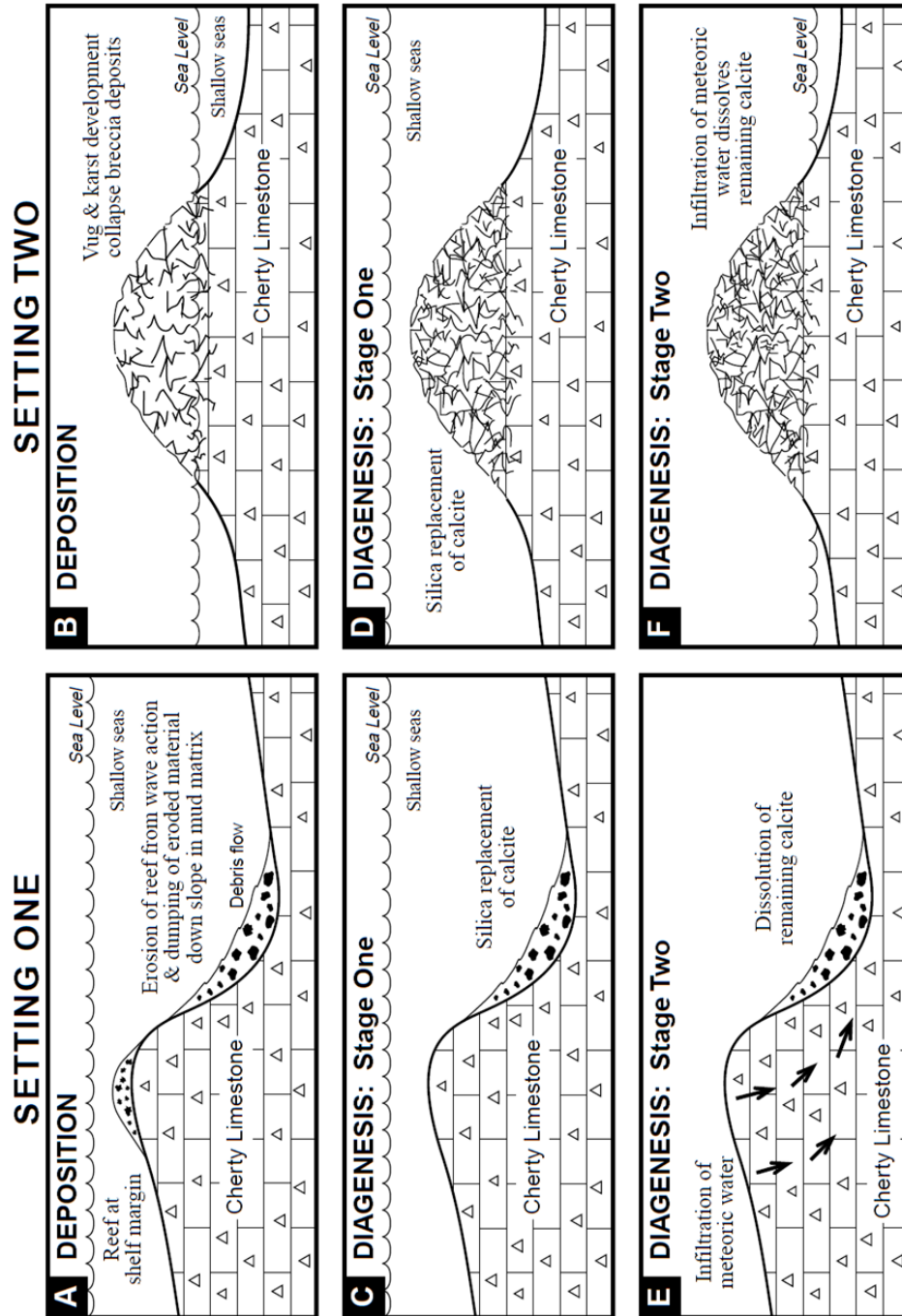
Figure 9: Models showing the depositional and diagenetic scenarios for the two types of chert lithologies. Deposition stage in setting one (a) involves fore-reef and/or shelf erosion of cherty limestone and redeposition of eroded material. Deposition stage in setting two (b) involves weathering-in-place on exposed paleohighs and development of porous chert. Diagenesis stage one is the silica replacement of calcite (c, d). Diagenesis stage two is the dissolution of any remaining calcite, possibly leaching by meteoric waters (e, f) (from Rogers, 2001).

CHAPTER 3: 3D PRESTACK SEISMIC PROCESSING

AVAILABLE DATA

Spyglass Energy, LLC, a small independent oil and gas exploration and production company located in Tulsa, Oklahoma, has provided me with a 3D prestack seismic survey acquired in northwestern Osage County, Oklahoma, near the town of Foraker. In this chapter, I present the most important results of my processing flows, with a detailed discussion in Appendix A and as a DVD to allow less experienced processors to mimic my workflow.

Figure 1 shows the location of the survey within Osage County. Table 1 summarizes the acquisition parameters representing common values used for a Midcontinent U.S.A. 3D seismic survey. The CMP bin spacing is 33.5 by 33.5 m (110 by 110 ft), the receiver group spacing is 67 m (220 ft) and the receiver line spacing is 201 m (660 ft). For each shot, there are ten live receiver lines, each with 52 active channels. The shot spacing is 67 m (220 ft) and the shot line spacing is 100 m (330 ft). The survey is mostly narrow azimuth, however; there are locations that come close to having wide azimuth acquisition. As the target zone is relatively shallow, the record length is 2 seconds at a 2 ms sampling interval, or 500 samples per second. The overall quality of the data is very good with recorded frequencies between 10 and 120 Hz. The dominant frequency at the target depth of 880 m (2900 ft, 0.530 s) is 50 Hz with a velocity of approximately 3048 m/s (10,000 ft/s), resulting in a tuning thickness vertical resolution of about 15.2 m (50 ft).

Receiver spacing	67 m (220 ft)
Receiver line space	201 m (660 ft)
Active receiver lines per shot	10 Lines
Live channels per receiver line	52 channels
Shot spacing	67 m (220 ft)
Shot line spacing	100 m (330 ft)
Source type	Vibroseis
Sweep parameters*	- Eight 10 second sweeps
	- 16-120 Hz
	- Increasing 3 dB/oct
	- 500 ms taper at start and end
Record length	2 seconds (2000 ms)
Sample interval	2 ms
CMP bin size	33.5 x 33.5 m (110 x 110 ft)
Maximum CMP fold	186
Average CMP fold	60
Tuning thickness	15.2 m (50 ft)
Lateral resolution (Fresnel Zone) for unmigrated data	80 m (280 ft)

Table 1: Summary of acquisition parameters for 3D prestack seismic survey. (*Sweep parameters are unknown, but the values presented in the table are typical for the Midcontinent U.S.A., and appear to be close approximates according to the raw spectrum (Karr and Hefner, 2010)).

PROCESSING

I begin with a 17 GB 3D prestack seismic survey that contains raw shot records, retaining the contractor's computed refraction and elevation statics. The target zone is relatively shallow at approximately 530 ms with basement occurring at approximately 700 ms. In order to improve vertical and horizontal resolution, my processing objective is to remove ground roll and coherent noise as much as possible and to reduce the acquisition footprint that contaminates the shallow section of the data. Prestack time migration will enhance subtle structure. Figure 10 shows the generalized processing workflow.

The first step is to load the data and make sure that the header geometry is consistent with the kinematics of the first breaks, thereby forming a quality control. Geometry QC is a critical step, and it is necessary to spend time and care to ensure that the data are properly loaded. The geometry database is created and applied to the trace headers, which includes defining the midpoint binning grid and binning the midpoints.

Figure 11a shows the source and receiver geometry for this survey. For each source, there are 10 live receiver lines with 52 geophones per line. The survey is a merge of two independently acquired patches: North and South. After defining the midpoint-binning grid and binning the midpoints, the CMP fold map shows a maximum fold of 186, although the fold is closer to 60 for the majority of the survey, shown in Figure 11b. Figure 12 shows the offset distribution, with the maximum offset approaching 3,658 m (12,000 ft), while the most commonly occurring offset is about 914 m (3,000 ft).
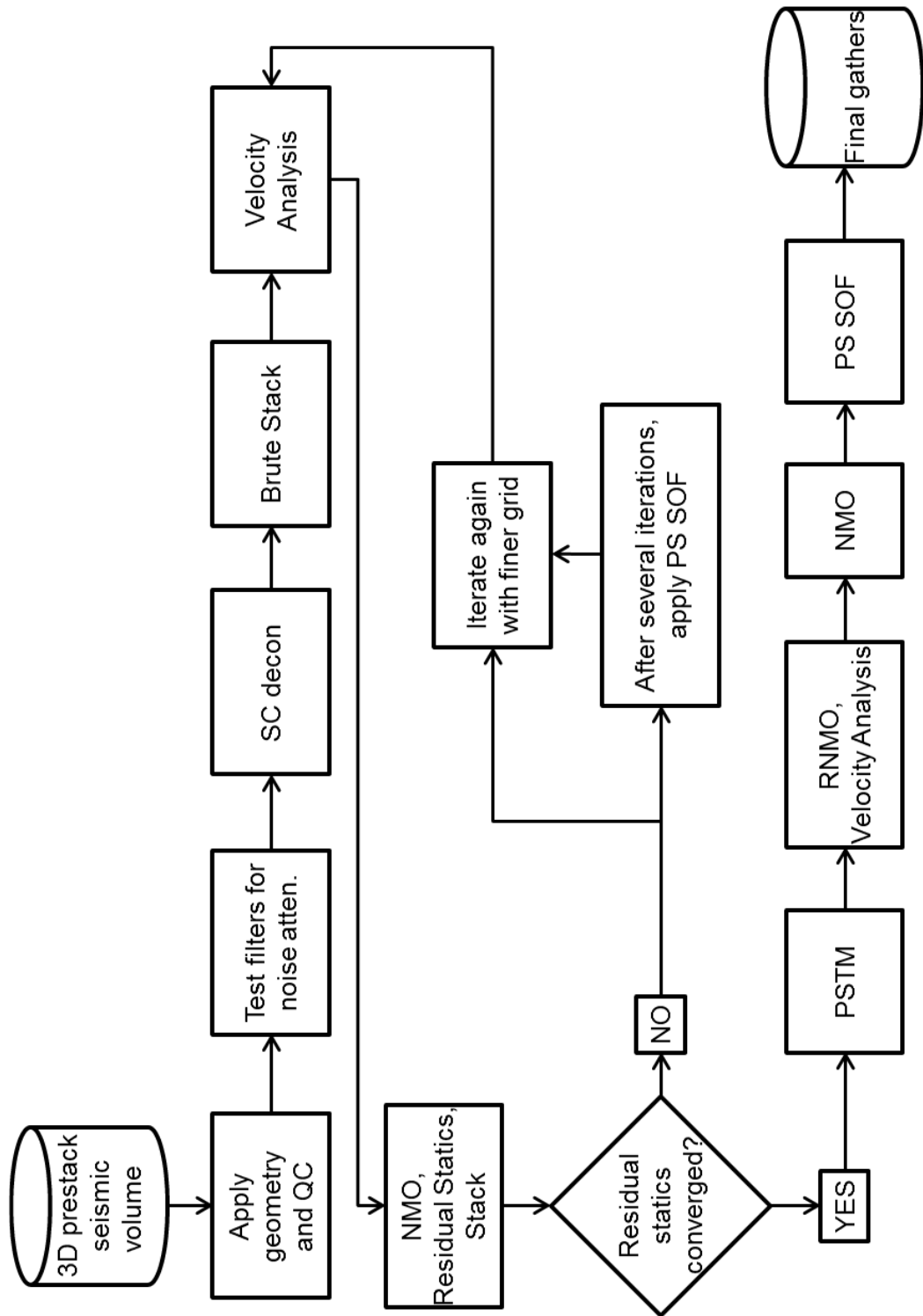
Figure 10: Generalized processing workflow used in this thesis.
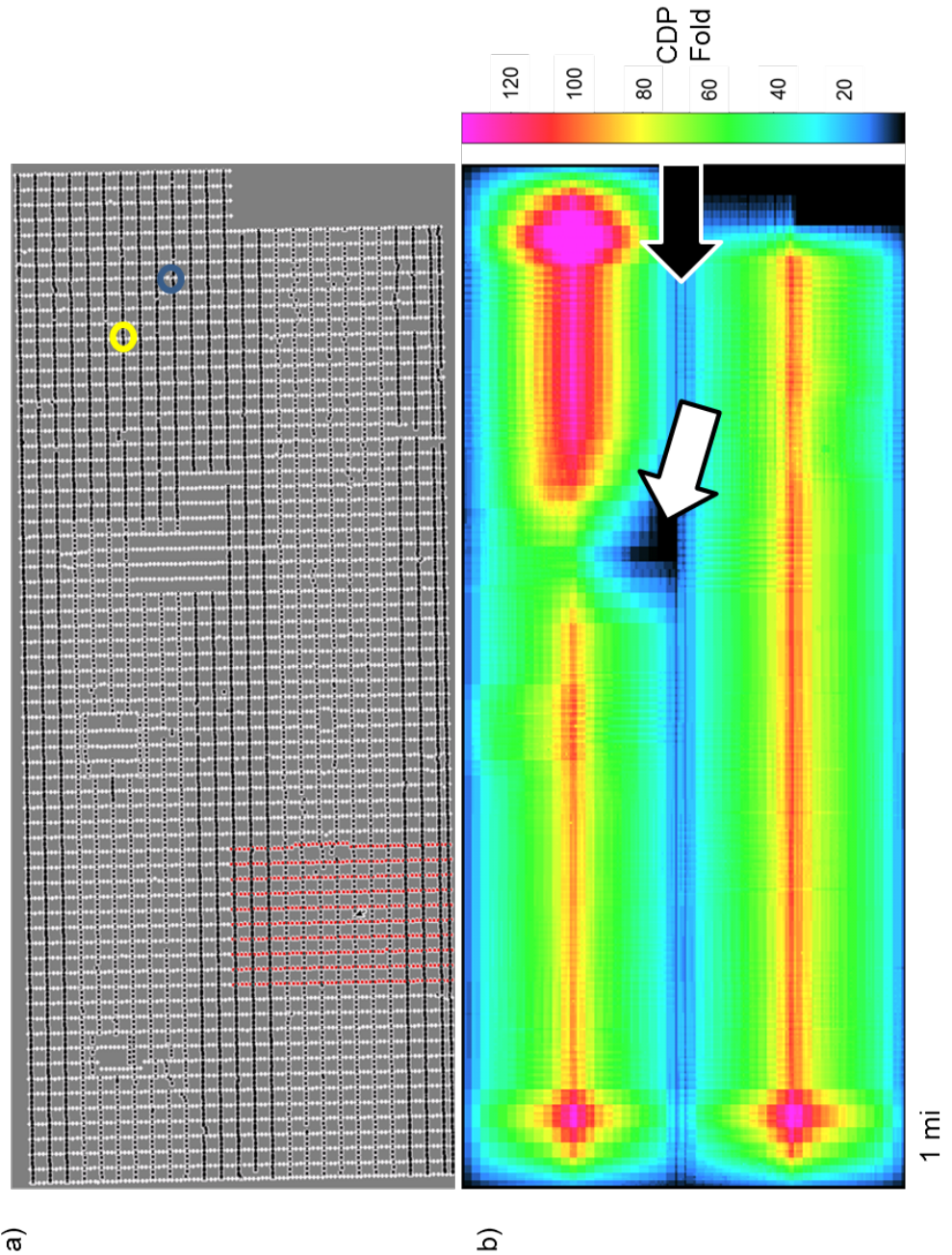
Figure 11: (a) Shot and receiver geometry for 3D prestack seismic survey. Black points represent shot locations and white points represent receiver locations. A representative shot gather geometry is shown in red. (b) CMP fold map showing a maximum fold of 186, although most of the survey has a fold between 60-80. The survey was acquired in two patches, which can be observed on the fold map. The low fold between the patches (black arrow) will result in lower signal to noise in this area. The low-fold hole near the center of the survey (white arrow) is a town site. The blue circle indicates the location of the CMP shown in Figure 16, while the yellow circle indicates the location of the shot gather shown in Figure 13.
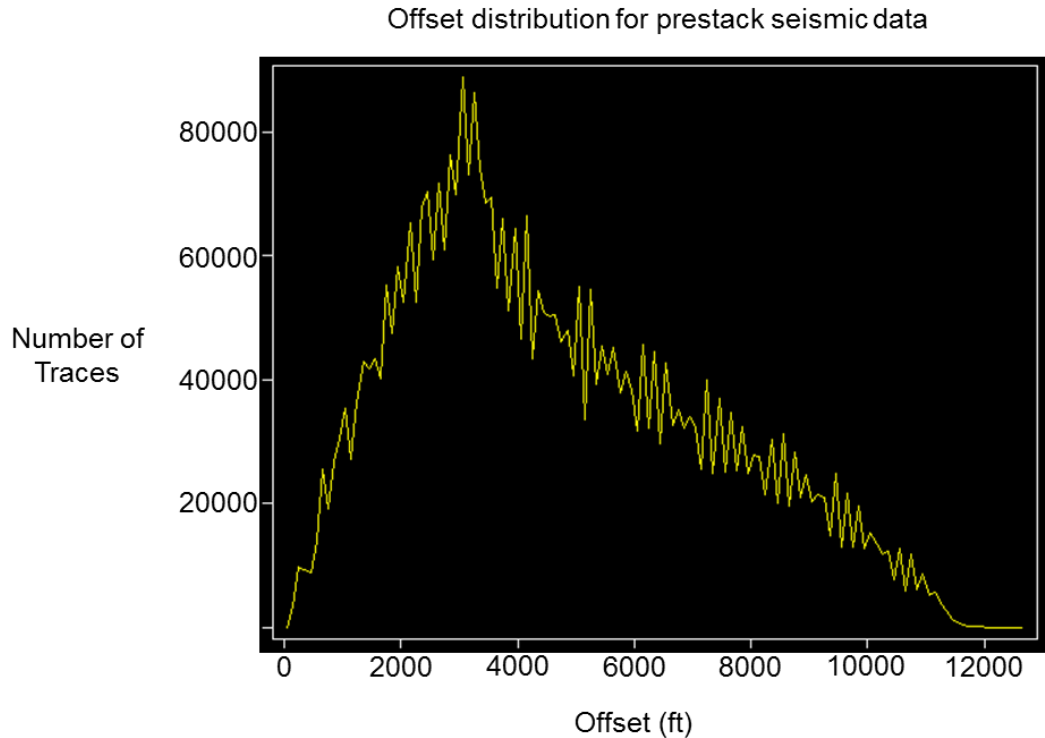
Figure 12: Offset distribution of the 3D prestack seismic survey.

Figure 13a shows a representative raw shot record indicated by the yellow circle in Figure 11a, sorted by source location number and channel number. Other than the previously applied refraction and datum statics and applying geometry, the records are raw. Groundroll is quite prevalent, especially at the near offsets. Figure 13b shows the spectral content of the shot record shown in Figure 13a. Frequencies below 10 Hz are below -60 dB. The slope between 10 and 18 Hz is about 80 dB/Octave. Frequencies between 15 and 110 Hz are at -25 dB and above, accounting for most of the data's spectral content. After a peak around 23 Hz at -0.15 dB, the frequencies begin to drop off. The frequencies between 45 and 110 Hz have a slope of -12 dB/Octave, and then the slope becomes -530 dB/Octave between 110 and 120 Hz. Figure

26

14 shows the same shot record, but the secondary sort is by the absolute value of the offset. Both the groundroll and air blast are noticeable, overwhelming actual signal at near offsets.
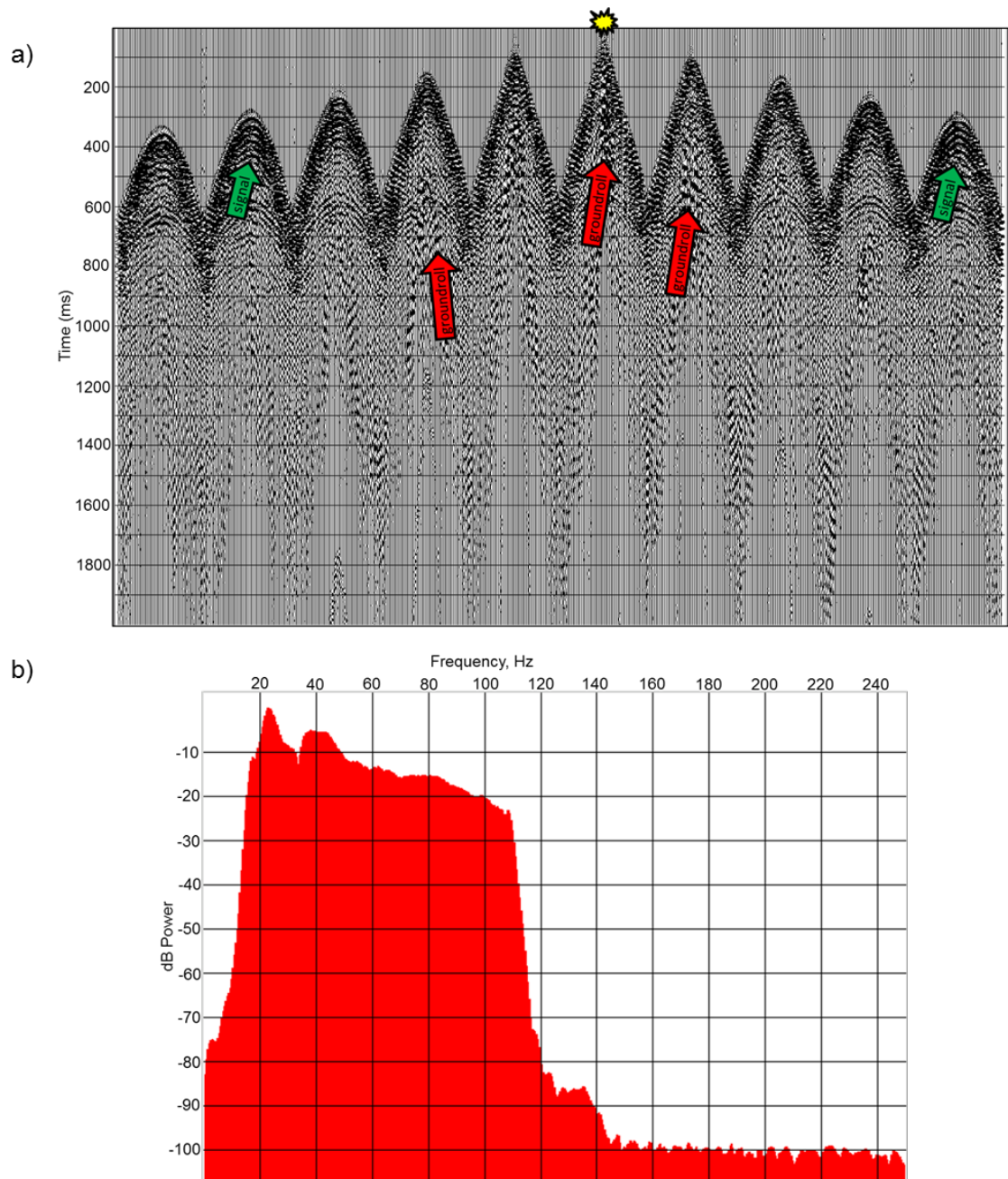
Figure 13: (a) Raw shot record after applying geometry, sorted by source station number and recording channel showing the ten live receiver lines in the patch. The yellow symbol indicates the source location. Groundroll (red arrows) dies off at further offsets where signal (green arrows) becomes more prevalent. (b) Spectral content for the same shot. Frequencies range between 18-110 Hz.
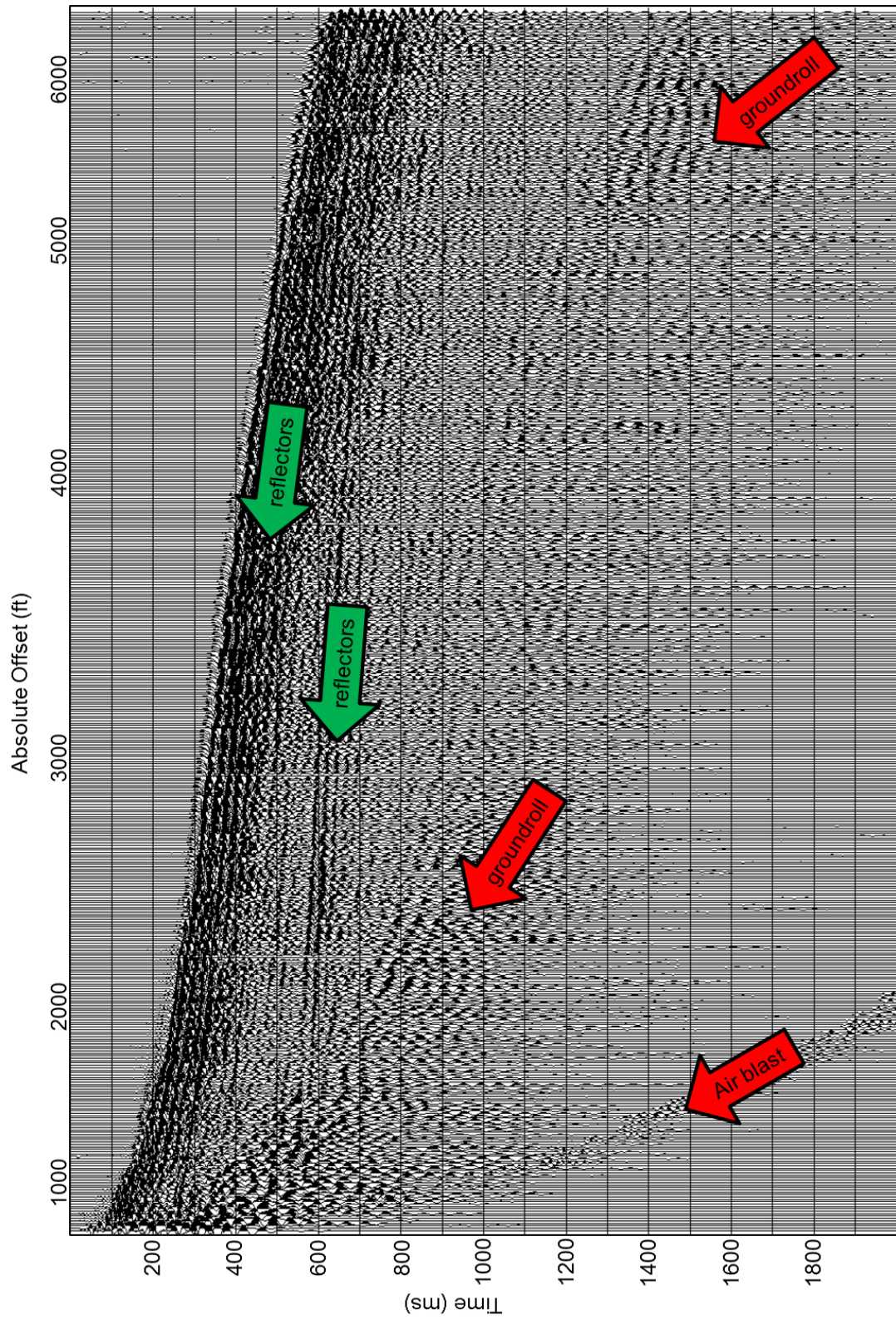
Figure 14: The same raw shot record from Figure 12a. Green arrows indicate signal and red arrows indicate groundroll and air blast.

Figure 15 shows a suite of records with various bandpass filters applied. Figure 15a shows the raw shot record with an Ormsby bandpass 0-0-10-20 Hz filter applied. Groundroll and the air blast dominate this frequency band, although there is some signal present. Figure 15b shows the shot record bandpass filtered with corner frequencies of 10-20-30-40 Hz. Groundroll is still very dominant in this frequency band. Figure 15c shows the shot record bandpass filtered between 90, 100, 110, and 120 Hz. This filter band contains some signal but also appears to contain some aliased noise. Finally, Figure 15d shows the shot record filtered between 10, 20, 90, and 120 Hz. Although the groundroll leaks up into the mid 20 Hz frequencies, preserving the low frequencies as much as possible is important. Setting the low cut corner at 10 Hz and the low pass corner at 20 Hz allows for a more gradual ramp, filtering out some of the offending groundroll while still preserving some of the lower frequencies. This is the filter design used for the rest of the processing flow, as well as for time-variant spectral whitening.
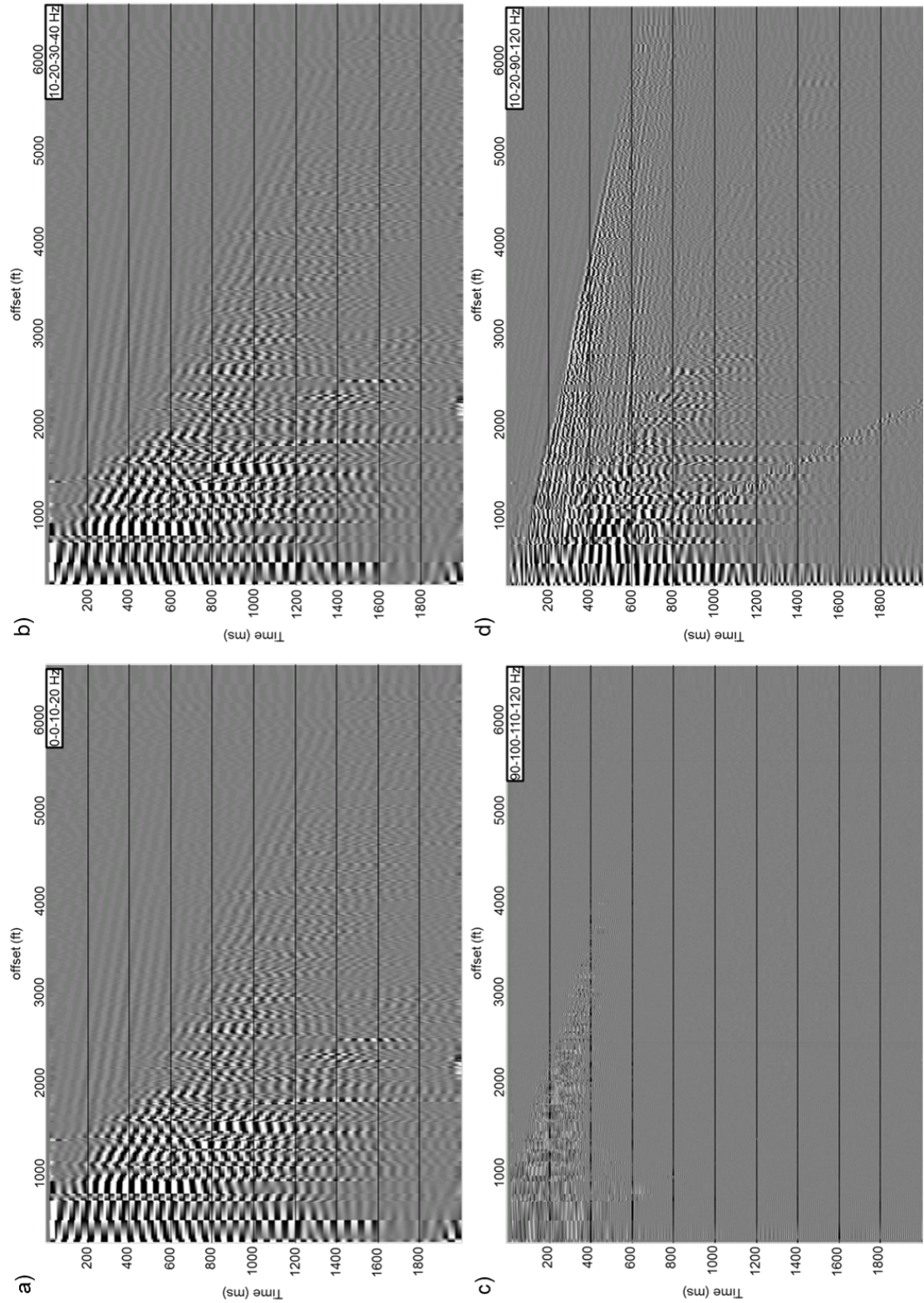
Figure 15: A series of bandpass filters applied to the same shot record. (a) Bandpass filtered 0-0-10-20 Hz. (b) Bandpass filtered 10-20-30-40 Hz. (c) Bandpass filtered 90-100-110-120 Hz. (d) Bandpass filtered 10-20-90-120 Hz.

31

After applying the geometry to the data, I begin testing for true amplitude recovery, using a parameter test of 2, 4, 6, 8, 10, and 12 dB/sec true amplitude recovery constant corrections, with the best correction to be 9 dB/s. A series of time gates are picked and then used to apply time-variant scaling to better balance the data. Trace statistics are calculated and used to perform trace edits. The trace statistics used for editing include spikiness (maximum amplitude divided by average amplitude), average trace energy, and statistical frequency deviation.

Before beginning velocity analysis, a "preliminary" deconvolved dataset is created. It is preliminary because it only uses spiking deconvolution, whereas later use surface-consistent deconvolution is used after having phase matched the two patches of the survey to one another. The spiking deconvolution uses a zero phase 120 ms operator with 0.1% white noise. I also apply a top mute, air blast attenuation, AGC and a 10-20-90-120 Hz bandpass filter. Figure 16 shows a representative CMP gather before and after spiking. The deconvolution and noise attenuation parameters have eliminated much of the groundroll and air blast and retained coherent reflector events visible down to almost 1100 ms at the far offsets. Figure 17 shows the corresponding spectral content of the CMP gather before and after.
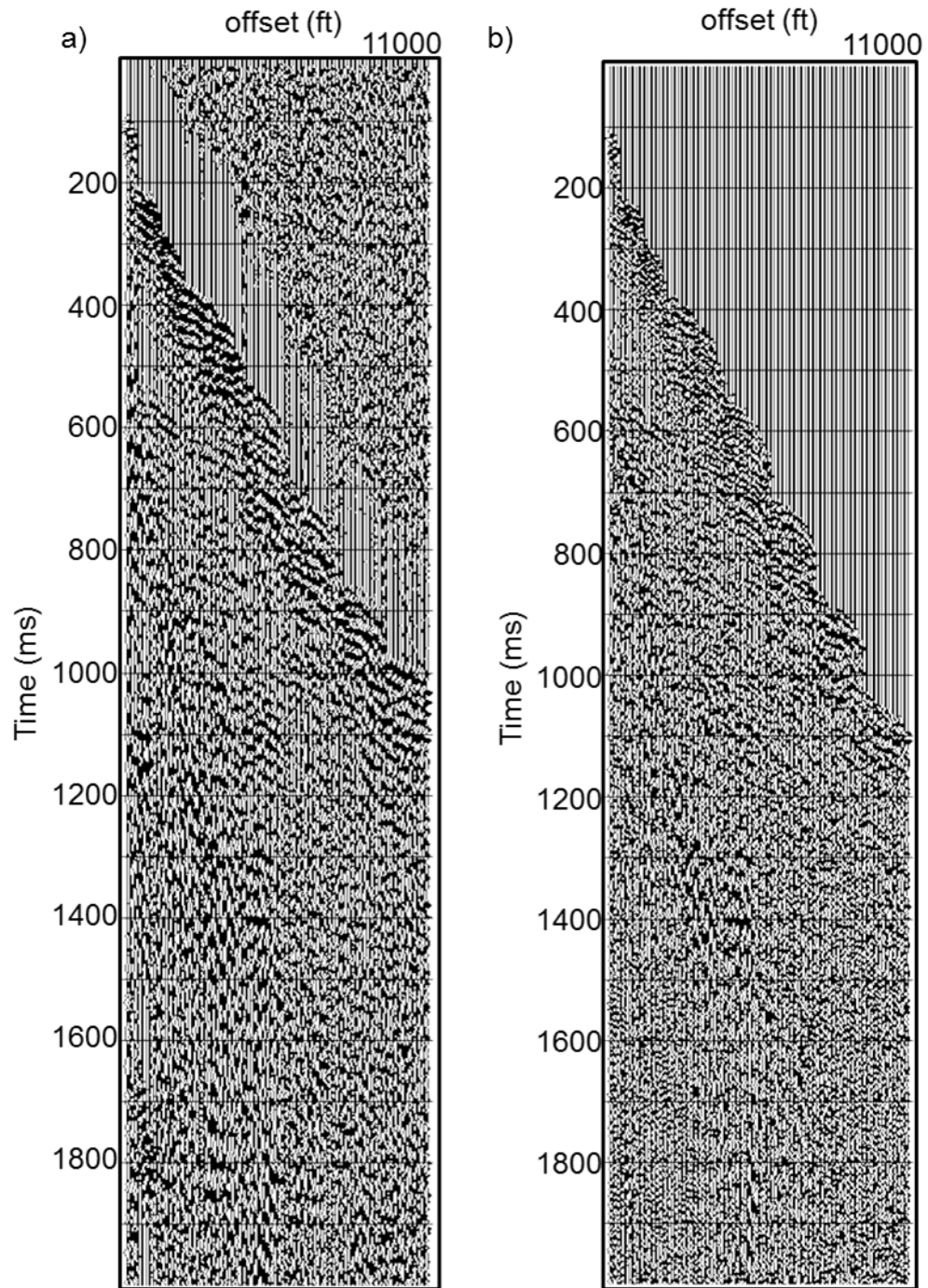
Figure 16: (a) A representative CMP gather after applying geometry and AGC. Groundroll and coherent noise is prevalent. The location of the CMP gather is indicated by a blue circle in Figure 11. (b) The same CMP after spiking deconvolution, top mute, air blast attenuation, AGC, and a 10-20-90-120 Hz bandpass filter. Groundroll is less prevalent and reflection events are better resolved.
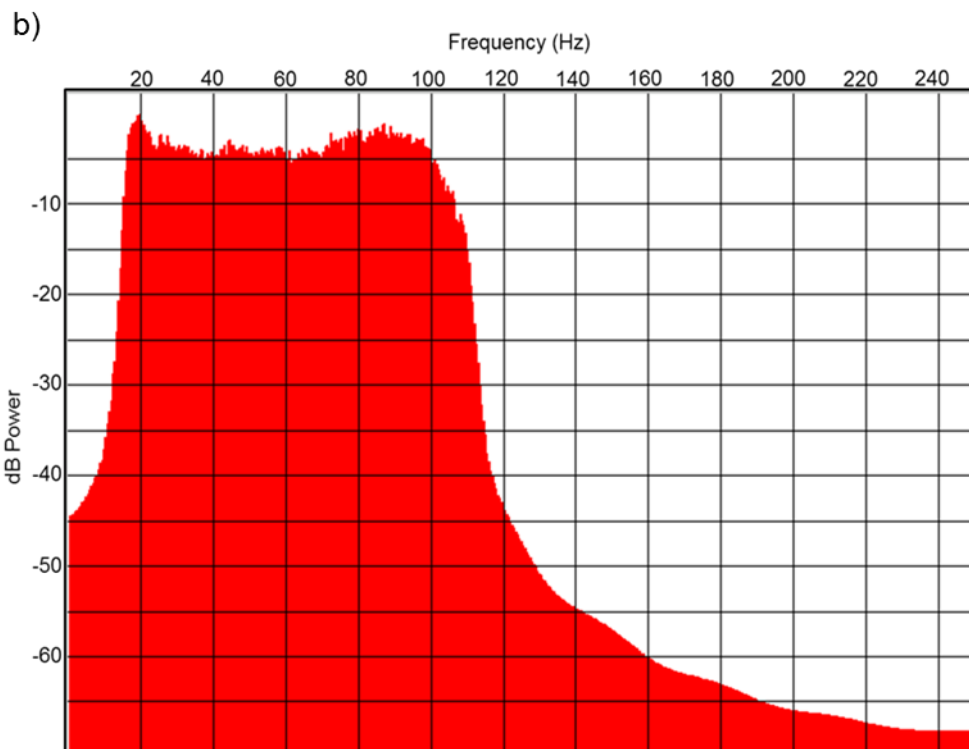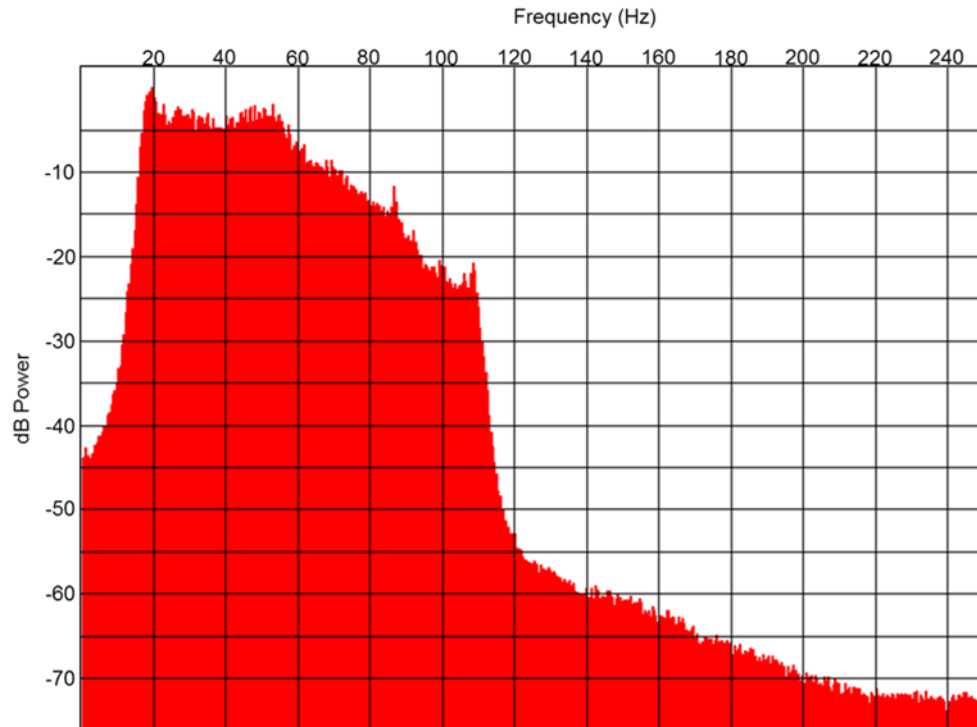
Figure 17: Spectrum of the CMP gather in Figure 16 (a) before and (b) after spiking deconvolution. The frequencies in (a) peak at 20 Hz and begin to fall off rapidly after 50 Hz. The spectrum in (b) is much flatter due to the spiking deconvolution operation.

An iterative process of velocity analysis and residual statics calculation begins by picking velocities for a single CMP. The corresponding NMO correction is applied to the deconvolved gathers using this single point velocity analysis, followed by calculating and applying residual statics, and then stacking the NMO corrected gathers to create a brute stack. After this first pass of residual statics, a new velocity analysis is performed picking on an 80x80 inline-crossline grid, applying the corresponding NMO correction to the deconvolved gathers using the new velocity field, and calculating new residual statics and stacking. This cycle of velocity analysis, NMO correction, residual statics calculation, and stacking continues using a 40x40 grid, and finally a 20x20 grid. Each time a new round of velocity analysis begins, the residual statics from the previous iteration are applied, and the previous velocity field serves as a guide function while picking on the finer grid. Ideally, the residual statics should eventually converge to a 0 ms correction. After the first pass, the residuals for most sources and receivers already fall between +/- 2.0 ms, which is the same as the data's sample interval. After the second pass, most residuals fall between +/- 1.0 ms. Figure 18a-d shows a representative CMP gather with NMO correction after each velocity analysis pass. As the velocity analysis becomes finer, events are better resolved. Figure 19-22 show the stack after each velocity analysis iteration.
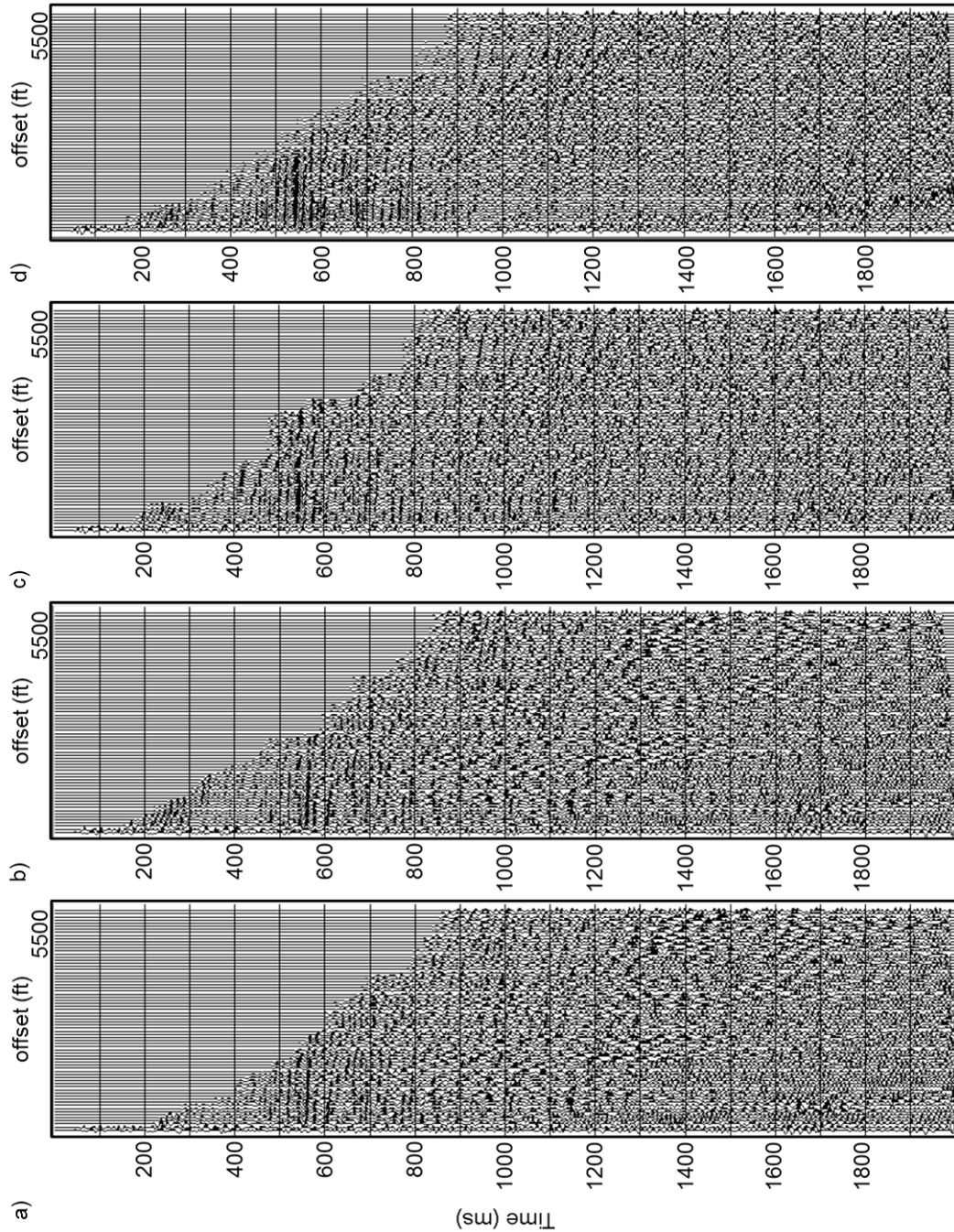
Figure 18: NMO-corrected CMP gather shown in Figure 16 using velocities computed a) on a single point, and on (b) an 80x80, (c) a 40x40, and (d) a 20x20 grid. The data in (d) were subjected to prestack structure-oriented filtering.
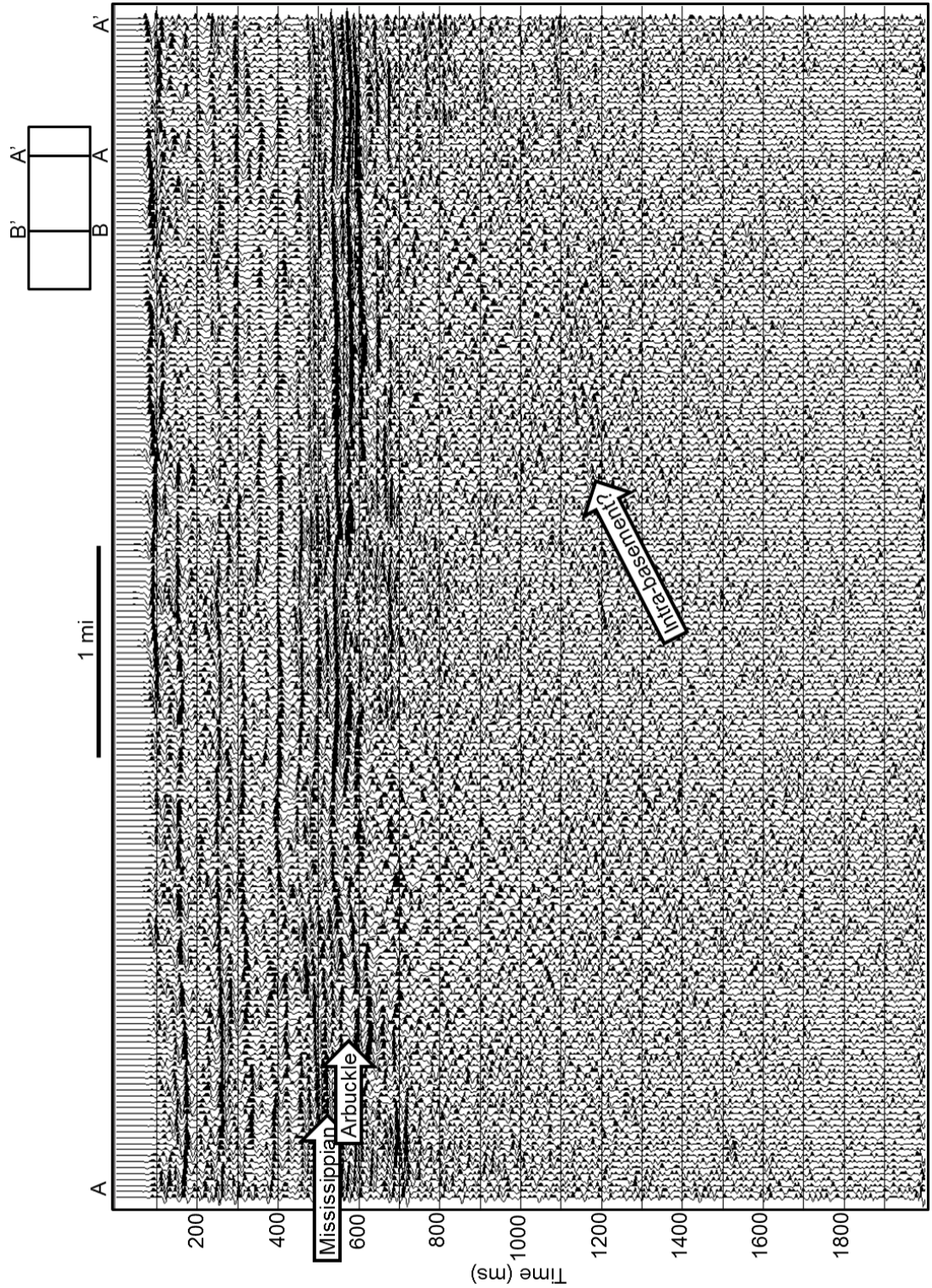
Figure 19: Line AA' through the brute stack, computed using a single velocity analysis location and after the first pass of residual statics.
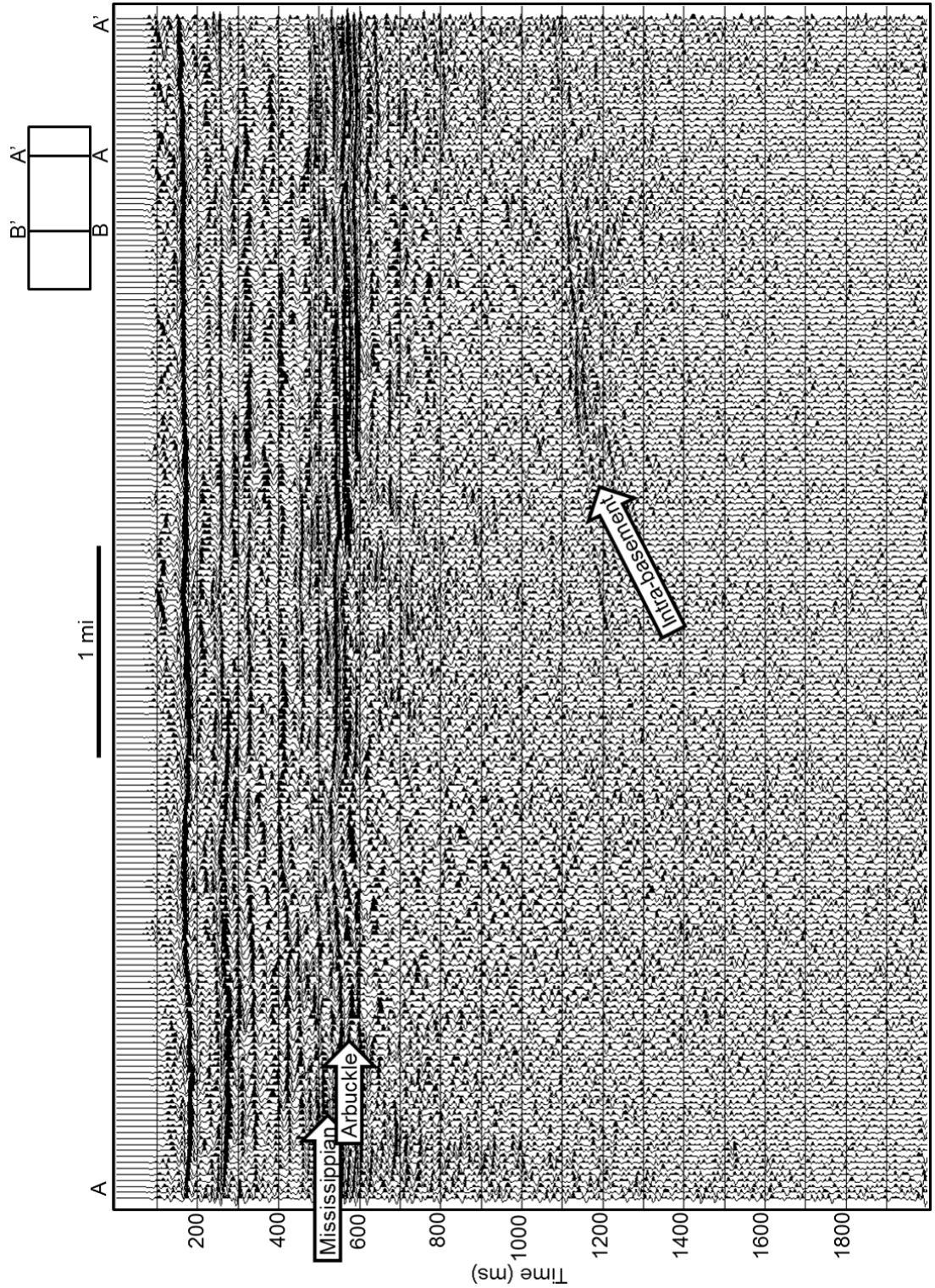
Figure 20: Line AA' through the stack after 80x80 grid velocity analysis and two pass of residual statics.. Reflectors between 200-700 ms are better resolved. The basement structure begins to be resolved.
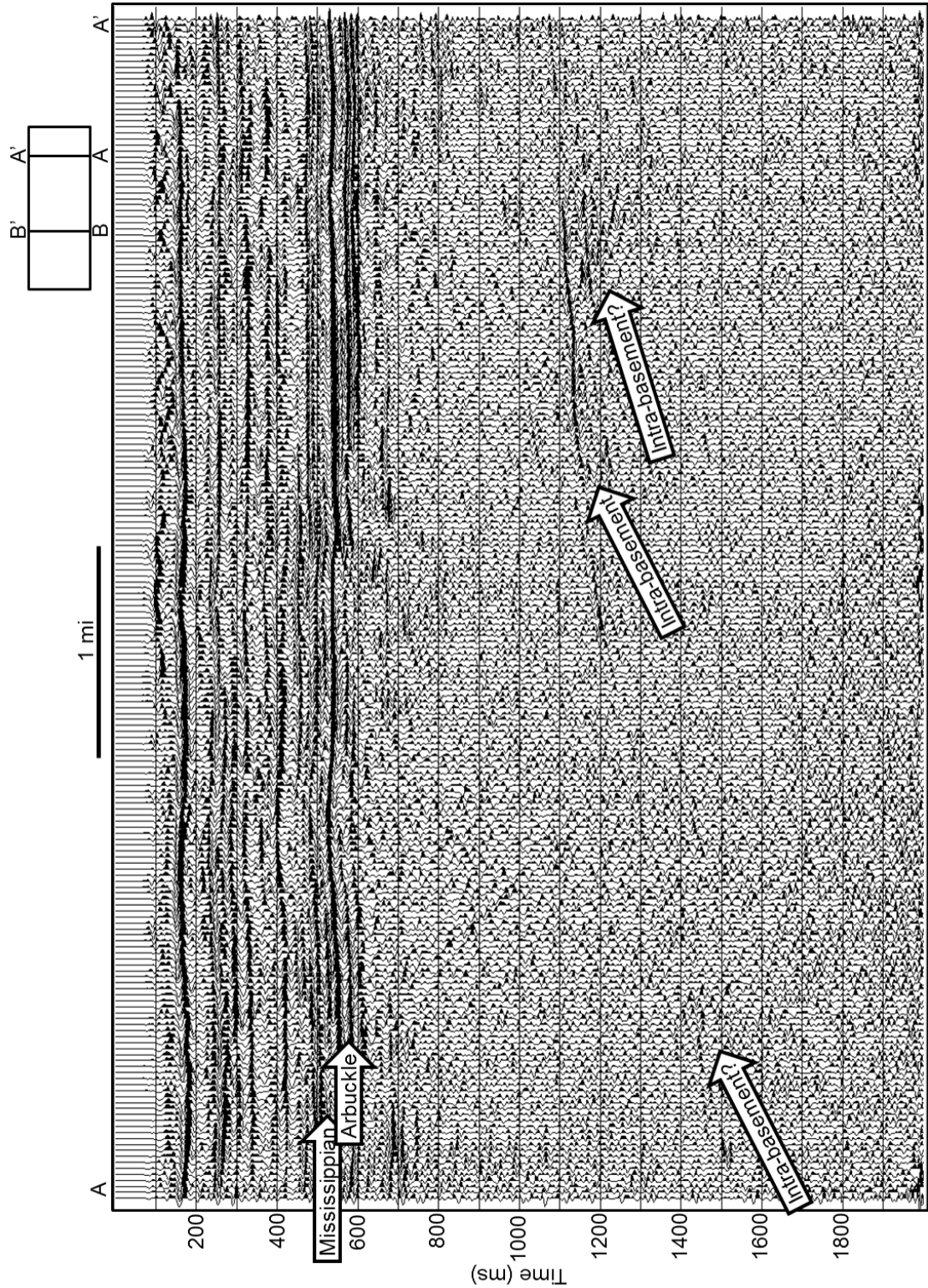
Figure 21: Line AA' through the stack after 40x40 grid velocity analysis, three passes of residual statics, and phase matching patch 1 to patch 2. Reflectors align better and the basement structure continues to be better resolved.

39
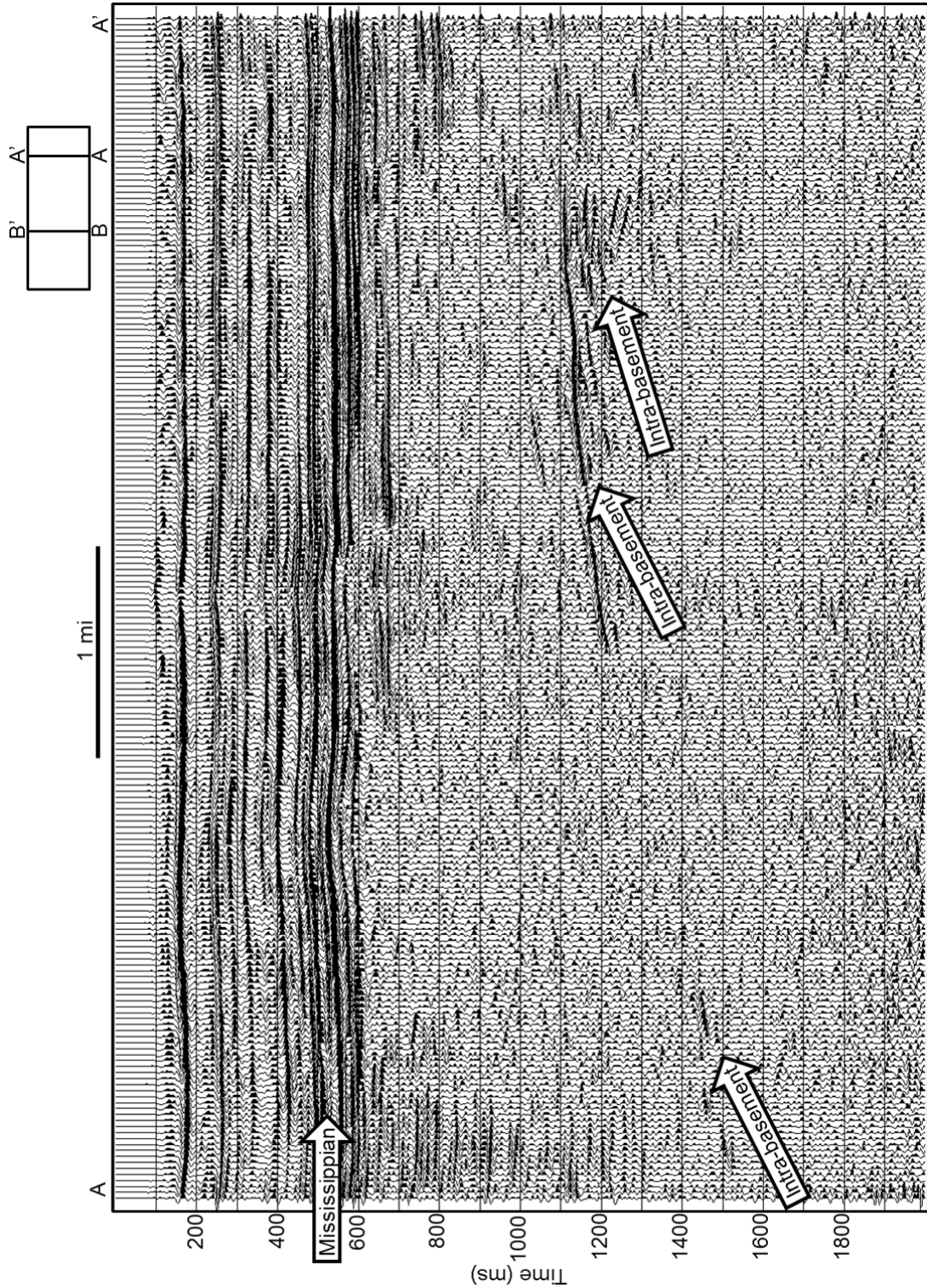
Figure 22: Line AA' through the stack after prestack structure-oriented filtering, 20x20 grid velocity analysis, phase matching, and four passes of residual statics. Resolution of reflectors between 400 and 600 ms increases. White arrows indicates an intra-basement reflector.

Once the second round of velocity analysis using the 80x80 grid is complete, a flow to phase match patch 1 to patch 2 is created. The fold distribution is more even in patch 2 while patch 1 has several obstacles due to the town of Foraker and no-permit zones, giving rise to holes in the fold map. The phase rotation patch 1 needs to match patch 2 is -50.47°. After applying the rotation, I restack using the 80x80 velocity field and compare it to the 80x80 stack before phase matching. The 80x80 stack shown in Figure 20 is before phase matching. The stack divided into patch 1 and patch 2 is shown in Figure 23 and the phase matched 80x80 stack in Figure 24. The reflectors now align much better and the "tear" or "seam" between the two patches is much less noticeable.

With the phase match filter derived, I return to the gathers that have geometry applied and trace edits and create a surface-consistent deconvolution flow. In this flow, the phase rotation, a top mute, air blast attenuation, time-variant spectral whitening, time-variant scaling, and a 10-20-90-120 Hz bandpass filter are all applied. The surface-consistent deconvolution goes between the top mute and the air blast attenuation steps. The surface-consistent deconvolution applies spiking deconvolution using the sources, receivers, offset, and CMPs for spectral decomposition. However, only the source and receiver components are applied. The operator is 120 ms in length with 0.1% white noise. The offsets are limited between 152 m (500.0 ft) and 1067 m (3500.0 ft) in calculating the operator, using five Gauss-Siedel iterations as recommended by Cary and Lorentz (1991).
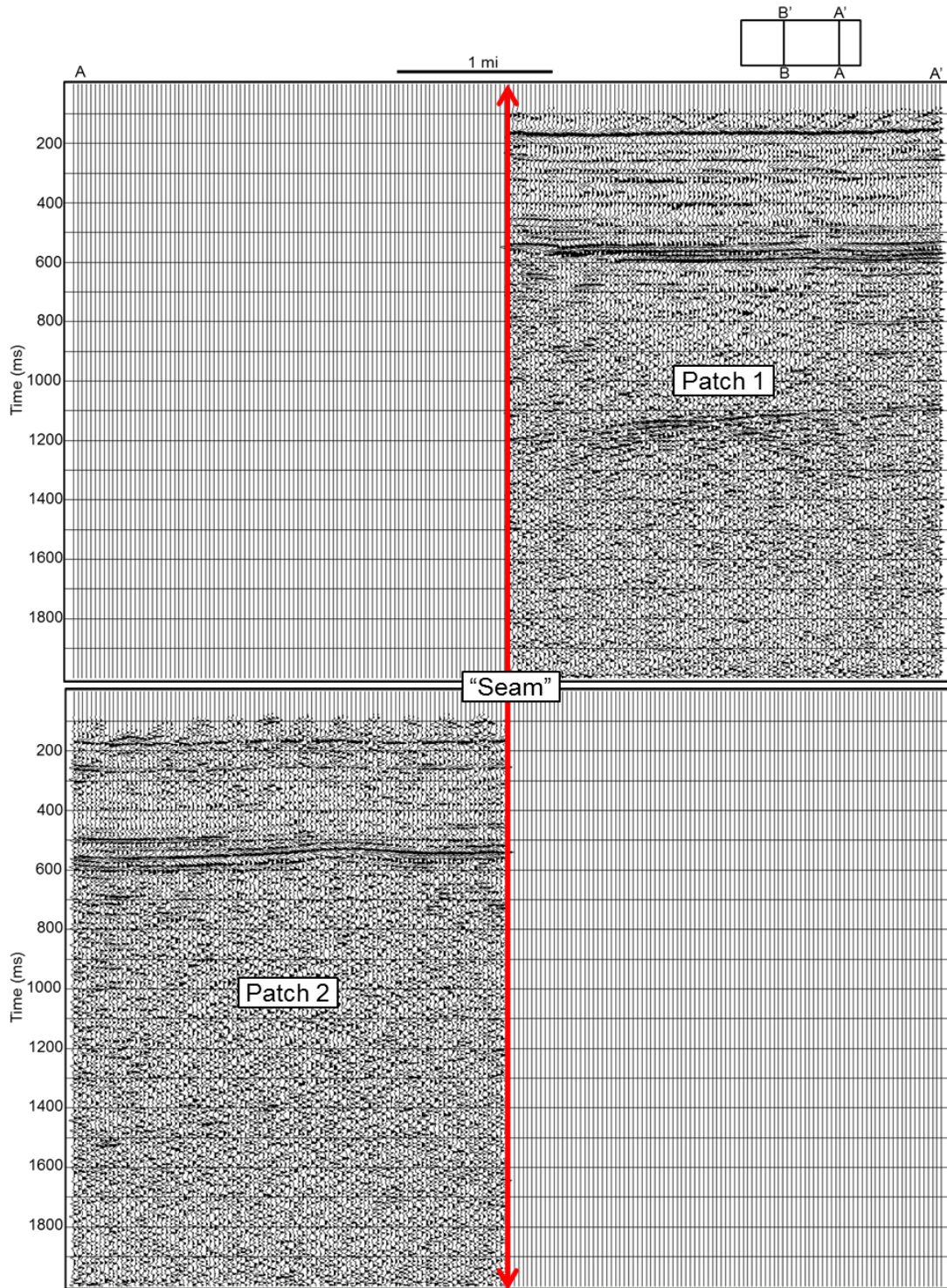
Figure 23: Stack after 80x80 grid velocity analysis divided into patch 1 (above) and patch 2 (below). The red line indicates the "seam" in the middle of the survey that results from the low fold between the two patches.
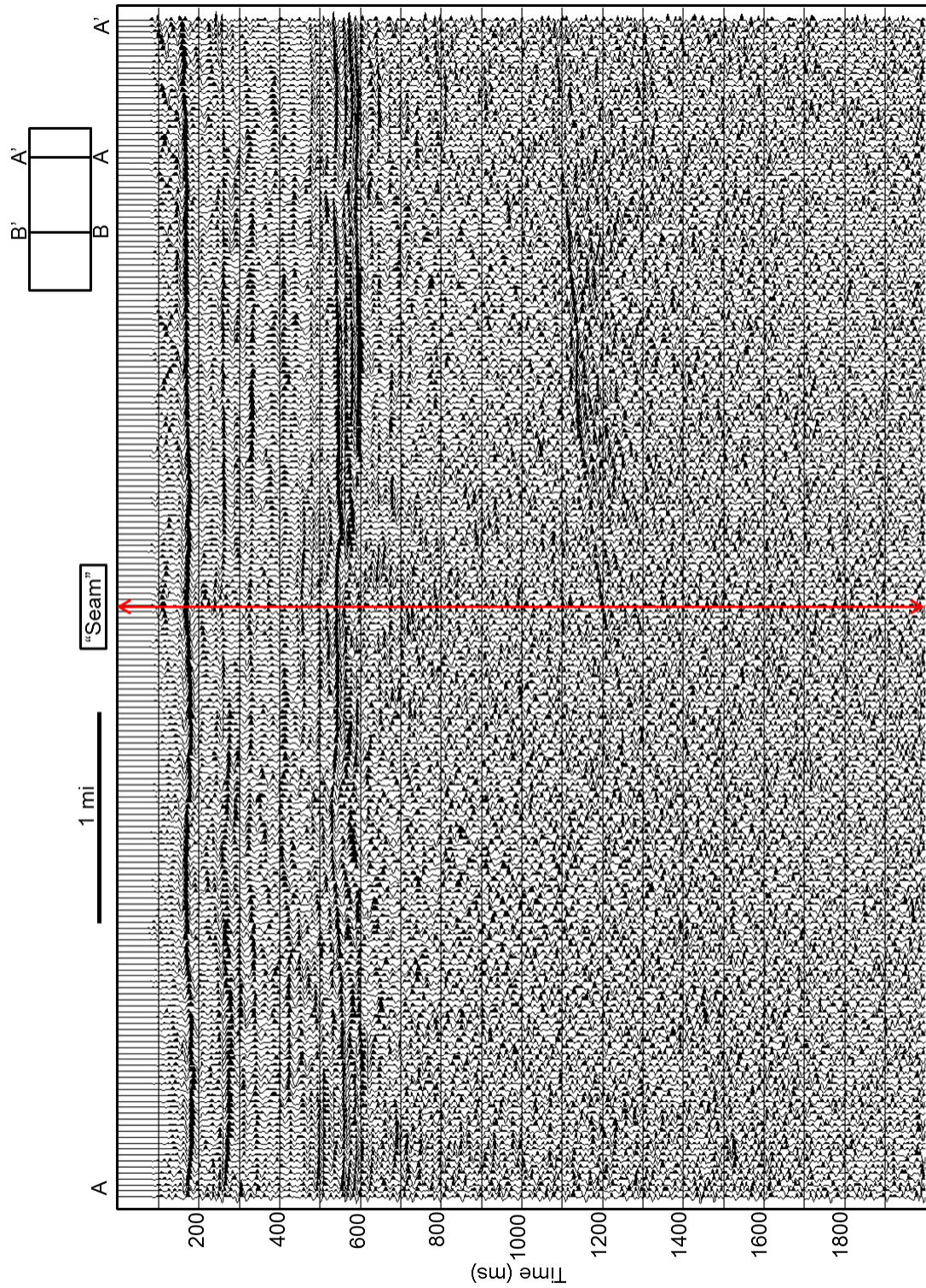
Figure 24: Stack after 80x80 grid velocity analysis with patch 1 phase rotated -50.47 degrees to match patch 2. The phase rotation is applied to gathers prior to stacking.

43

The previous spiking deconvolution facilitated velocity analysis, residual statics, and phase matching, but is suboptimal to surface-consistent deconvolution. I retain the velocity analysis and statics corrections but apply surface consistent deconvolution to the gathers as shown in Figure 10. Figure 25a shows a CMP gather after applying surface-consistent deconvolution and the noise attenuation processes (top mute, air blast attenuation, time-variant spectral whitening, time variant scaling, and bandpass filter). There is a significant reduction in groundroll contamination, and events down to 1200 ms are better resolved across almost all offsets. Figure 25b shows the spectral content of the CMP in Figure 25a. The frequencies are now much flatter throughout and there has been a slight extension of the low frequencies before they roll off.

Once completing the third round of velocity analysis using the 40x40 grid, the surface-consistent deconvolved CMP gathers are written out to SEGY. While the gathers are cleaned up fairly well, application of a prestack structure-oriented filter will further enhance signal and reduce noise and groundroll. The structure-oriented filter works as follows: a stack of the NMO corrected input gathers is used to calculate the dip using a maximum correlation technique. This dip model is then used to guide the filter planes along modeled constant offset gathers. The applied filter is a robust statistics filter with edge preserving properties. After filtering the modeled data, the estimated noise model is adaptively subtracted from the original input gathers. The filtered gathers are imported back into the processing software to continue with the final 20x20

44

velocity analysis and residual statics calculation. The prestack structure-oriented filter vastly improves the data's signal-to-noise ratio (SNR). Groundroll and coherent noise is almost negligible while the actual events, or signal, are very clear. Figure 26a shows a representative CMP gather after applying the filter. Figure 26b shows the spectral content of the data.
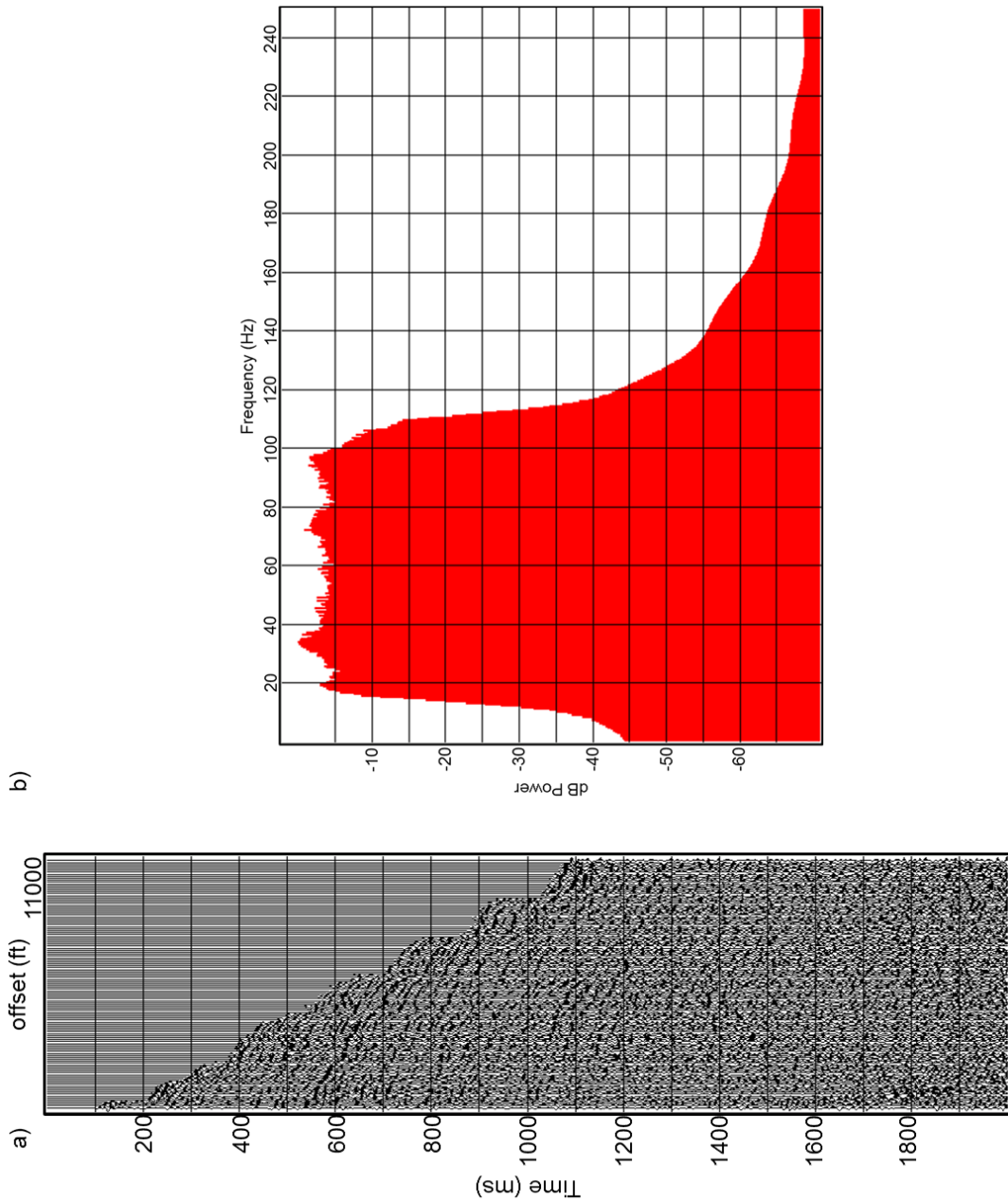
Figure 25: (a) CMP gather after applying surface-consistent deconvolution, air blast attenuation, time-variant spectral whitening, time-variant scaling, and a bandpass filter. Suppression of noise brings out signal almost down to 1200 ms. (b) Spectrum of the CMP gather, which is now quite flat

46
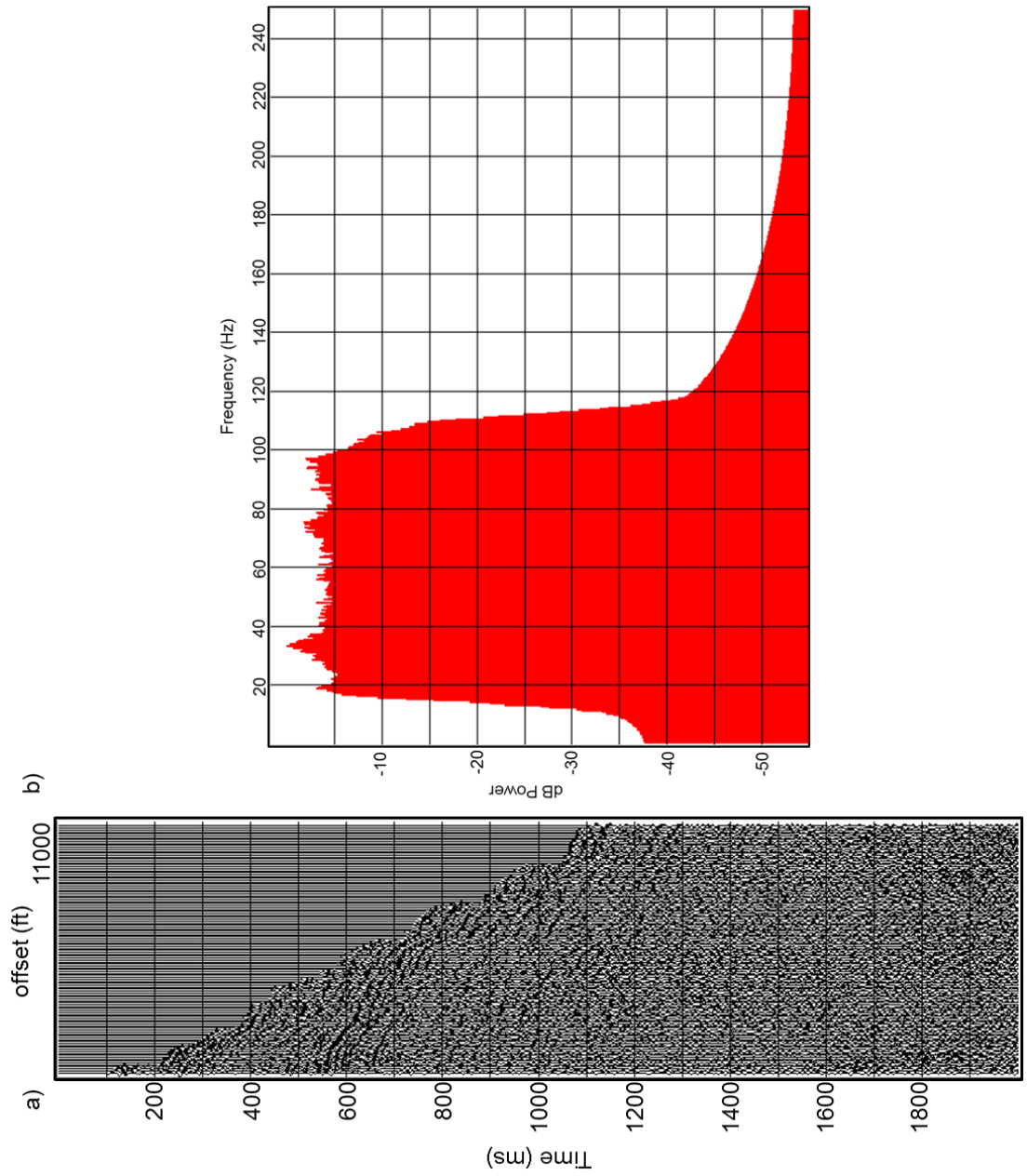
Figure 26: (a) Surface-consistent deconvolved CMP gather after applying a prestack structure-oriented filter. Noise contamination is almost indiscernible. (b) Spectrum of the CMP after applying a prestack structure-oriented filter.

Applying a prestack structure-oriented filter not only removes groundroll and coherent noise; it also improves the semblance calculations for velocity analysis. This enhances velocity picking, increasing both the accuracy of the picks and the number of reflectors resolved. Figure 27 shows a semblance panel from velocity analysis prior to applying the prestack structure-oriented filter, while Figure 28 shows a semblance panel from velocity analysis after applying the filter.

After the 20x20 velocity analysis, the surface-consistent deconvolved gathers with the prestack structure-oriented filter applied are written out as the final gathers. The final velocity field facilitates the application of a 1/distance spherical divergence true amplitude recovery, followed by applying a final time-variant spectral whitening, time-variant scaling, and bandpass filter, using the frequencies 10, 20, 90, and 120 Hz for the corners of both the time-variant spectral whitening and bandpass filter. Figure 29a shows a representative CMP from the final gathers, and the spectral content is shown in Figure 29b. The final velocity field is exported to SEGY, first interpolating it to a 1x1 grid so there is a pick at every CMP, and then smoothing the velocity field at a 3x3 increment. Resampling the velocity field to a 2.0 ms sample interval matches it to the seismic data. Figure 30 shows a line from the final velocity field that for prestack time migration.
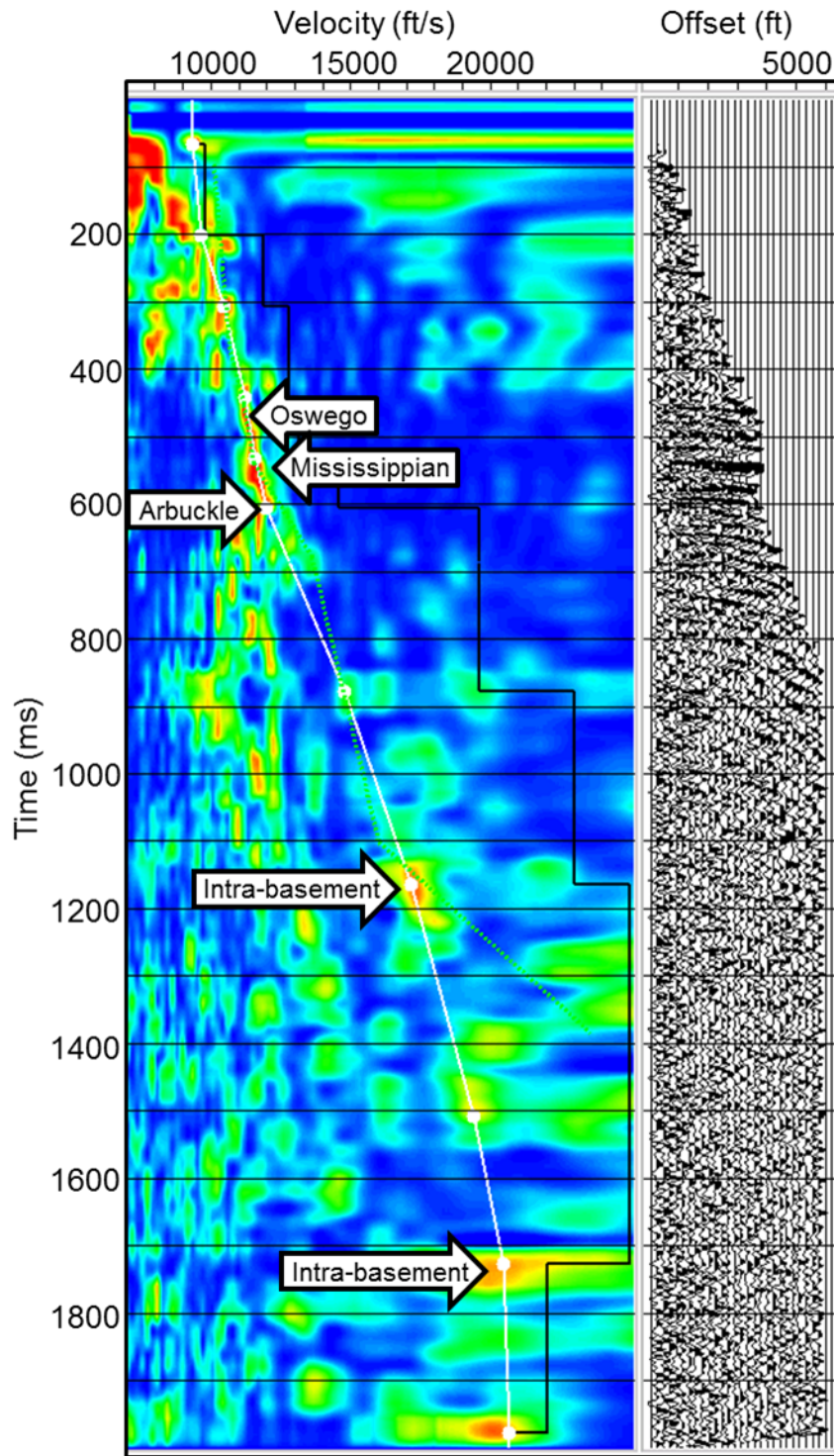
Figure 27: Velocity analysis semblance panel and CMP supergather prior to the application of a prestack structure-oriented filter. I am able to resolve events between 400 and 700 ms fairly well, but noise overwhelms signal outside of this window.
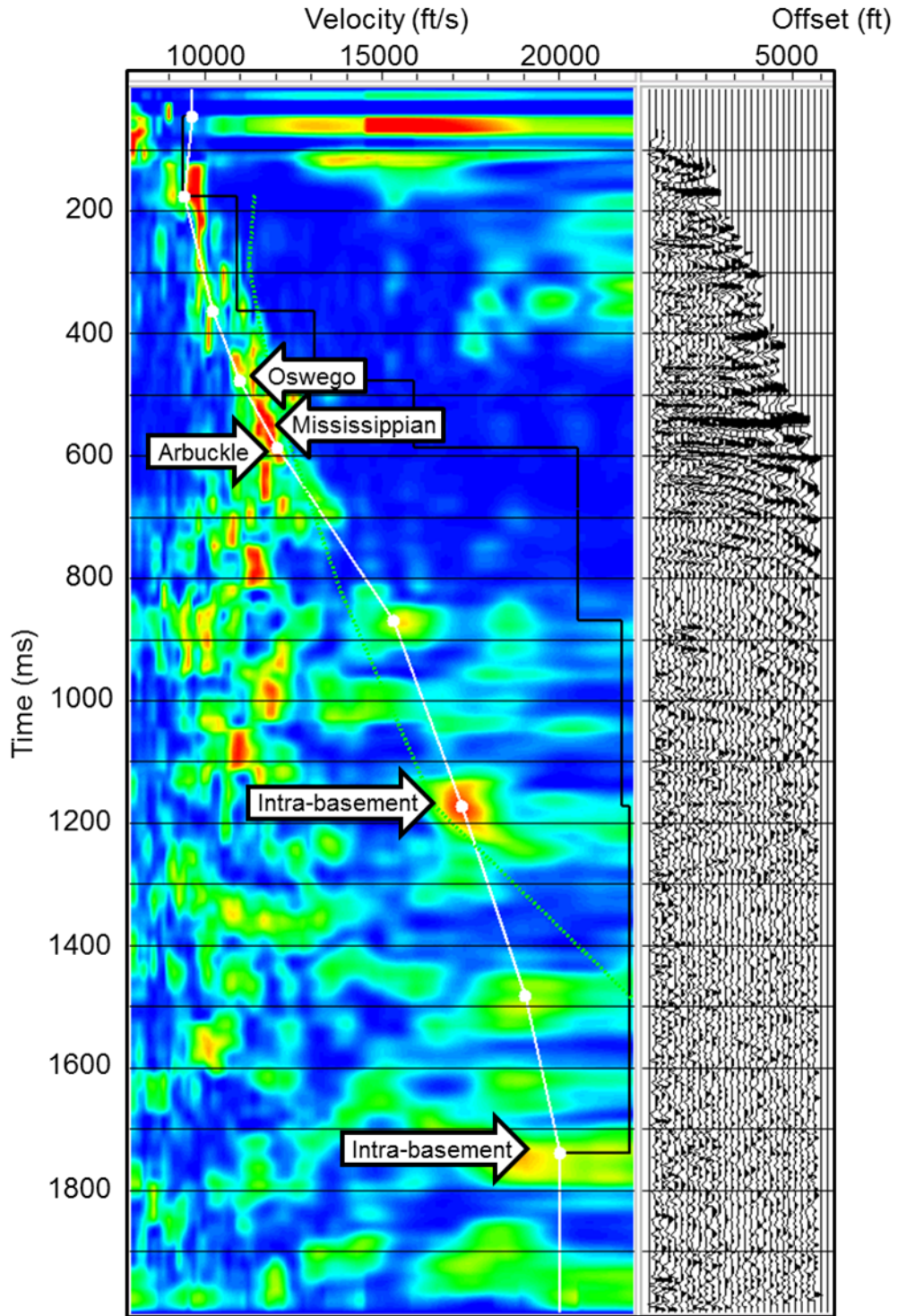
Figure 28: Velocity analysis semblance panel and CMP supergather after applying a prestack structure-oriented filter to the data. Semblance "bullseyes" are clearer and I am able to resolve reflectors from 150 to 700 ms very well. Additionally, basement structure is now more visible with the presence of groundroll drastically reduced.
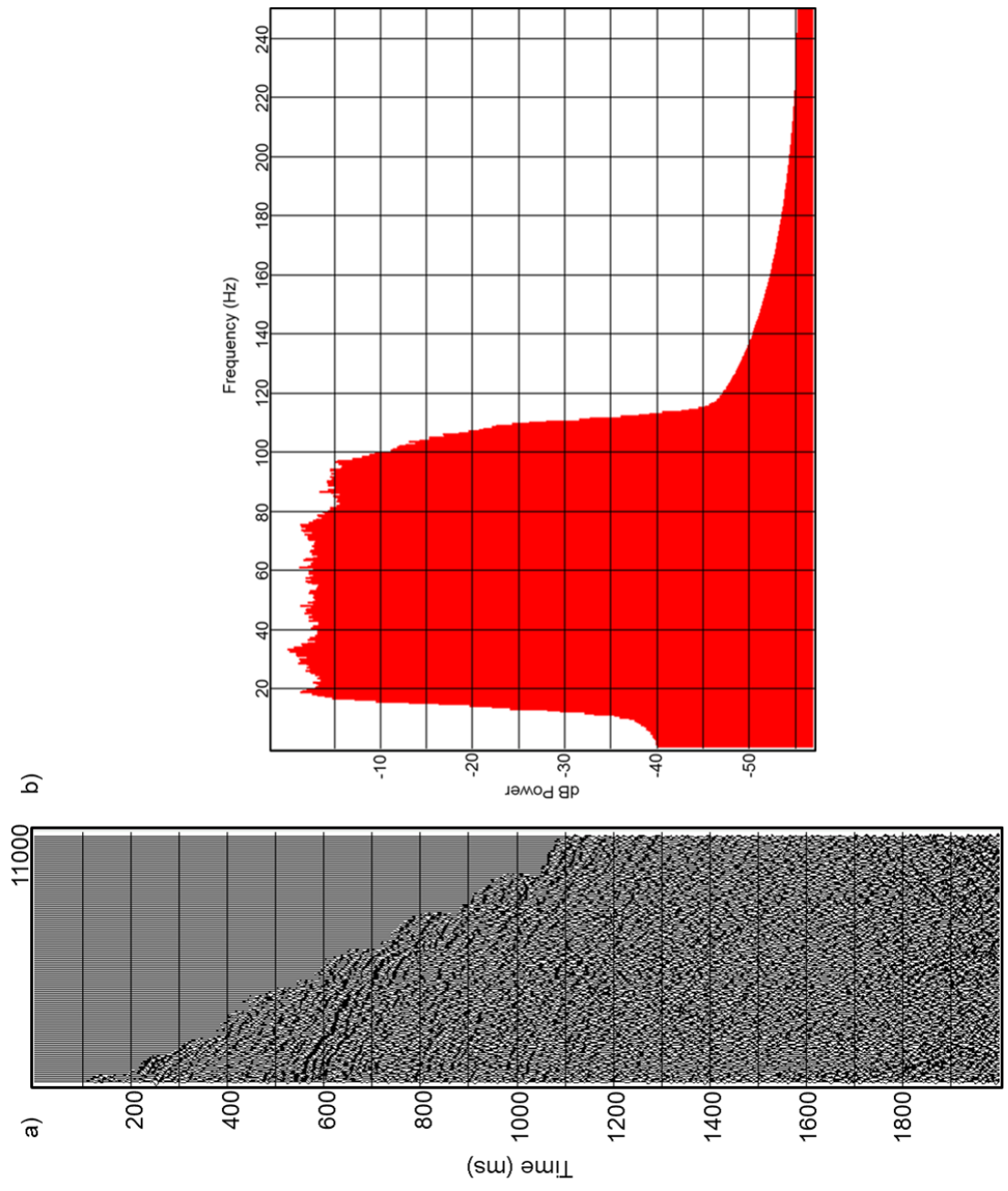
Figure 29: (a) Final gathers for PSTM, and (b) Spectrum of final gathers.
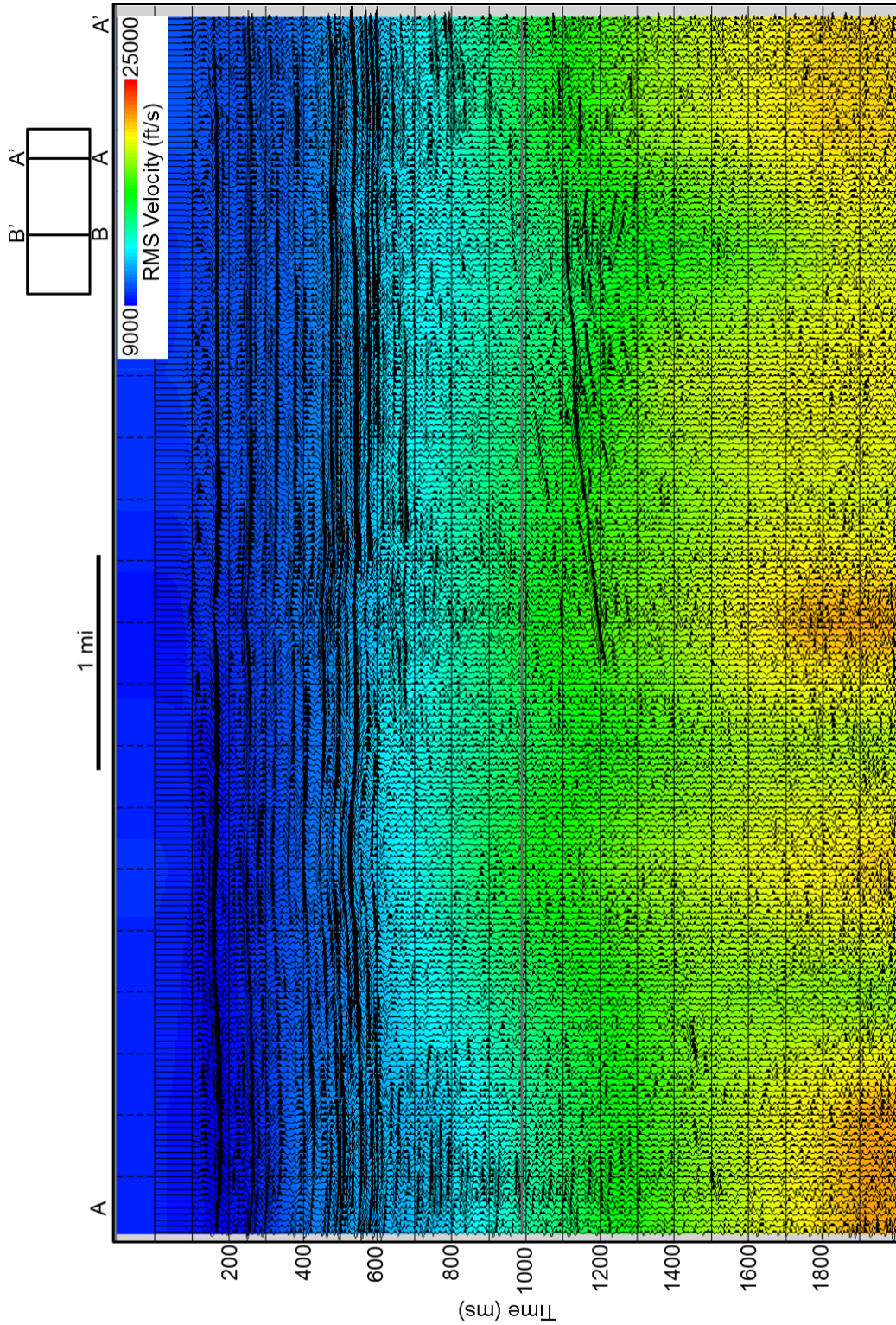
Figure 30: Line AA' through the final RMS velocity field, co-rendered with seismic amplitude. The velocities are interpolated for every CMP from the 20x20 grid, smoothed 3x3, and resampled to 2.0 ms to match the seismic data. This velocity field will be used for PSTM.

52

PRESTACK TIME MIGRATION

Now that the bulk of the processing is complete, the data are ready for migration. Given irregularities in shot and receiver lines (Figure 11) and the smooth lateral variation in velocity (Figure 30), a Kirchhoff prestack time migration (PSTM) algorithm is well suited. PSTM allows for better imaging of subtle discontinuities in an otherwise mostly flat terrain and improves the seismic data's lateral resolution. Kirchhoff algorithms use diffraction imaging and summing to locate properly an event in the subsurface.

This particular Kirchhoff PSTM algorithm has the ability to bin both offsets and azimuths. For this migration, only a single azimuth bin and 60 offset bins are selected, setting the maximum offset at 3048 m (10,000 ft) which will result in incident angles of greater than 45° at my target depth of approximately 910 m (3000 ft), illustrated in Figure 31. The high angle offsets allow inversion for densities. The migration aperture is 3048 m (10,000 ft). By applying time-variant scaling during processing, the data must be scaled by t^{-1} (t = time) because the migration code expects the amplitudes to decay by t^{-1}. Figure 32 shows the same CMP gather shown in Figure 16 after migration.

Migration moves the data laterally as well as vertically, and thus usually needs a slightly different velocity. Therefore, using a reverse NMO algorithm with the migration velocities unflattens the gathers, followed by picking new velocities on a 20x20 grid using the migrated, un-flattened gathers. Using the new velocities, an NMO correction is applied to the gathers with a 50% stretch mute to retain as many of the far offsets as possible. Following NMO is a final

prestack structure-oriented filter and spectral whitening. Figure 33 shows a final common reflection point (CRP) gather after applying NMO with the new velocity field and the final prestack structure-oriented filter and spectral whitening.

$$\theta = \arctan\left(\frac{5000}{3000}\right) = 78°$$
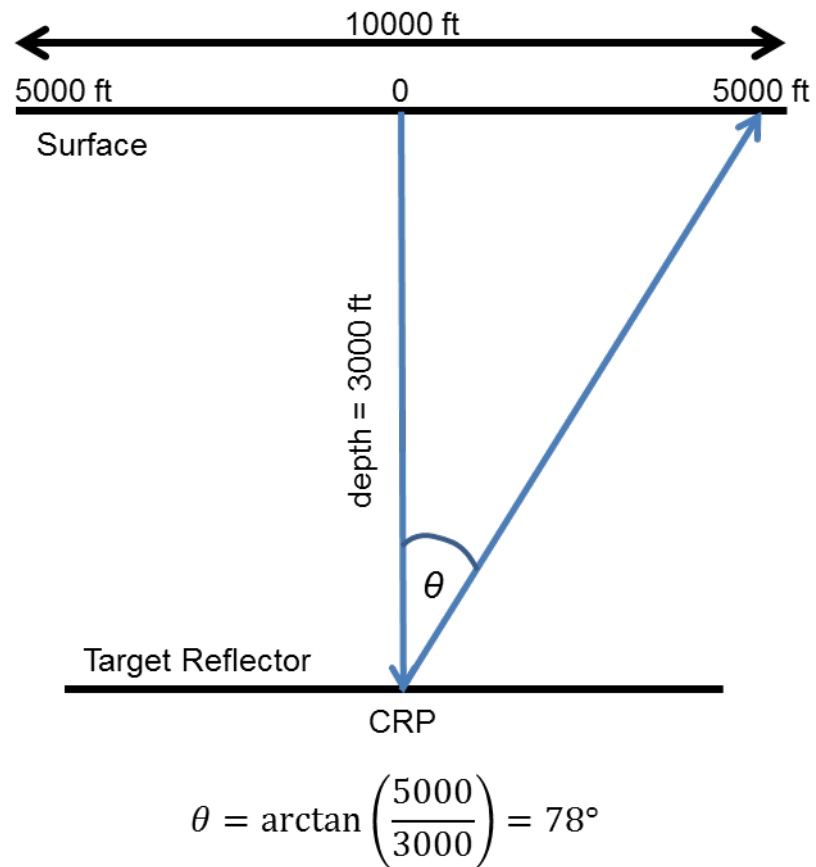
Figure 31: Illustration showing that with a maximum offset of 10,000 ft for migration and a target depth of 3000 ft, I can recover greater than 45° incident angle, allowing me to invert for densities in addition to Z_P and Z_S.
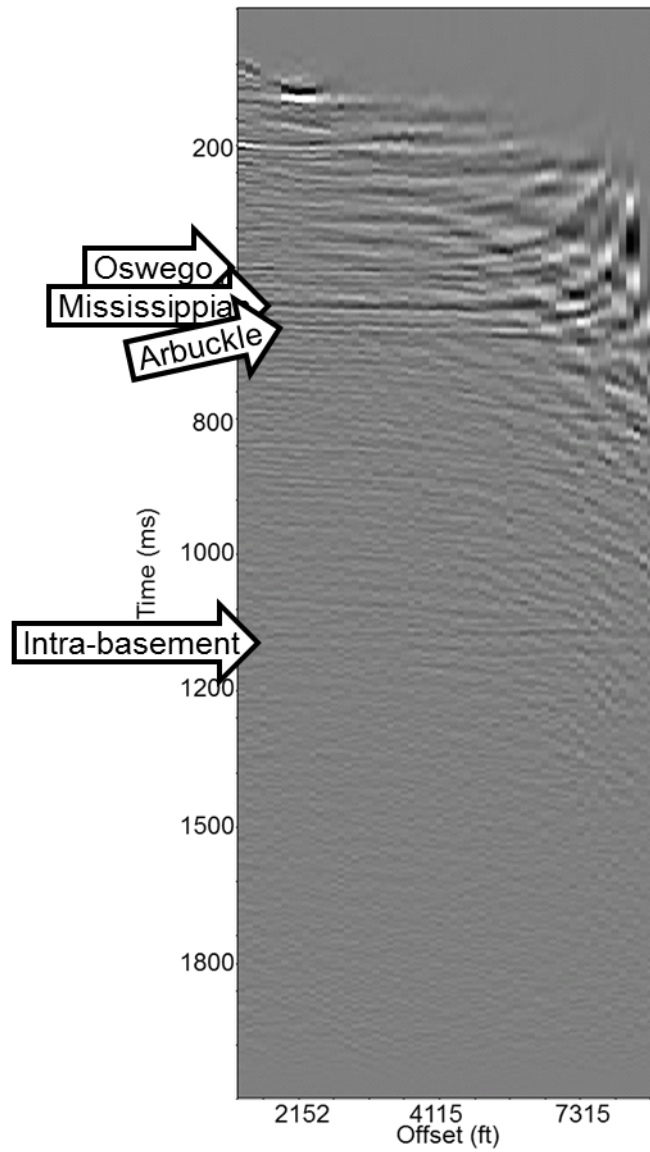
Figure 32: CMP gather after Kirchhoff PSTM using 60 offset bins and 1 azimuth bin, and an emergence angle of 60 degrees.
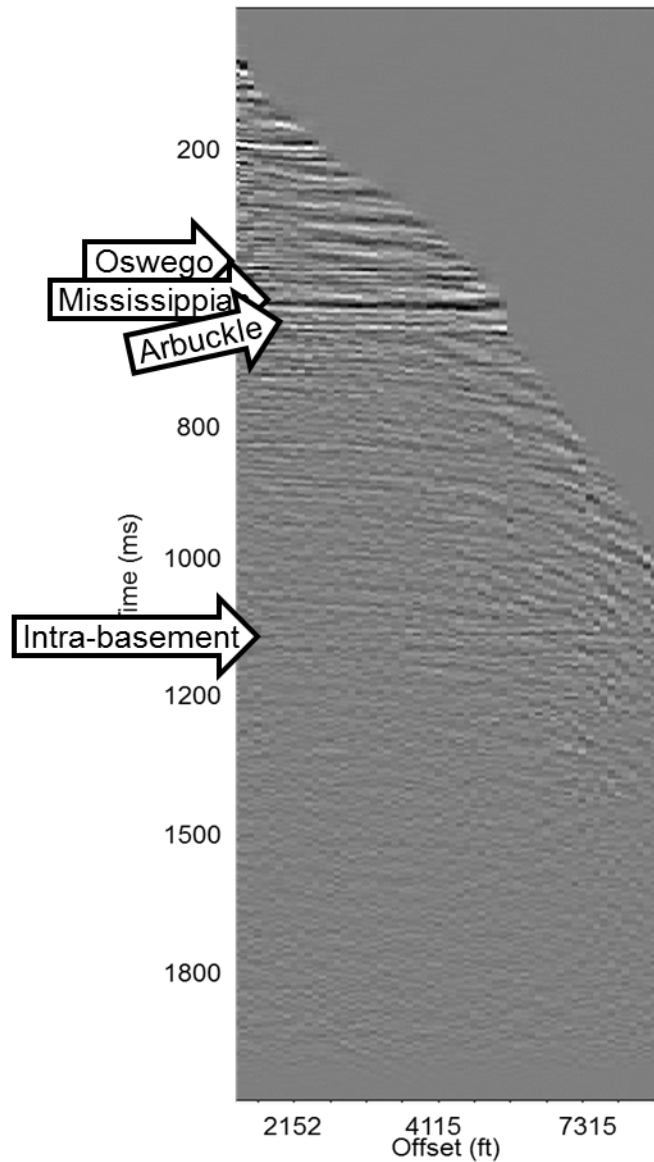
Figure 33: Migrated gathers after reverse NMO, picking new velocities, applying an NMO correction with a 50% stretch mute to retain as many far offsets as possible, and a final prestack structure-oriented filter and spectral whitening.

COMPARISON WITH VENDOR-PROCESSED DATA

A significant advantage of reprocessing is access to the previous images and therefore insight into not only the geologic objective but also limitations of the previously used processing workflow (such as acquisition footprint). Figure 34a shows line AA' from the vendor provided stack. From the EBCDIC header, the vendor's processing history includes the application of refraction and elevation statics, PSTM, time-variant scaling, a 14/112 Hz bandpass filter, and FX deconvolution. The spectra of the vendor's processed data is shown in Figure 34b. After 70 Hz, the frequencies begin to fall off, decreasing by more than 5 dB by 100 Hz.

For comparison, vertical line AA' through the stack of the reprocessed data after PSTM, new velocities, NMO, prestack structure-oriented filtering and spectral whitening is shown in Figure 35a. Note that the reflectors are not only more continuous but exhibit higher bandwidth as well. Additionally, by avoiding FX deconvolution, the sub 700 ms basement structure resolves better and is more believable. FX deconvolution has over-smoothed these reflectors resulting in the wormy appearance of the basement in the vendor's stack section, and also reduces some of the higher frequency content. Figure 35b, shows the spectrum of the final reprocessed stack section. The spectrum is much flatter and retains the higher frequencies better than the vendor's retains.
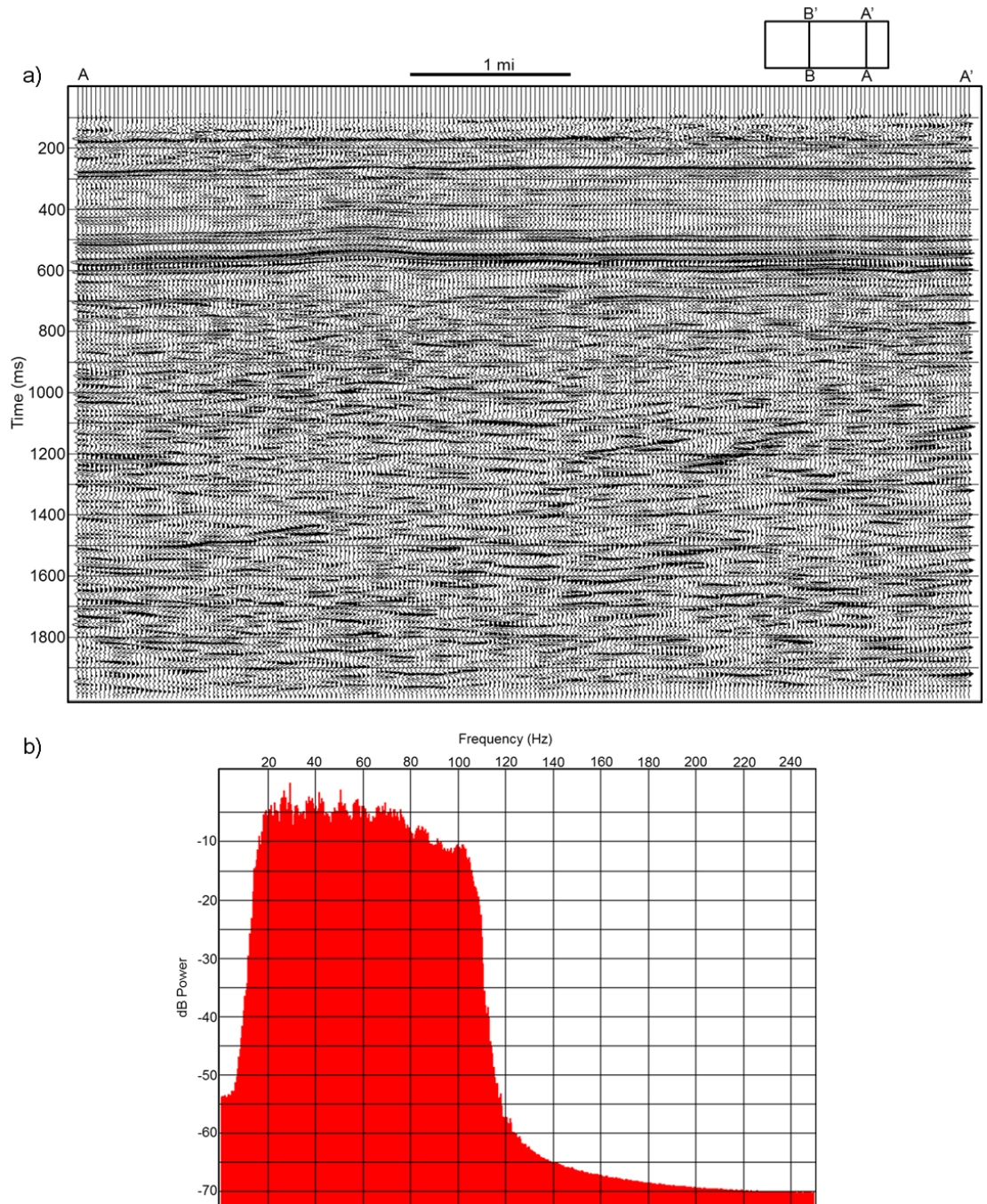
Figure 34: (a) Line AA' through the previous vendor supplied migrated data volume. The target zone between 500 and 600 ms does not show as many reflectors or as high of frequency. The sub 700 ms basement is wormy in appearance due to FX deconvolution, which masks the basement structure. (b) the spectrum of the vendor supplied migrated data volume. The frequencies begin to roll off around 70.
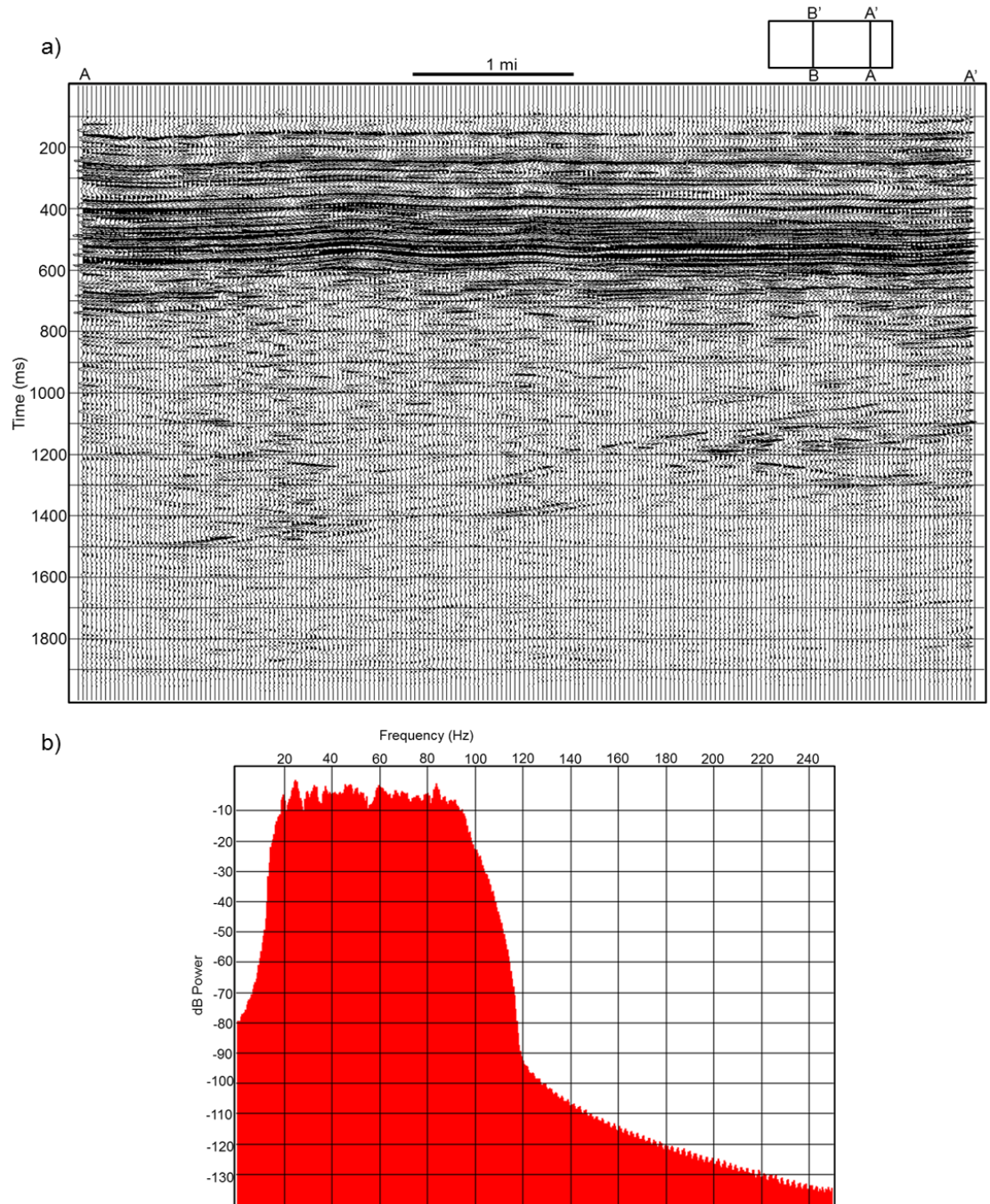
Figure 35: (a) Final stack section after PSTM, residual velocity analysis, NMO, prestack structure-oriented filtering and spectral whitening. More reflectors are resolved and the basement structure is more apparent. (b) Spectrum of the final stack section after PSTM and residual velocity analysis. The spectrum is flatter and better preserves the high frequencies.

Figure 36 shows a time slice of coherence through the vendor's data at the approximate Arbuckle level at t = 560 ms, which is compared to a time slice of coherence through the final reprocessed data in Figure 37. Coherence is useful in comparing the resolution of the two volumes. Counter-intuitively, better resolution will result in more incoherence because the subtle features of the seismic are better resolved. The subtleties are better imaged in the reprocessed volume, especially in the northeast corner. However, the linear east-west trend in the center of the reprocessed volume is likely the effect of the seam between the two patches.
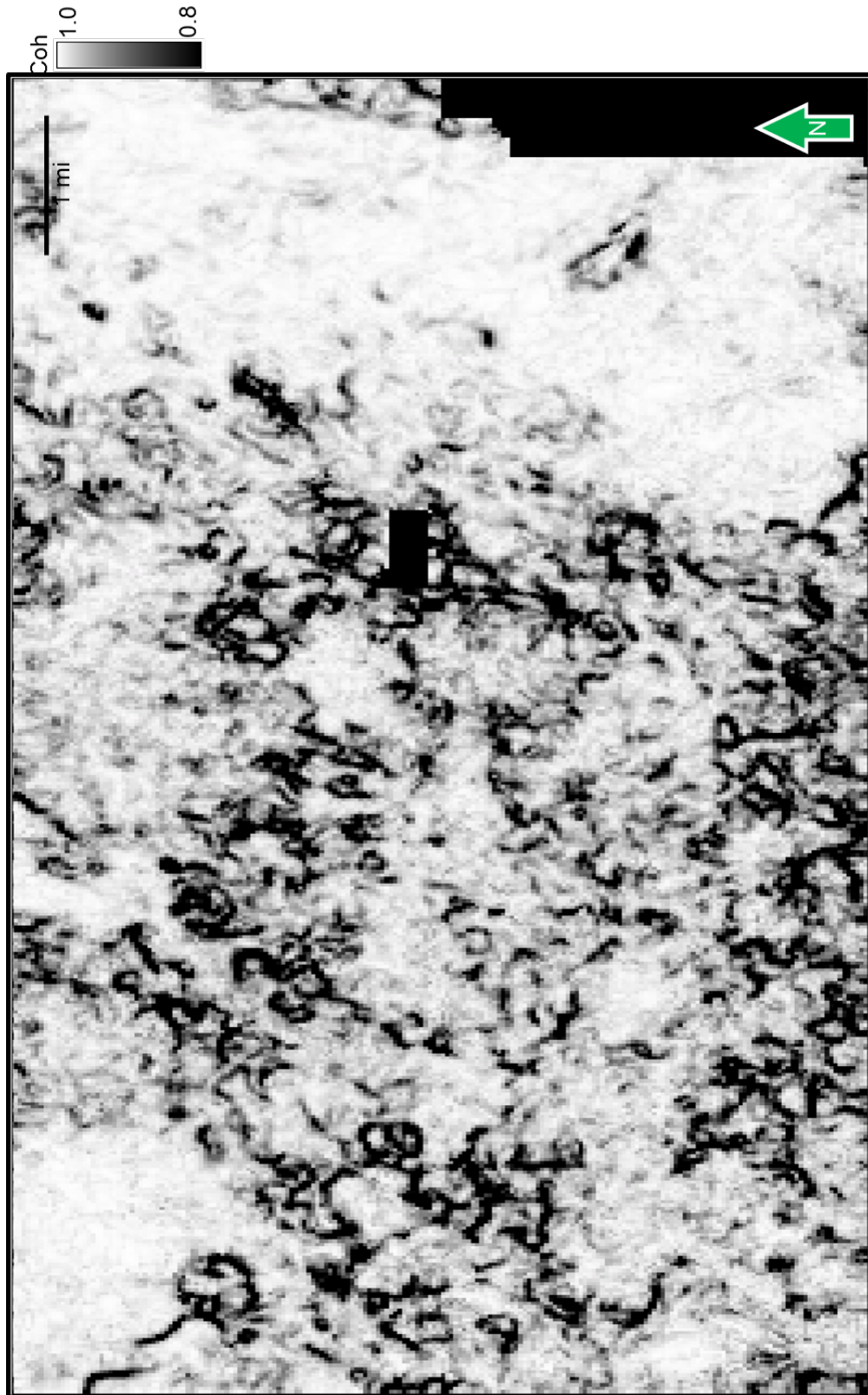
Figure 36: Coherence time slice (t=560 ms) through the vendor's processed data at the approximate Arbuckle level.

Figure 37: Coherence time slice (t=560 ms) through my final stack section at the approximate Arbuckle level.

CHAPTER 4: ATTRIBUTE CHARACTERIZATION OF A

MISSISSIPPI LIME SURVEY

THEORY

The P-wave velocity, V_P, of sound in a linearly elastic media is:

$$V_P = \sqrt{\frac{\lambda + 2\mu}{\rho}},$$ (4.1)

where λ is the incompressibility, μ is the shear modulus, and ρ is the density of the rock. Together, λ and μ are the Lamé parameters in linear elasticity. The first parameter, λ, is often called the incompressibility and is sensitive to pore fluids. The second parameter, μ, is often called the rigidity of the rock and is unaffected by any present fluids as shear stress is not supported by fluids or gases. Similarly, the S-wave velocity, V_S, is:

$$V_S = \sqrt{\frac{\mu}{\rho}},$$ (4.2)

indicating that V_S is not sensitive to pore fluids but instead to the rock matrix.

The P-Impedance, Z_P, is:

$$Z_P = \rho V_P,$$ (4.3)

where ρ is the density of the rock and V_P is the P-wave velocity. Impedance contrasts between layers in the Earth allow us to record seismic reflections and is the basis for defining reflection coefficients. The S-Impedance, Z_S, is:

$$Z_S = \rho V_S,$$ (4.4)

where again ρ is the density of the rock and V_S is the S-wave velocity. Both Z_P and Z_S are sensitive to changes in lithology; however, Z_S is not sensitive to changes in pore fluid.

Goodway et al. (1997) proposed that by rearranging the equations for V_P and V_S in terms of λ and μ and scaling by ρ, the orthogonal Lamé parameters can be extracted from logs or seismic data via the impedance equations. Rearranging equation 4.1 to solve for λ and equation 4.2 to solve for μ gives:

$$\lambda = V_P^2 \rho - 2\mu, \tag{4.5}$$

$$\mu = V_S^2 \rho, \tag{4.6}$$

while equation 4.5 is reduced to:

$$\lambda = V_P^2 \rho - 2V_S^2 \rho, \tag{4.7}$$

expressing λ and μ in terms of P- and S-wave velocity and density. Multiplying equations 4.6 and 4.7 by ρ allows λ and μ to be expressed in terms of Z_P and Z_S, which are both easily extracted from well logs and prestack seismic data. This gives the attributes $\lambda\rho$ and $\mu\rho$, defined as:

$$\lambda\rho = Z_P^2 - 2Z_S^2, \tag{4.8}$$

$$\mu\rho = Z_S^2, \tag{4.9}$$

and allow us to better extract rock properties from 3D prestack seismic data using elastic parameters directly linked to the rock's bulk and shear moduli (Goodway et al., 1997). Additionally, Poisson's ratio (σ), the ratio of transverse to axial strain when a material is compressed, can be derived using Z_P and Z_S:

$$\sigma = \frac{1}{2}\frac{(\frac{Z_P}{Z_S})^2 - 2}{(\frac{Z_P}{Z_S})^2 - 1},$$ (4.10)

and by using this relationship, deriving a Poisson's ratio volume using the P- and S-Impedance volumes is straightforward.

Generating several surface seismic attributes to aids interpretation. Coherence is an edge-detection attribute and measures the similarity between neighboring waveforms. When neighboring traces are very similar, the data exhibit high coherence, which is an indication that there is a low amount of lateral and vertical variations in the seismic data. If the neighboring traces are not similar, the data exhibit low coherence, and in the absence of strong acquisition footprint contamination can be useful for interpreting structural discontinuities. In particular, I use the energy-ratio similarity for computing coherence. Energy-ratio similarity is computed along structure and uses the analytic trace (the original data and its Hilbert transform or quadrature) in the computation (Chopra and Marfurt, 2007). Numerically, it is the ratio of the energy of the Karhunen-Loeve filtered data over the total (unfiltered) energy of the input data within an analysis window (Chopra and Marfurt, 2007). In carbonate terrains, circular features that exhibit low coherence commonly correspond to karst collapse or karst tower features. More linear features detected by coherence attributes commonly correspond with faults. Channel edges often give rise to meandering features.

Curvature is a mathematical measure of a quadratic surface's deviation from a plane and can be useful for interpreting structure in 3D seismic data. In 2D curvature is computed by fitting a circle to a curved region such that:

$$\kappa = \frac{1}{R},\tag{4.11}$$

where R is the radius of the circle which fits the curved surface. In 3D, any quadratic surface can be described by two orthogonal "principal" curvatures. k_1, called the most-positive principal curvature is the larger of the two in signed value and describes ridge-like structures.. k_2, the most-negative principal curvature, describes valley-like structures. Most-positive and most-negative implies there is no other apparent curvature that is more positive than k_1 or more negative than k_2. While both k_1 and k_2 can have positive values (for a dome) or negative values (for a bowl), k_1 is always greater than or equal to k_2. Of particular interest to my work are experiments conducted by Staples (2011) and White (2013) which show a direct relationship between curvature and fractures, indicating that curvature extracted from 3D seismic data can be used as a proxy for fracture detection.

PETROPHYSICAL PROPERTIES

Snyder et al. (2013) present a characteristic type log for the tripolitic chert versus the tight limestone and tight chert, which is shown in Figure 38. The type log comes from a well that penetrates the Highway 60 East Hardy tripolitic chert trend in western Osage County. Compared to the tight limestone and tight chert that accounts for most of the Mississippian section, tripolitic chert shows low density, low resistivity, and low gamma ray.
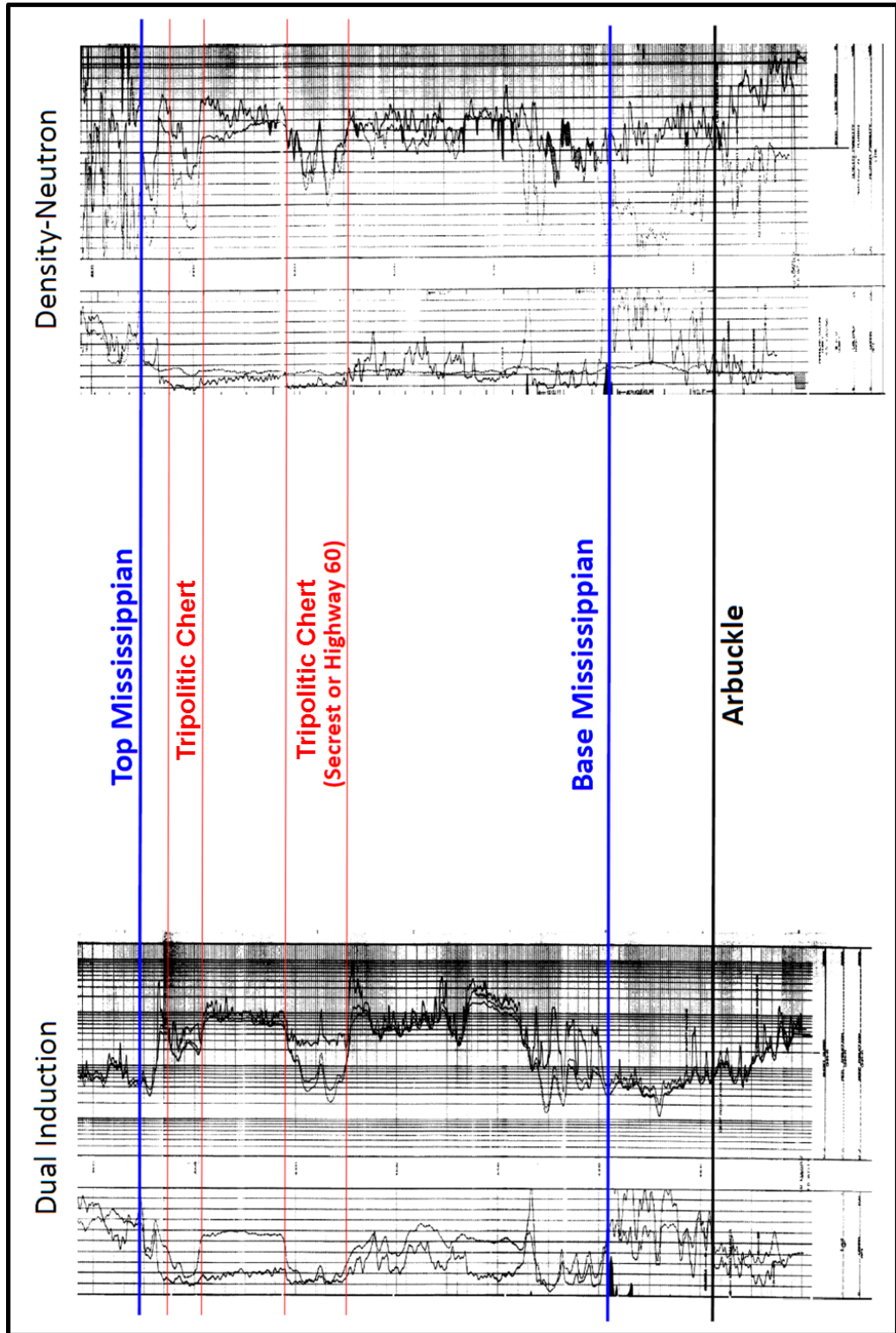
Figure 38: Type log showing the response of tripolitic chert and tight limestone and tight chert. The left set of logs is gamma ray and induction (resistivity), and the right set of logs is gamma ray and neutron density.

Matson (2013) defines three unique intervals in the Mississippian section of Osage County near the study area. "Osage A" is encountered at the top of the Mississippian, lying unconformably beneath the Pennsylvanian Cherokee Shale, and is characterized as siliceous limestone with high susceptibility for diagenetic alteration to tripolitic chert. "Osage B" occurs both with and below "Osage A" and contains interbedded tight, highly fractured limestone and tight nonporous chert, having low potential of diagenetic alteration. The St. Joe Limestone (Kinderhookian) lies below "Osage B" and consists of limestone, showing some dolomitization, and is a chert free interval.

Figure 39 shows the log response at "Well B" through the Mississippian, which is used for prestack inversion. The top section, colored in blue, is characteristic of "Osage A". The middle section, colored in brown, is characteristic of "Osage B". The lower section, colored in green, is characteristic of the St. Joe Limestone. The caliper track shows significant washout issues at the top of the Mississippian, as well as several more throughout the section. Therefore, the logs required some editing, which included outlier cleaning and despiking, linear interpolation and splining if required, and the application of a Gaussian smoother. Figure 40 shows the log editing workflow.
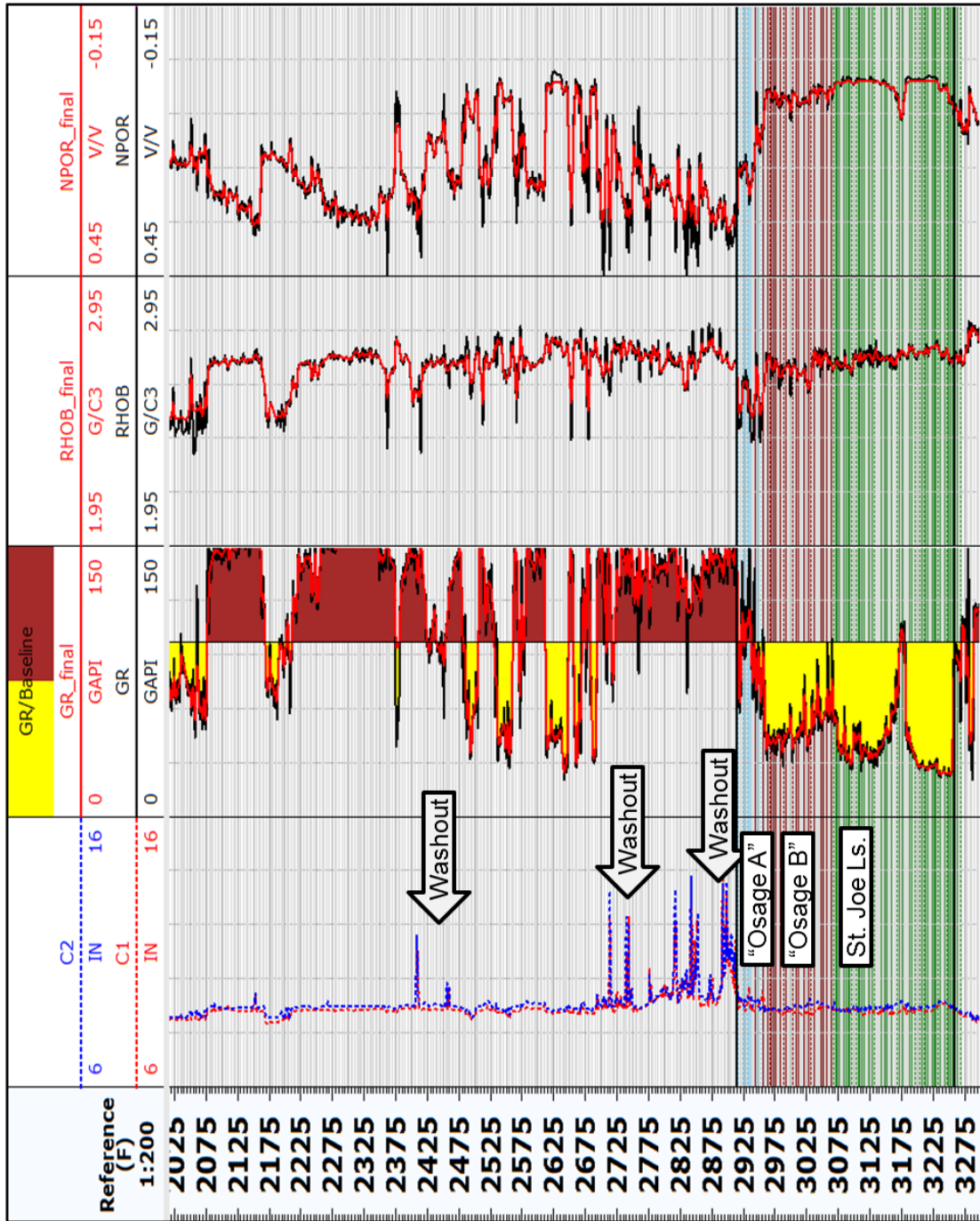
Figure 39: Selected logs at "Well B" before (black) and after (red) log editing. The dual calipers in track 1 (left) show significant borehole washout problems, indicated by arrows. The Mississippian starts at approximately 888.5 m (2915 ft) and extends to approximately 990.6 m (3250 ft), for a thickness of approximately 102.1 m (335 ft). "Osage A" is colored in blue, "Osage B" in brown, and the St. Joe Limestone in green.
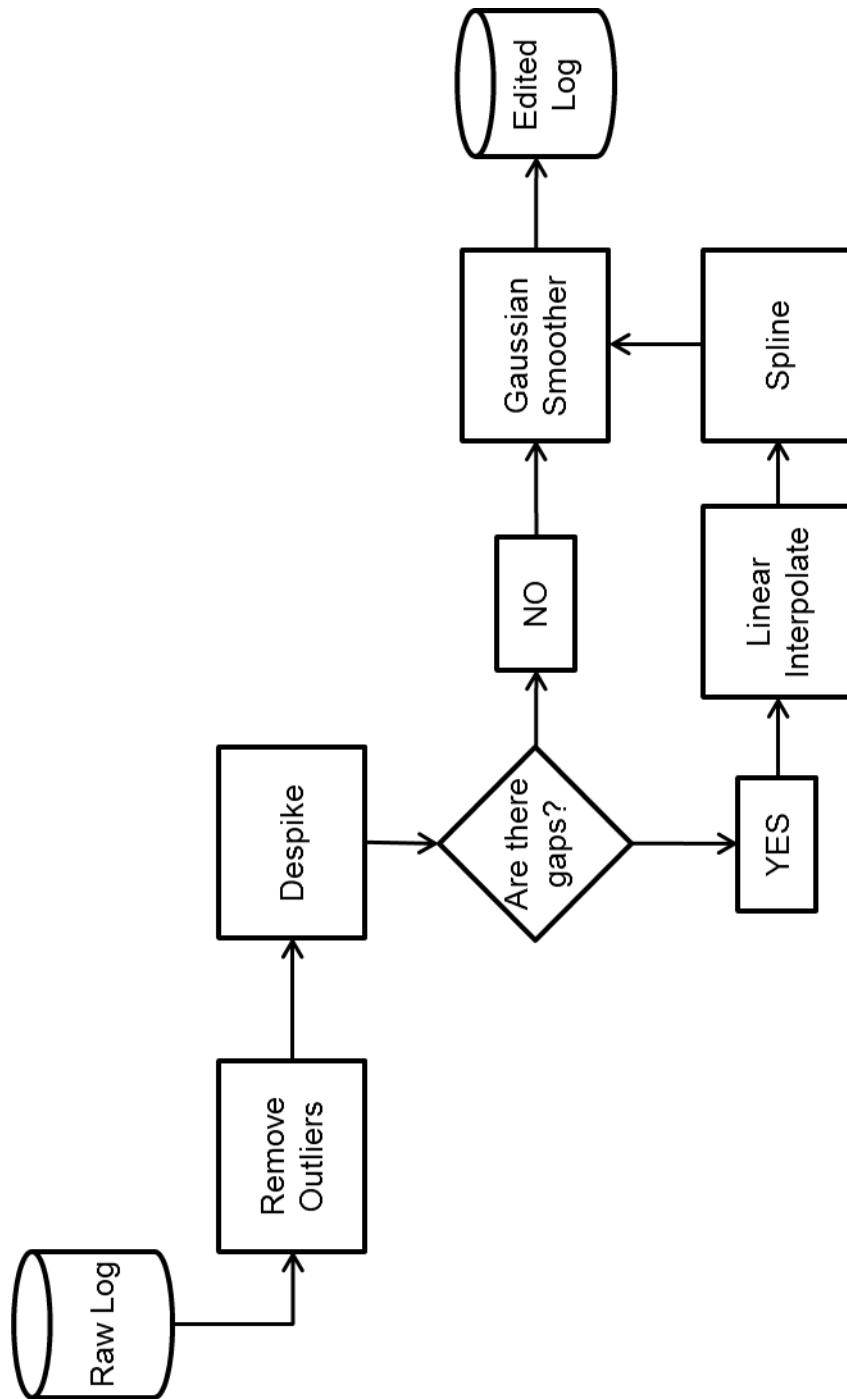
Figure 40: Workflow used to edit logs.

Total porosity (PHIT), which includes secondary porosity such as fractures, and the density of the apparent matrix (RHOMAA) are calculated using bulk density (RHOB) and enhanced thermal neutron porosity (NPOR). P- and S-Impedance (Z_P and Z_S, respectively), lambda-rho and mu-rho ($\lambda\rho$ and $\mu\rho$, respectively), and V_P/V_S are calculated using the P- and S-wave sonic logs and bulk density log. The volumetric photoelectric factor of the apparent matrix (UMAA) is derived using RHOMAA and the photoelectric factor (PEF) log, which is sensitive to changes in mineralogy. Figure 41 shows log responses at "Well B" after editing and deriving the previously mentioned properties.

RHOMAA values for "Osage A" are higher than bulk density (RHOB) values for two reasons: first, RHOMAA measures only the density of the matrix and discounts any porosity or fluid effect, and second, the matrix is highly silicified and exhibits densities close to quartz. RHOMAA values for "Osage B" and the St. Joe do not vary as much for two reasons: first, porosity, both primary and secondary, in these two intervals is much less than observed in "Osage A", so the porosity and fluid effect is not as pronounced on bulk density (RHOB) measurements, and second, because these intervals are much less silicified, the rock matrix is much less altered. Zhao (2011) observes similar results comparing bulk density to rock matrix density from core plug measurements made on core from the a well which is a township north and a range east of "Well B" in Osage County.
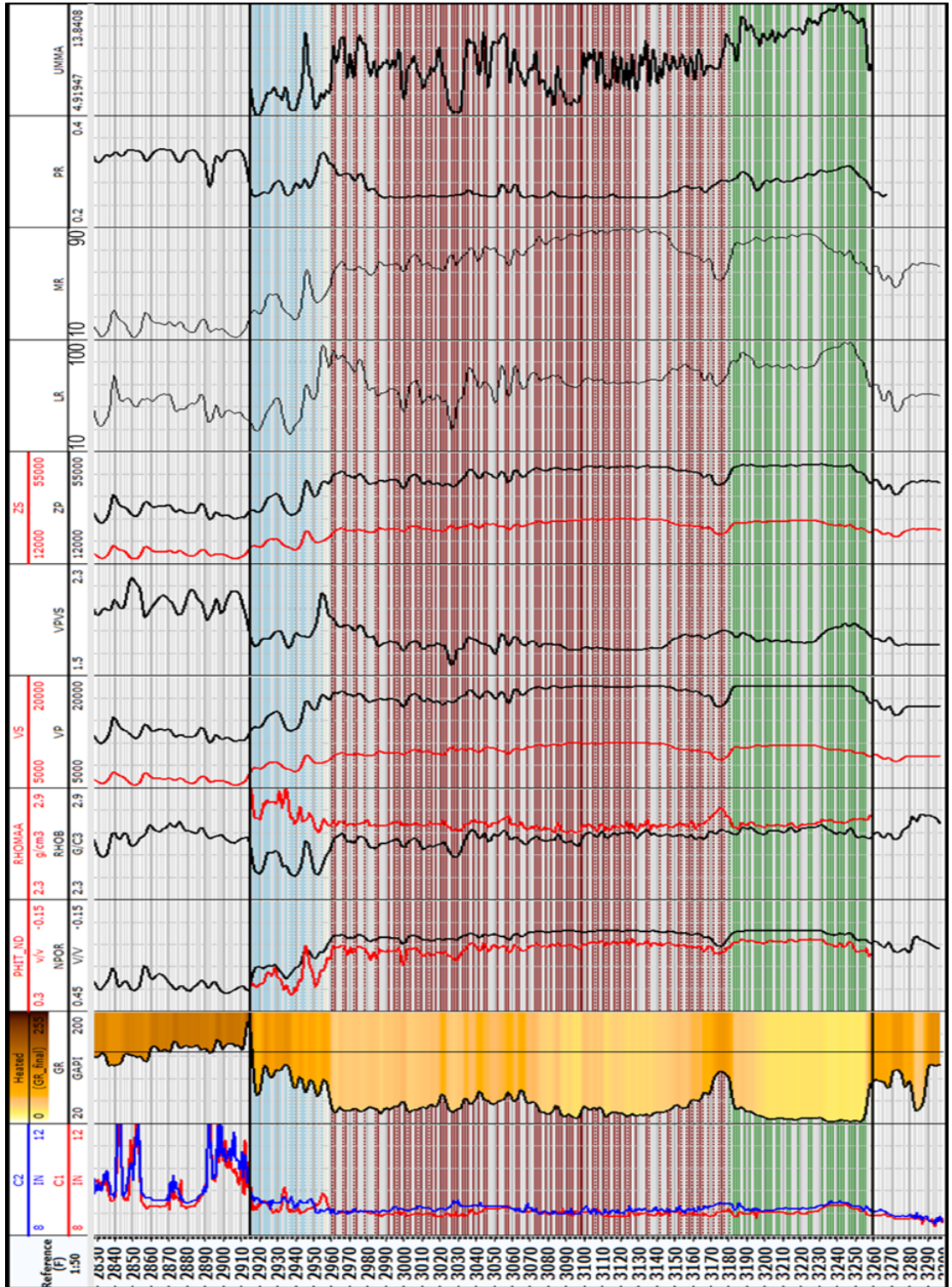
Figure 41: Log response at "Well B" after edits and calculating PHIT, RHOMAA, V_P/V_S, Z_P, Z_S, $\lambda\rho$, $\mu\rho$, and UMAA. Density is the best discriminator for tripolitic chert/"Osage A"-type silicified limestone. "Osage A" is colored in blue, "Osage B" in brown, and the St. Joe Limestone in green.

Figure 42 shows a crossplot of RHOB versus NPOR through the Mississippian section. The St. Joe Limestone (in green) plots mostly along the limestone line. "Osage B" (in brown), which consists of interbedded limestone and chert, plots between the limestone and sandstone lines. "Osage A" (in blue), which is expected to plot near the sandstone line due to its highly siliceous content, plots between the limestone and dolomite lines. However, "Osage A" also exhibits the highest porosities and lowest densities of the three intervals in the Mississippian.

Figure 43 shows a crossplot of RHOMAA versus UMAA, both of which contain information about the apparent rock matrix. The St. Joe (in green) plots near the calcite corner, as expected. "Osage B" (in brown) plots between the quartz and calcite corners along the bottom edge, also as expected. "Osage A" (in blue) now plots well into the quartz region, which confirms that the rock matrix of this section is very silica rich. Therefore, in the previous figure, "Osage A" is plotting erroneously most likely due to borehole washout problems, which affect RHOB measurements.

Figure 44 shows a crossplot of Z_P versus PHIT through the Mississippian, while Figure 45 shows a crossplot of Z_S versus PHIT. "Osage A" clearly separates from "Osage B" and the St. Joe Limestone in both plots. "Osage A", which contains tripolitic chert, shows the lowest impedance and highest porosities, confirming the hypothesis that as porosity increases, impedance decreases.

73
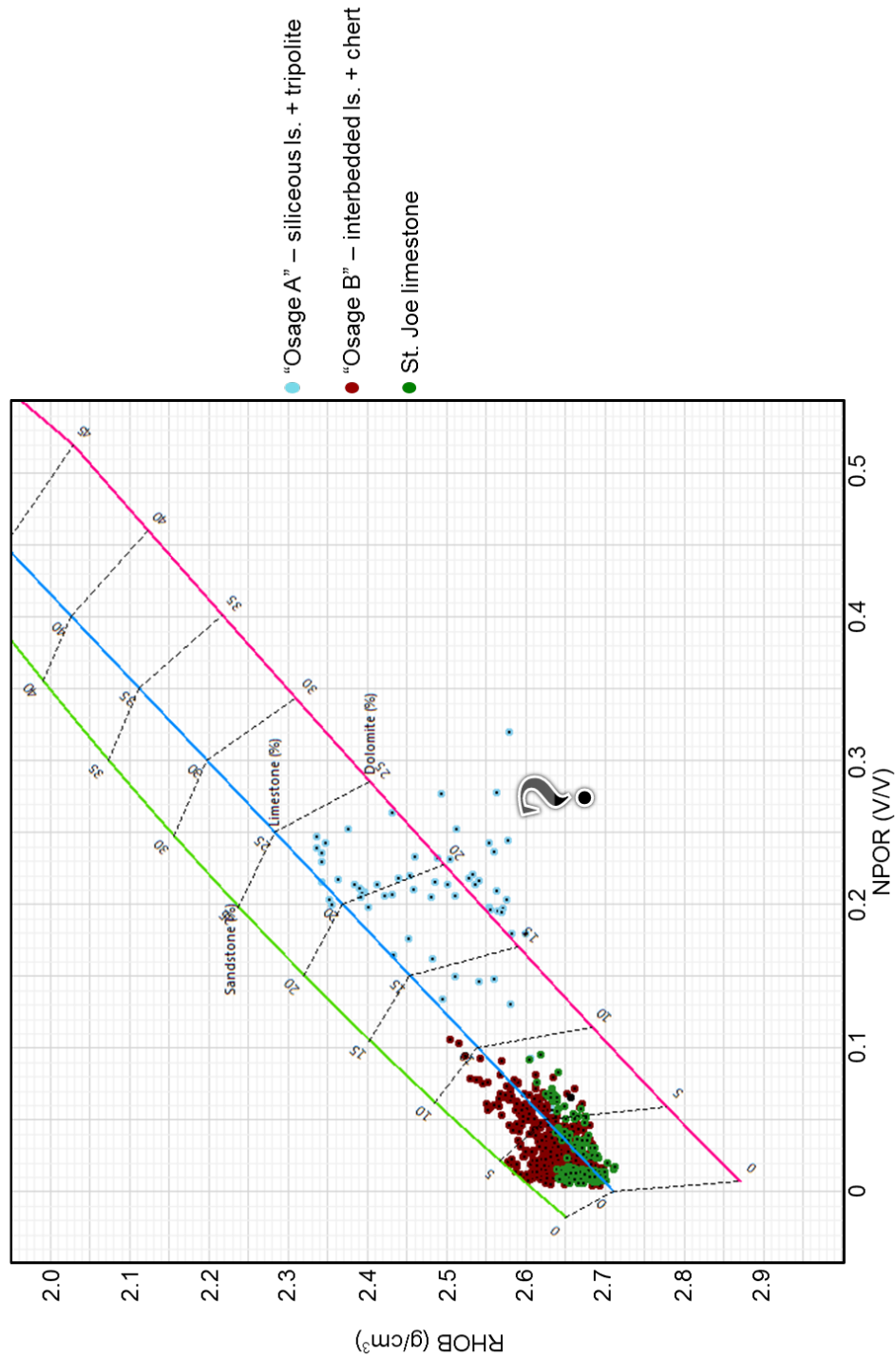
Figure 42: Crossplot of bulk density (RHOB) versus enhanced thermal neutron porosity (NPOR) through the Mississippian at "Well B". The St. Joe Limestone (green) plots mostly on the limestone line, while "Osage B" (brown) plots between the limestone and sandstone line, due to the presence of interbedded nonporous chert. "Osage A" (blue) plots between the limestone and dolomite line, which is unexpected; however "Osage A" also exhibits the highest porosities and lowest densities.

74
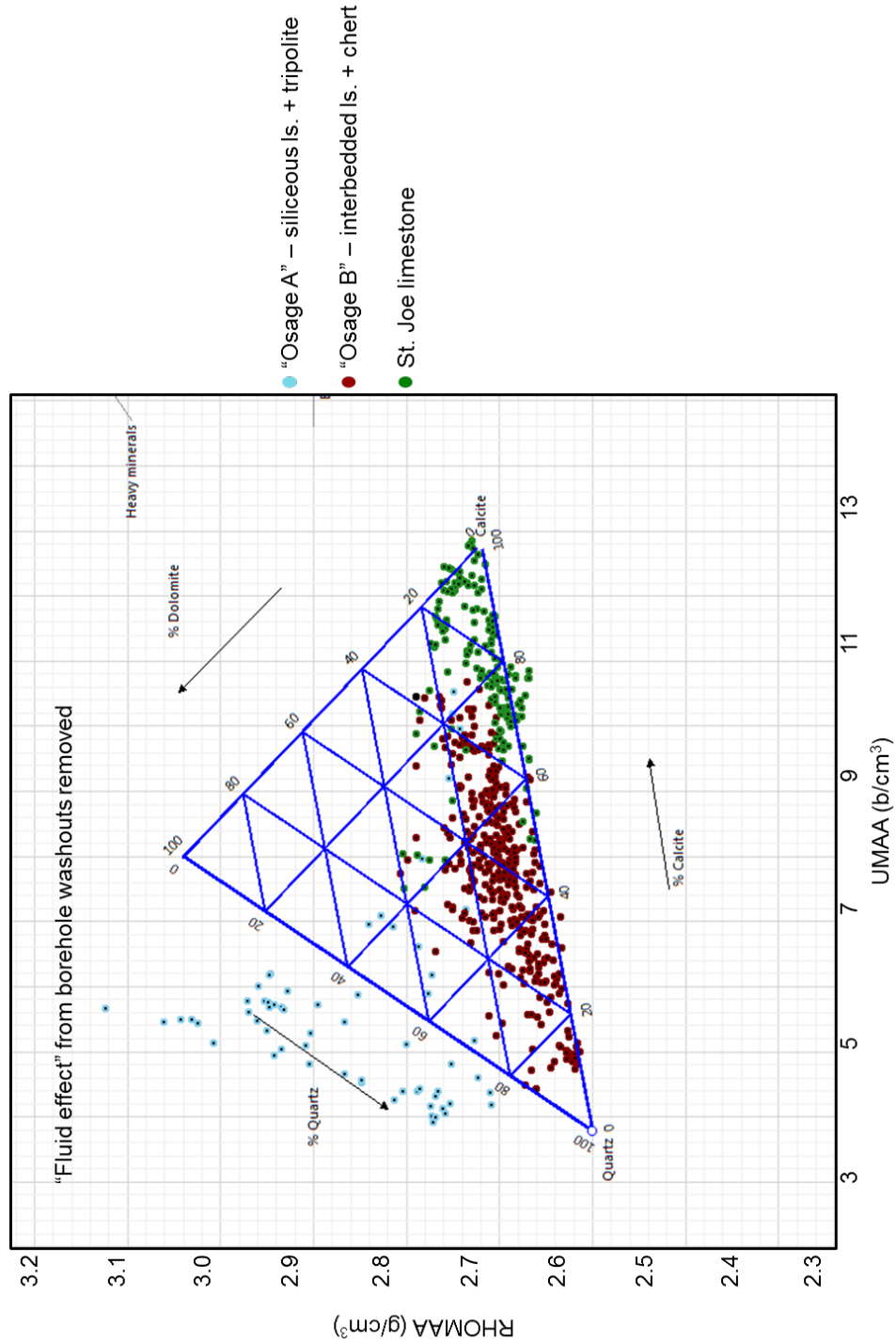
Figure 43: Crossplot of RHOMAA versus UMAA through the Mississippian. Both RHOMAA and UMAA measure only the apparent matrix, discarding any fluid or porosity effects. The St. Joe Limestone (green) plots near the calcite corner, and "Osage B" (brown) plots between the quartz and calcite corners, both as expected. "Osage A" now plots well into the quartz region, indicating a highly silicified matrix. Borehole washout problems are likely the cause of "Osage A" erroneously plotting in the previous figure.

75
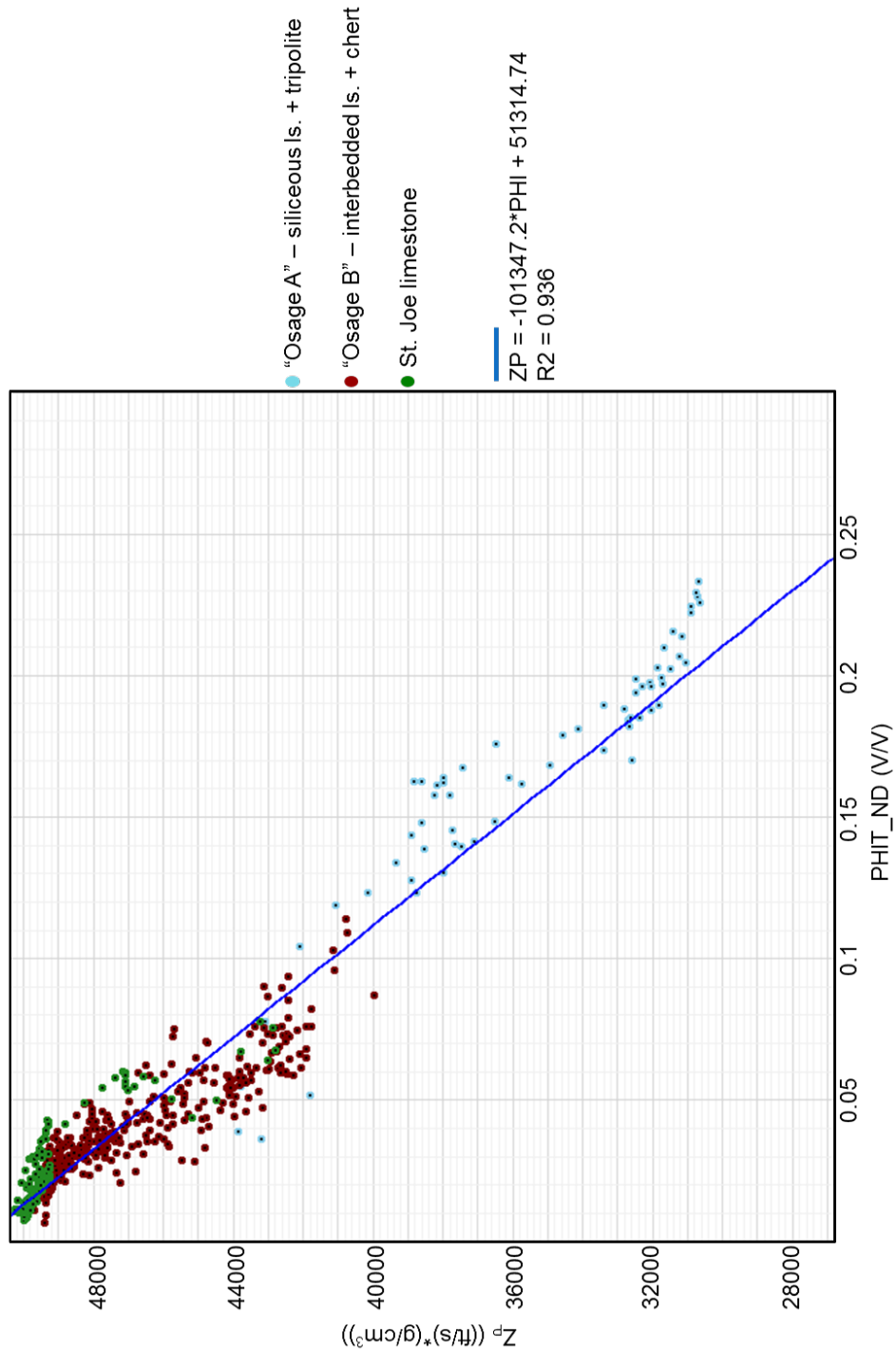
Figure 44: Crossplot of Z_P versus PHIT through the Mississippian. "Osage A" (blue) is clearly separated from "Osage B" (brown) and the St. Joe Limestone (green), and exhibits the lowest impedances and highest porosities.

The figure axes and legend read:

- "Osage A" – siliceous ls. + tripolite
- "Osage B" – interbedded ls. + chert
- St. Joe limestone
- $ZP = -101347.2*PHI + 51314.74$
- $R2 = 0.936$

X-axis: PHIT_ND (V/V) — 0.05, 0.1, 0.15, 0.2, 0.25

Y-axis: Z_P $((ft/s)*(g/cm^3))$ — 28000, 32000, 36000, 40000, 44000, 48000
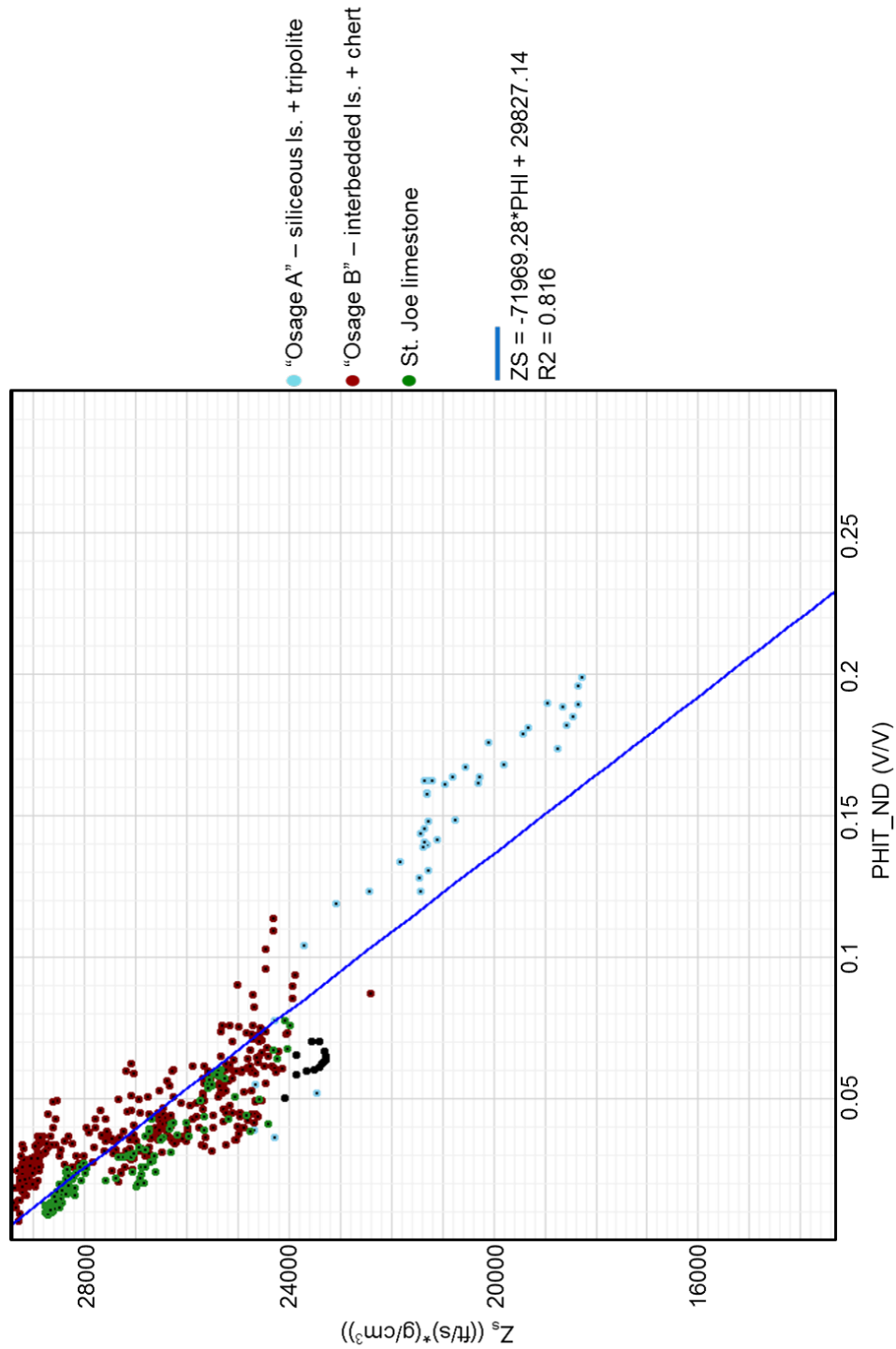
Figure 45: Crossplot of Z_S versus PHIT through the Mississippian. "Osage A" (blue) is clearly separated from "Osage B" (brown) and the St. Joe Limestone (green), and exhibits the lowest impedances and highest porosities.

Figure 46 shows the logs for total porosity (PHIT), bulk density (RHOB), density of the apparent matrix (RHOMAA), and intrinsic permeability (KINT) through the Mississippian, colored by interval, as before. Figure 47a shows a histogram of intrinsic permeability through "Osage A", Figure 47b shows a histogram of intrinsic permeability through "Osage B", and Figure 47c shows a histogram of intrinsic permeability through the St. Joe Limestone. These results show an important feature of the Mississippi Lime play. Although typical tripolitic chert of "Osage A" exhibits high porosities ranging from 20-50% (4-24% in "Well B"), permeability tends to be low (0.01-13.3 mD in "Well B"), which is due to the unique nature of porosity in carbonates. Porosity in the tripolitic chert consists mostly of moldic, vuggy and micro-porosity, which tend not to be well connected, and hence the importance of the natural fracture network in the interbedded tight limestone and nonporous chert (Rogers, 2001; Zhao, 2011; Dowdell et al., 2012; White et al., 2012). Permeability observed in "Osage B" is likely due to fractures, as the interbedded limestone and chert of this interval are mainly nonporous. "Reservoir quality" permeability typically needs to be greater than 100 mD; however, the Mississippi Lime is an unconventional resource play and requires on average 95 drops of water to produce 5 drops of oil.
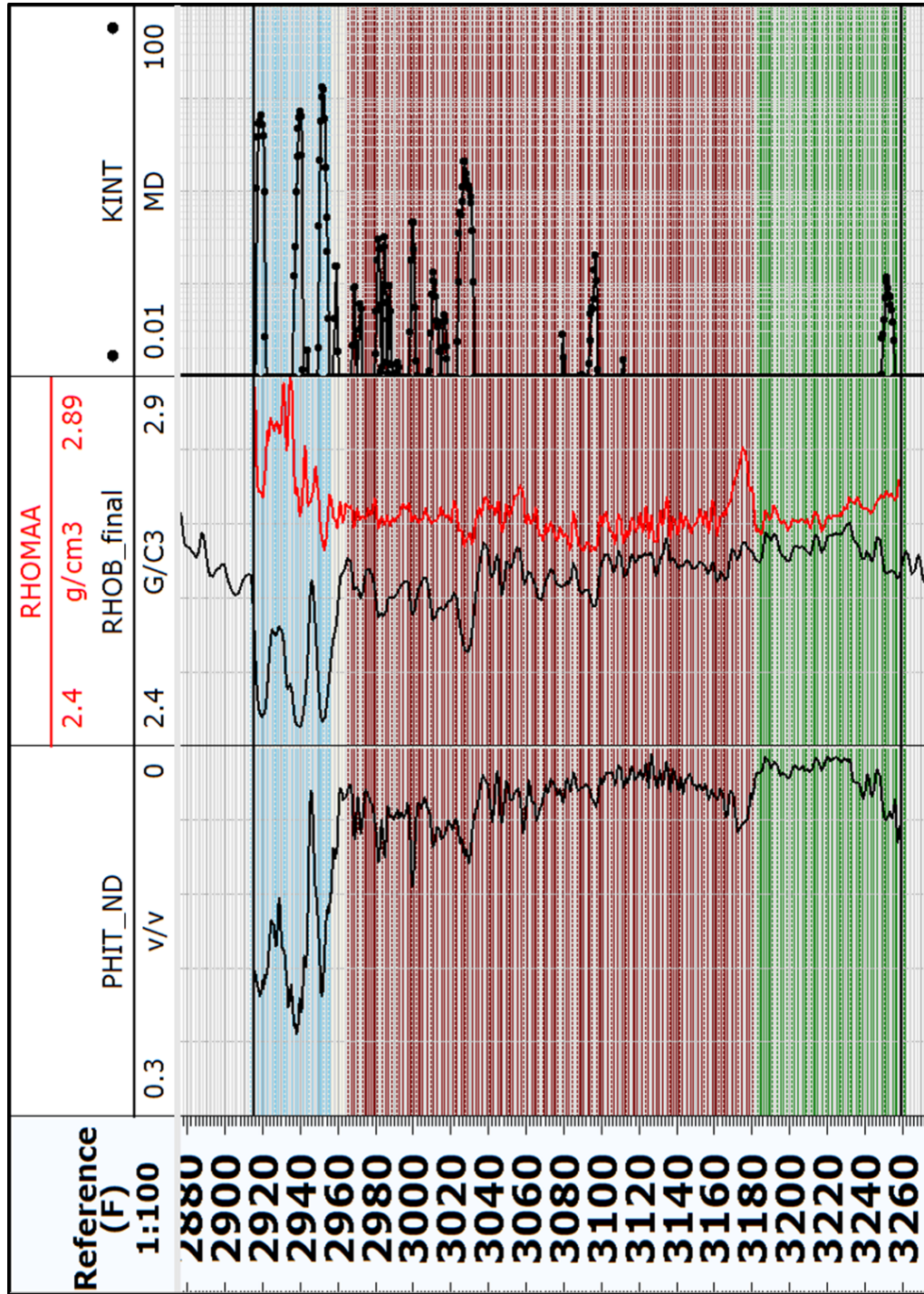
Figure 46: Total porosity (PHIT), bulk density (RHOB), density of the apparent matrix (RHOMAA), and intrinsic permeability (KINT) for the Mississippian in "Well B". "Osage A" is colored in blue, "Osage B" in brown, and the St. Joe Limestone in green. While "Osage A" exhibits high porosity, permeability is relatively low. Porosity in tripolitic chert is mostly moldic, vuggy, and microporosity in the matrix, all of which tend not to be well connected (Rogers, 2001; Zhao 2011).
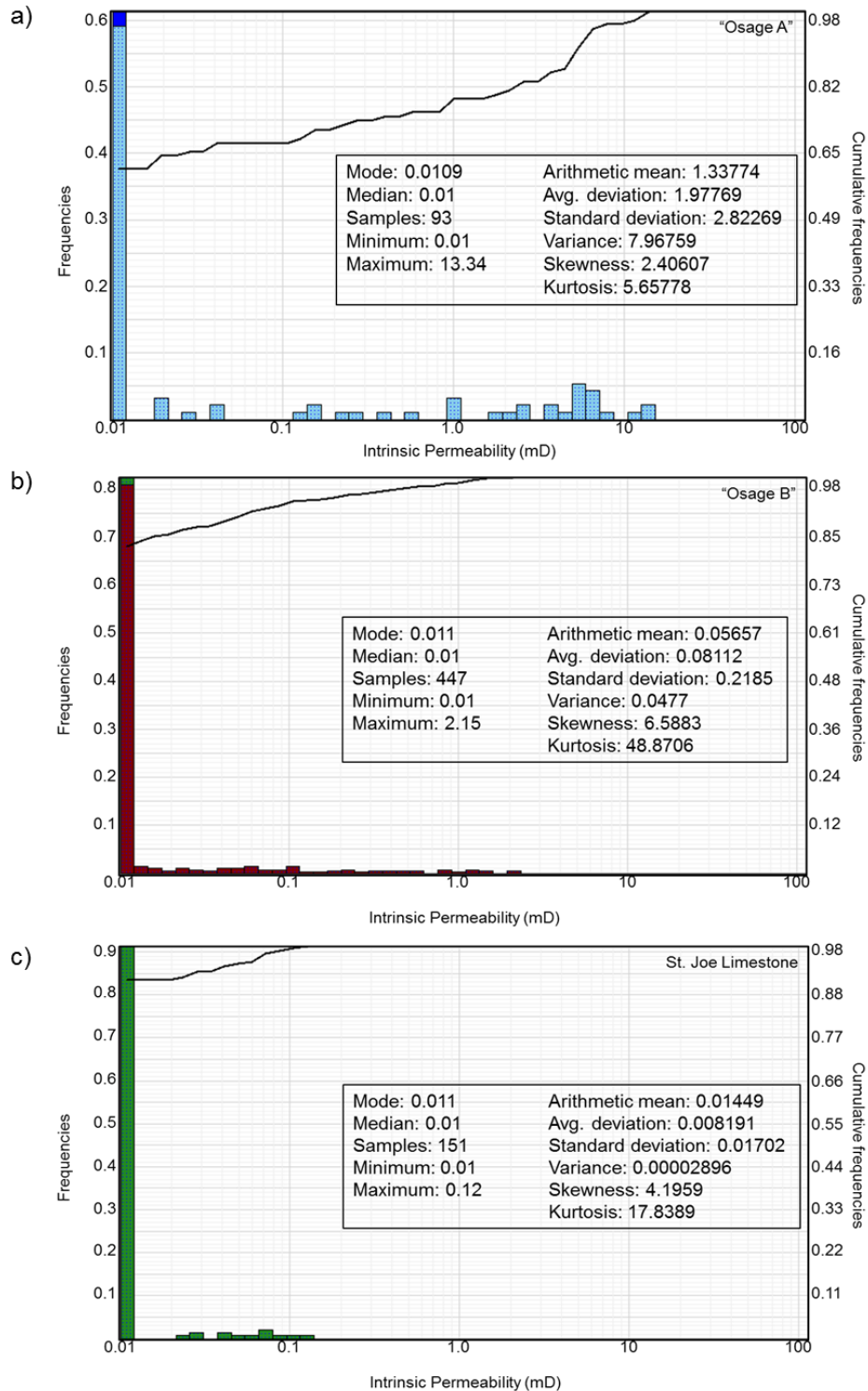
Figure 47: Histogram of intrinsic permeability for (a) "Osage A", (b) "Osage B", and (c) the St. Joe Limestone in "Well B". "Osage A" exhibits the highest permeability of 13.34 mD. "Osage B" exhibits a maximum permeability of 2.15 mD, possibly due to fracture porosity. The St. Joe Limestone exhibits very little permeability.

80

INVERSION

Before performing simultaneous prestack seismic inversion, "Well B" needs to be tied to the prestack time migrated seismic data. Figure 48 shows the seismic-well tie. The left tracks show the P-wave sonic log, density log, and enhanced thermal neutron porosity log. The synthetic trace calculated from Z_P is shown in blue while the extracted trace from the seismic is shown in red. The seismic data is shown in the furthest right trace, showing only offsets from 100 to 2000 ft, which were used in extracting a trace to tie to the zero-offset synthetic. The correlation between the synthetic and seismic is 80% in the window between 450 and 550 ms.

The prestack time migrated data are stacked and loaded into an interpretation package to pick the top Oswego, Mississippi, and Arbuckle horizons, using well tops as guide. Figure 49 shows a vertical section adjacent to the well location and the three picked horizons. A strong reflection at 700 ms is the top of the granitic basement. Figure 50, Figure 51, and Figure 52 show the two-way time (TWT) structure maps created from the picked Oswego, Mississippi, and Arbuckle horizons, respectively.
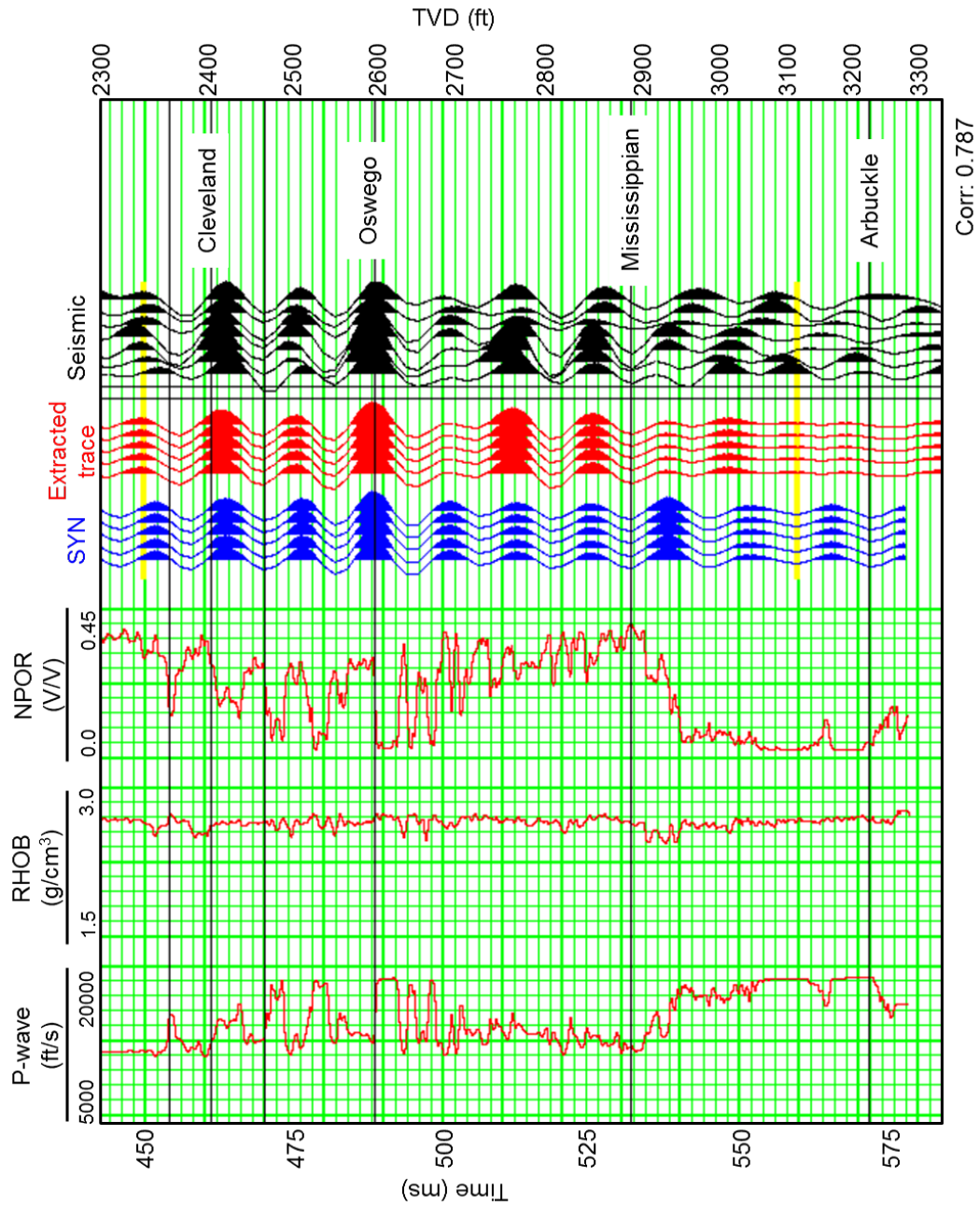
Figure 48: Seismic-well tie showing the synthetic generated from the P-wave sonic log and bulk density log using a statistical extracted wavelet. The correlation coefficient between 450 and 550 ms is 80%.

82
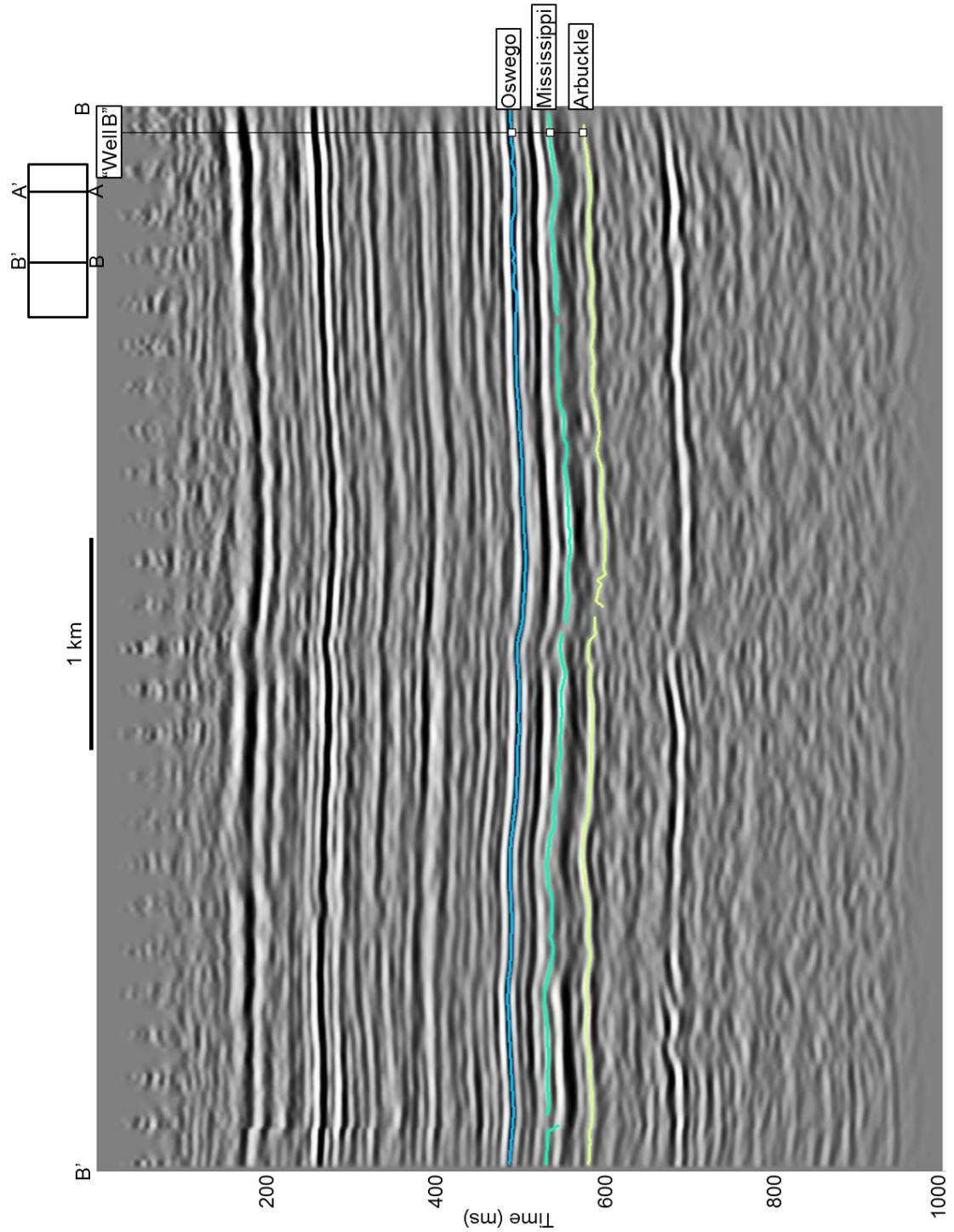
Figure 49: Vertical slice BB' through the seismic data near the well tie. The Oswego, Mississippian, and Arbuckle top horizons are picked using well tops. There is an apparent vertical fault in the middle of the line; however, this is more likely an artifact of the "seam" between the two patches.

83
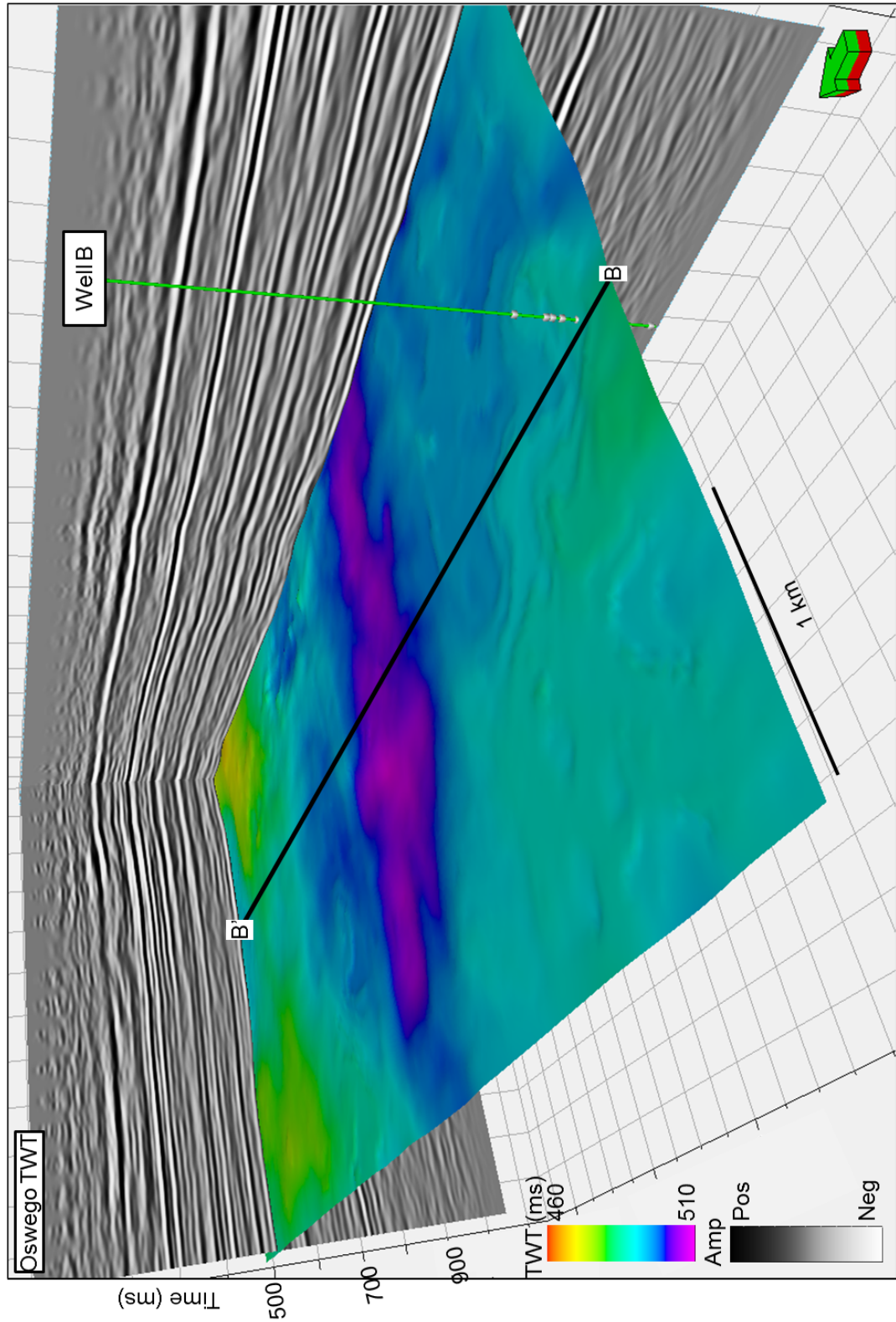
Figure 50: Seismic amplitude inline-crossline chair back with the Oswego TWT structure map from the picked Oswego horizon. A black line across the Oswego surface indicates the location of vertical slice.
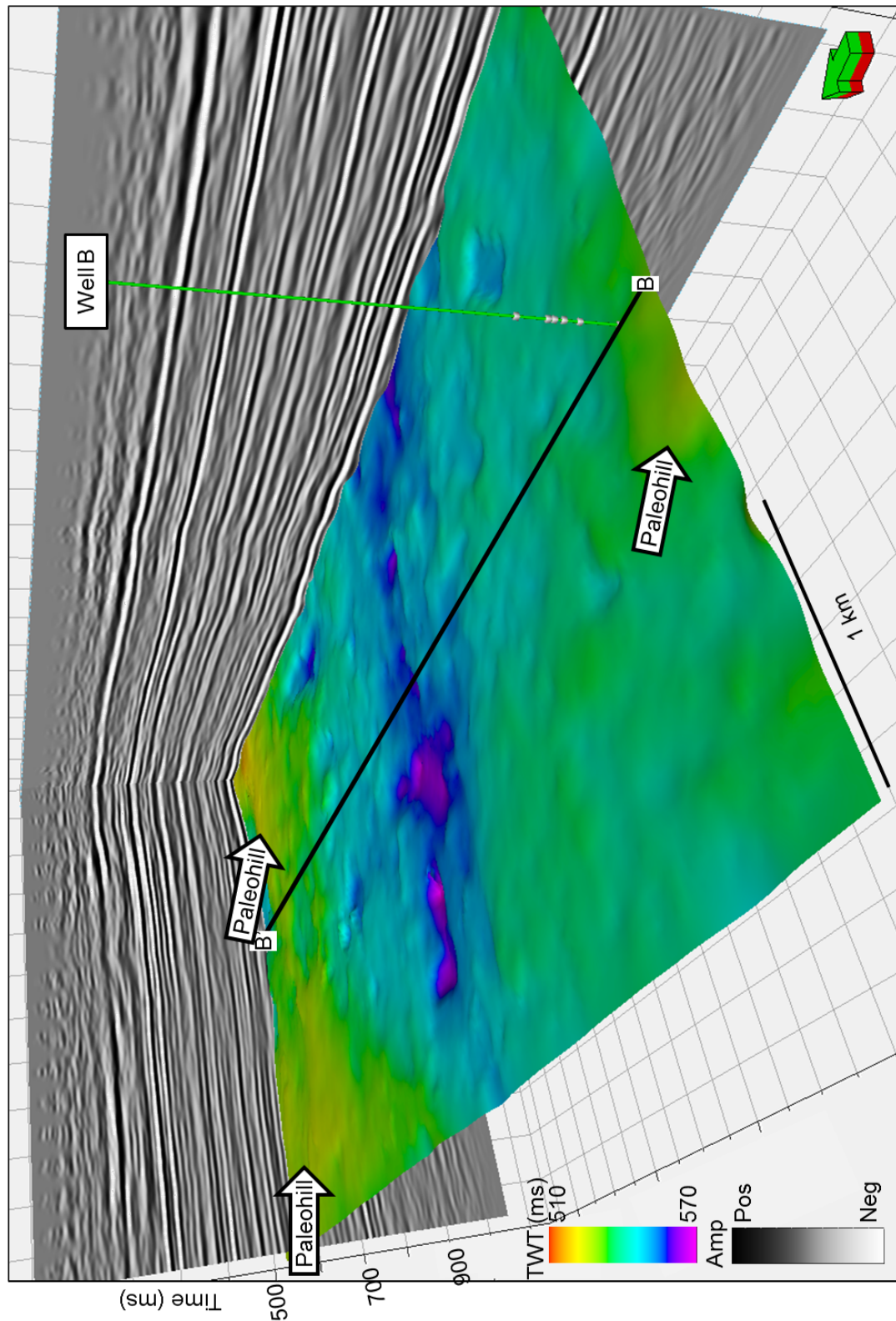
Figure 51: Seismic amplitude inline-crossline chair back with the Mississippian TWT structure map from the picked Mississippian horizon.
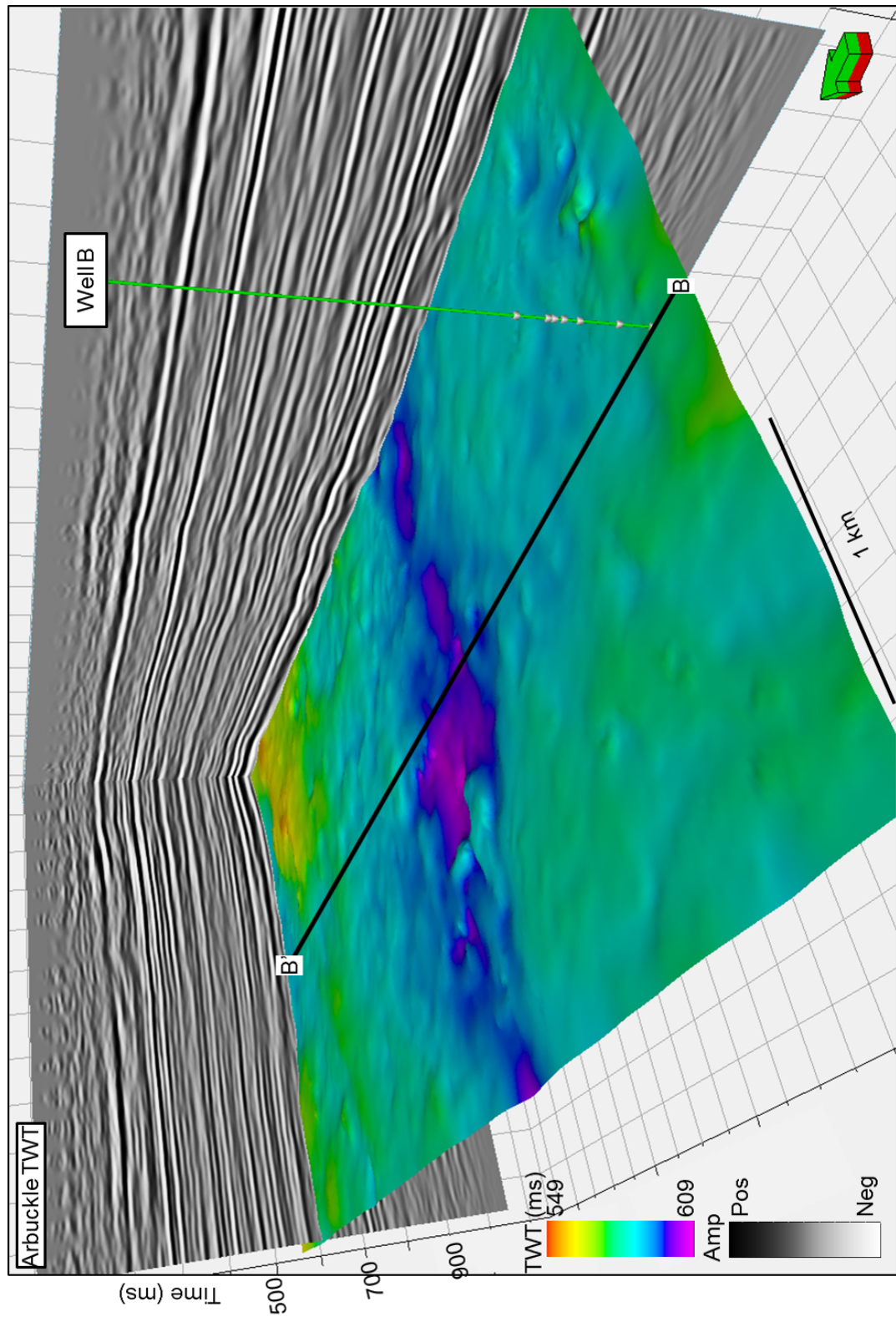
Figure 52: Seismic amplitude inline-crossline chair back with the Arbuckle TWT structure map from the picked Arbuckle horizon.

Next, the prestack time-migrated data are converted to angle gathers ranging from 0 to 45°, shown in Figure 53, and then low-frequency models for inverting Z_P, Z_S, and density from the seismic data and well logs are constructed. While the picked horizons can be used in creating the low-frequency models, in this instance they are not, as using the horizons in the model can bias the final inversion results. Figure 54-56 show the low frequency models for Z_P, Z_S, and density inversion, respectively. Simultaneous prestack inversion uses the low-frequency models, generating volumes for Z_P, Z_S, and density. Once the inversion is complete, $\lambda\rho$ and $\mu\rho$ volumes are transformed from the Z_P and Z_S volumes using equations 4.8 and 4.9.
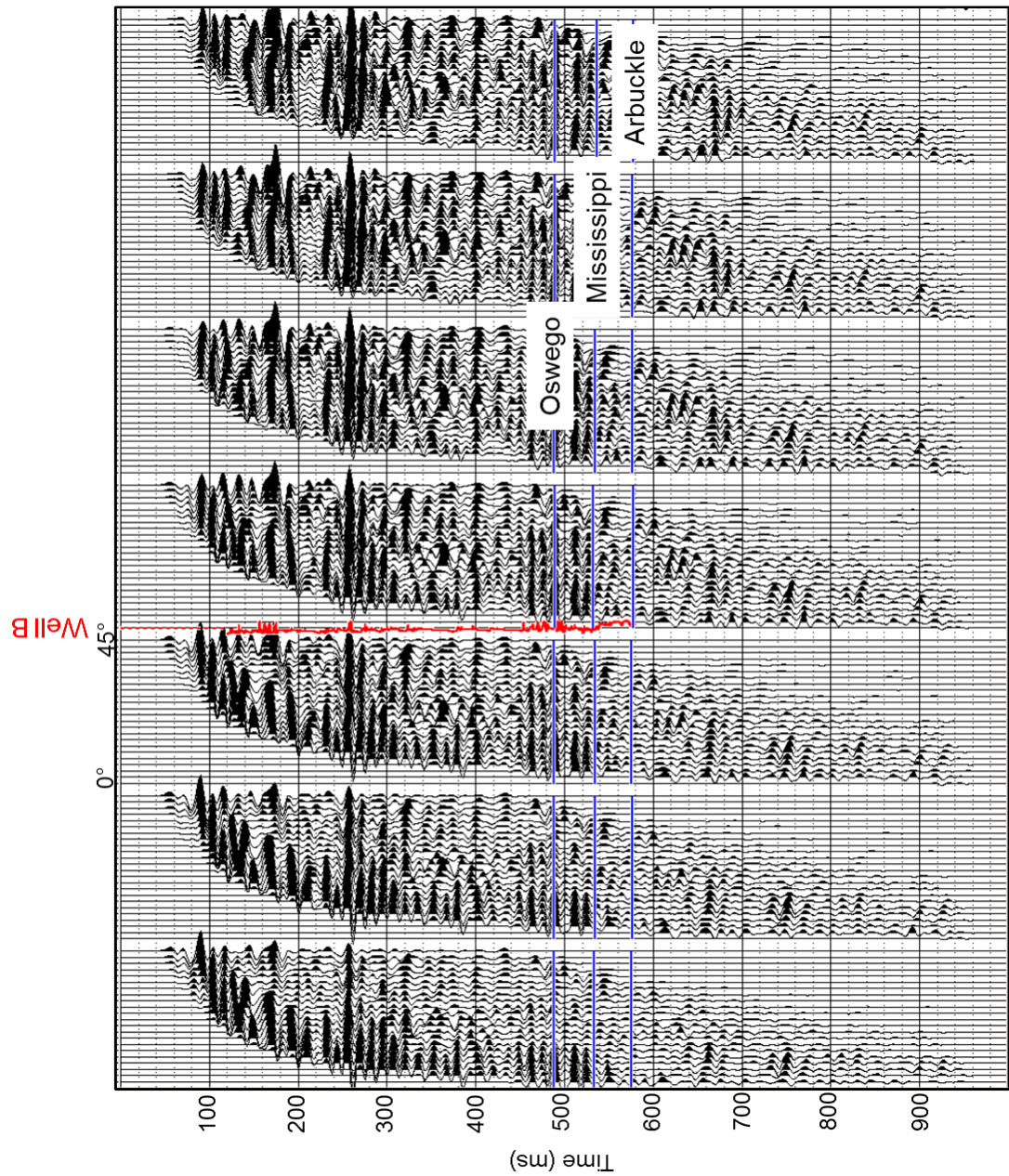
Figure 53: Seven angle gathers from 0-45 degrees created from the input prestack time migrated seismic data. The red P-wave log denotes the well location, and the picked horizons are shown in blue.

88
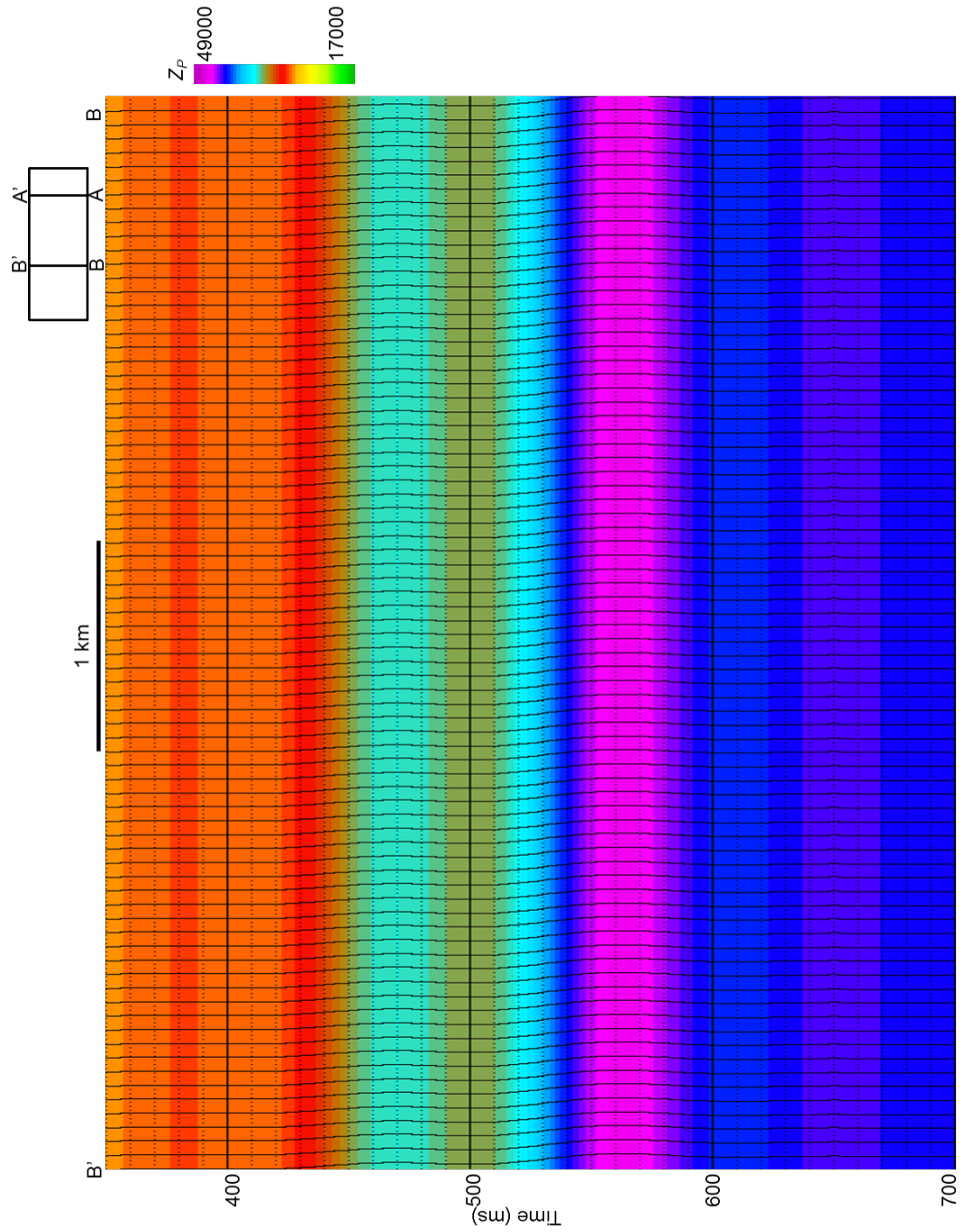
Figure 54: vertical slice BB' through the low frequency model used for Z_P inversion generated from horizon picks and logs.
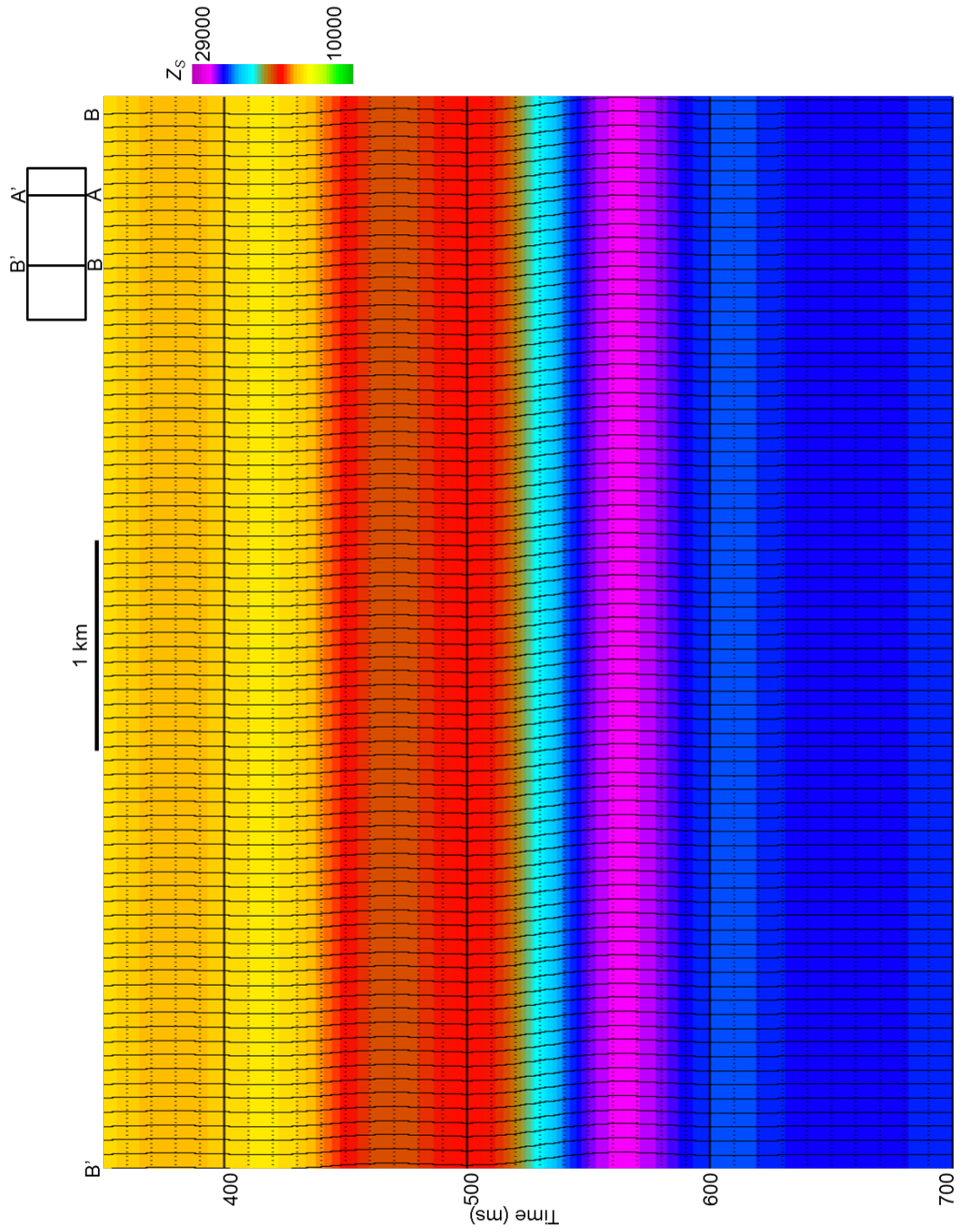
Figure 55: vertical slice BB' through the low frequency model used for Z_S inversion generated from horizon picks and logs.
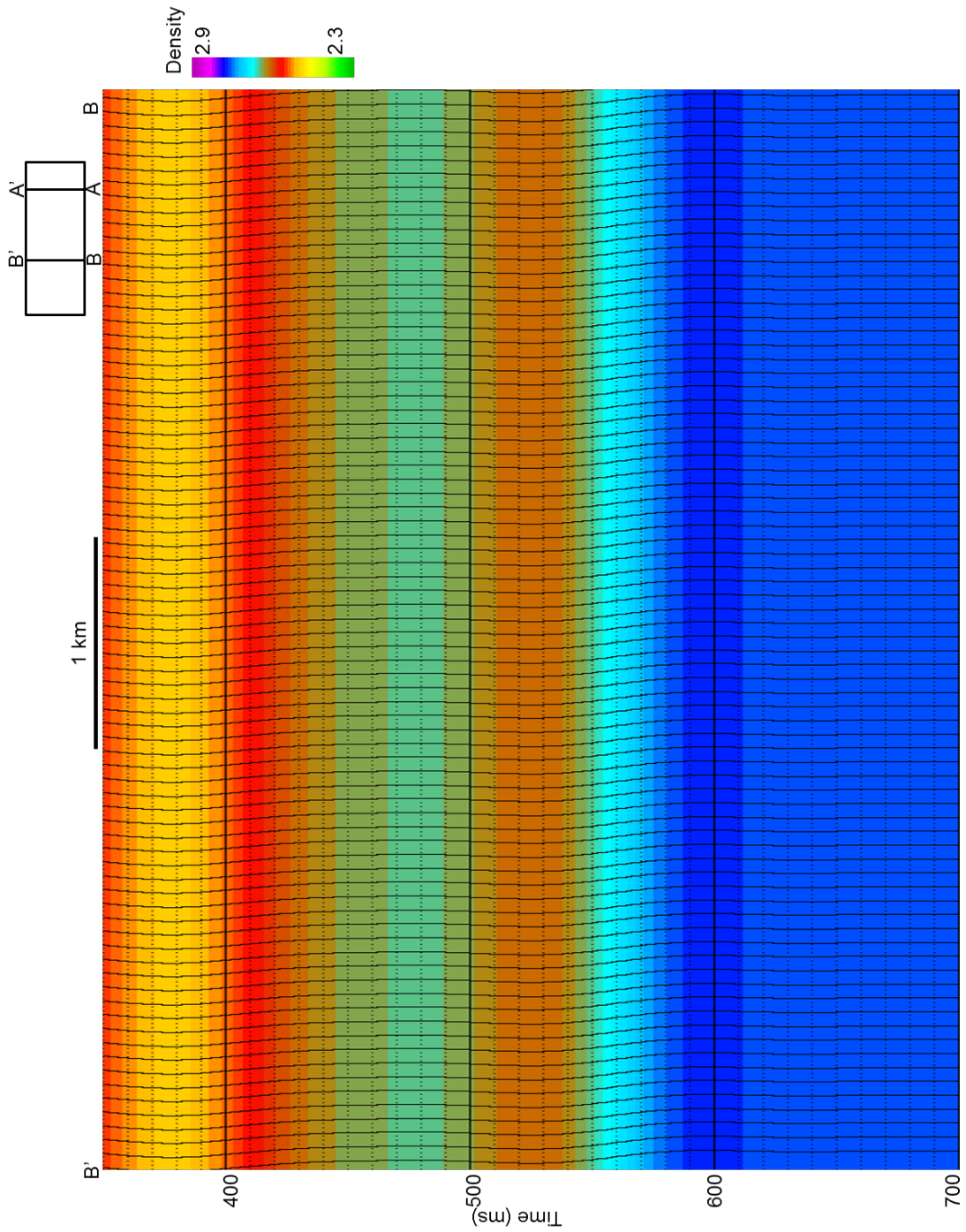
Figure 56: Vertical slice BB' through the low frequency model built for density inversion using the angle gathers and the density log.

INTERPRETATION

Figure 57-61 shows vertical line BB' through the inverted Z_P, Z_S, density, $\lambda\rho$, and $\mu\rho$ estimates with seismic amplitude displayed as wiggle traces with variable area. Warm colors indicate low values while cool colors indicate high values. The crossplots in Figure 44 and 45 show that tripolite should occur as low values for each inversion volume, occurring near the top of the Mississippian. White arrows indicate pockets of low Z_P along the Mississippian. There is an abrupt change in Z_P at the transition from siliceous limestone, which has high potential for diagenetic alteration to tripolite, to the interbedded chert and limestone, which has a significantly lower potential for diagenetic alteration to tripolite, and finally into the St. Joe limestone which contains no chert at all. Each of these attributes shows similar patterns. As observed on well logs, density is the best discriminator of tripolitic chert ("Osage A"), from interbedded tight limestone and chert ("Osage B"), and tight limestone (St. Joe). The scaled $\lambda\rho$ and $\mu\rho$ volumes enhance the tripolite anomalies, but also indicate low anomalies at the top of the Arbuckle. However, the well logs end right at the top of the Arbuckle, so the estimates for the Arbuckle and below are not calibrated to log control.
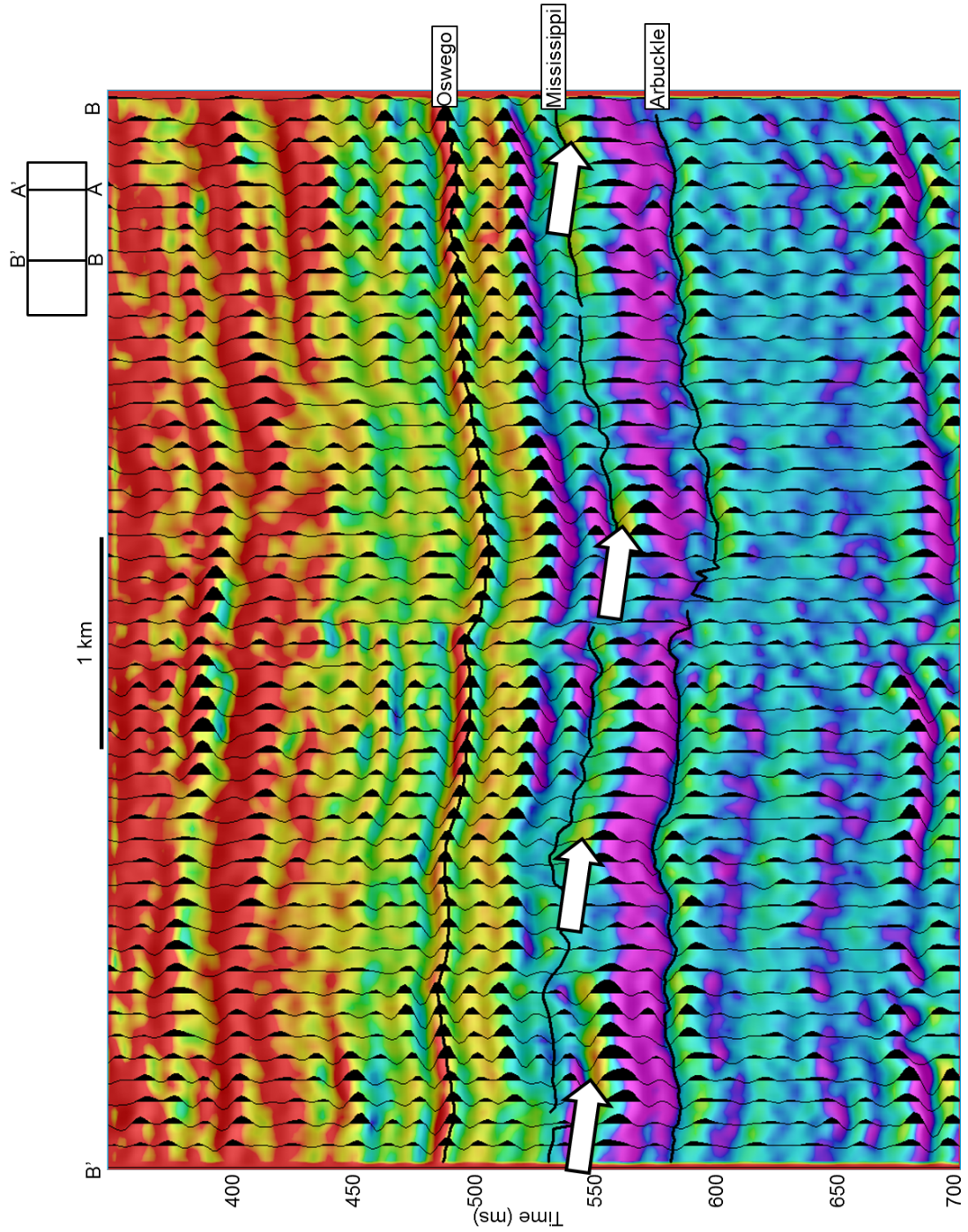
Figure 57: Vertical slice BB' through seismic amplitude corendered with Z_P. White arrows indicate potential pockets of tripolite within the Mississippian. Warm colors correspond with low Z_P.

93
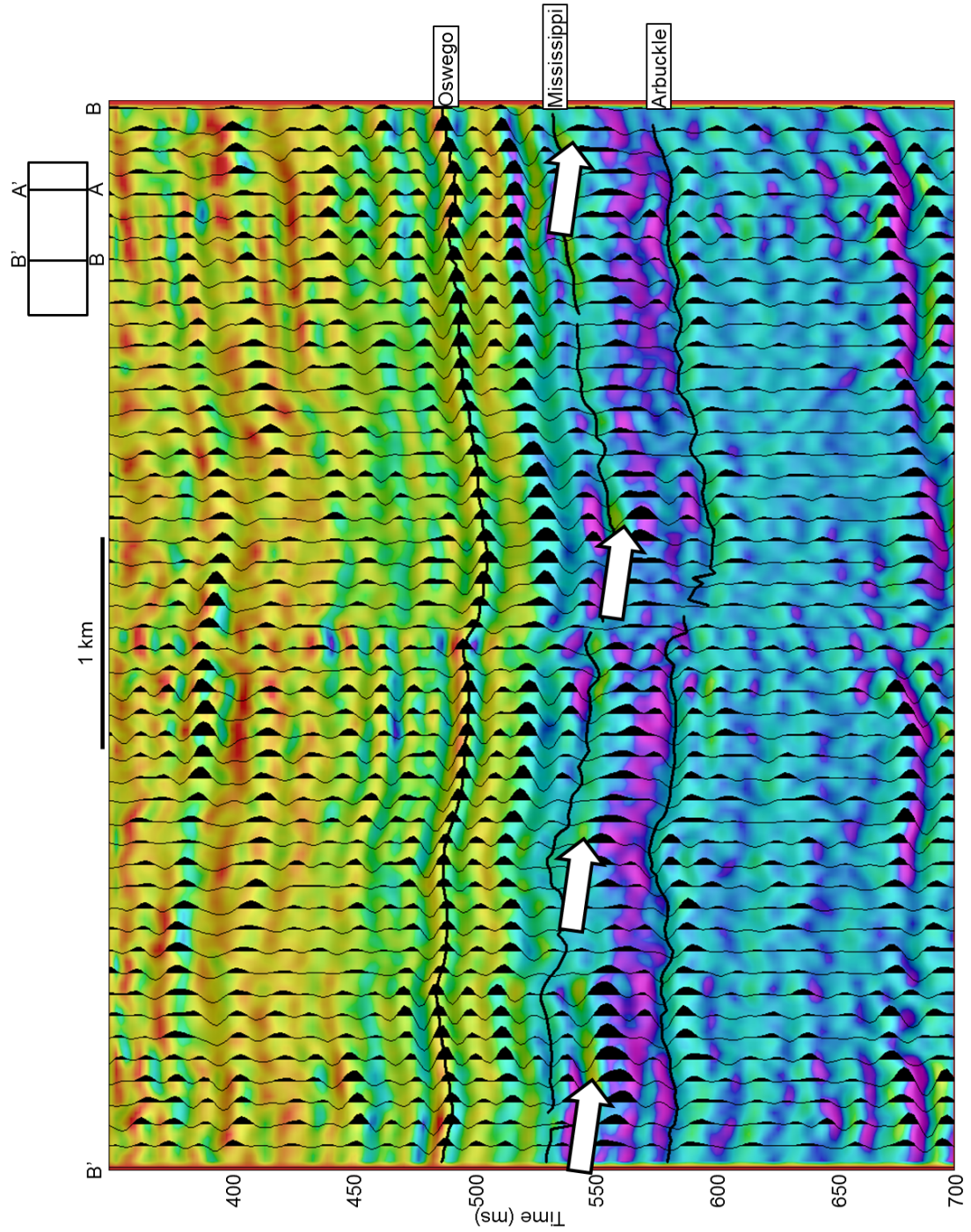
Figure 58: Vertical slice BB' through seismic amplitude corendered with Z_S. White arrows indicate potential pockets of tripolite within the Mississippian. Warm colors correspond with low Z_S.
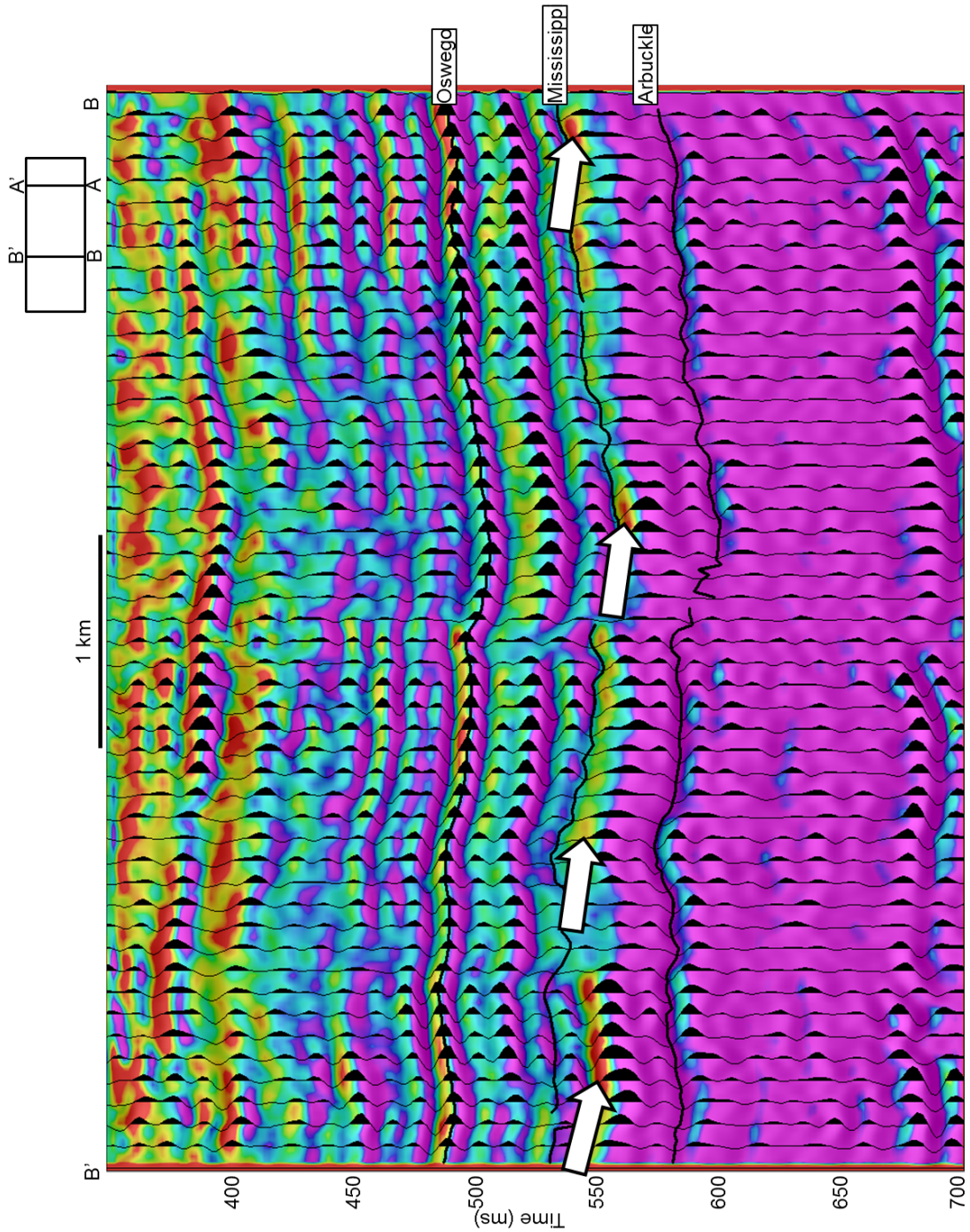
Figure 59: Vertical slice BB' through seismic amplitude corendered with density. White arrows point out low values of density, which is characteristic of tripolite. Warm colors correspond with low density. As observed on well logs, density is the best discriminator for tripolitic chert and "Osage A"-type siliceous limestone.
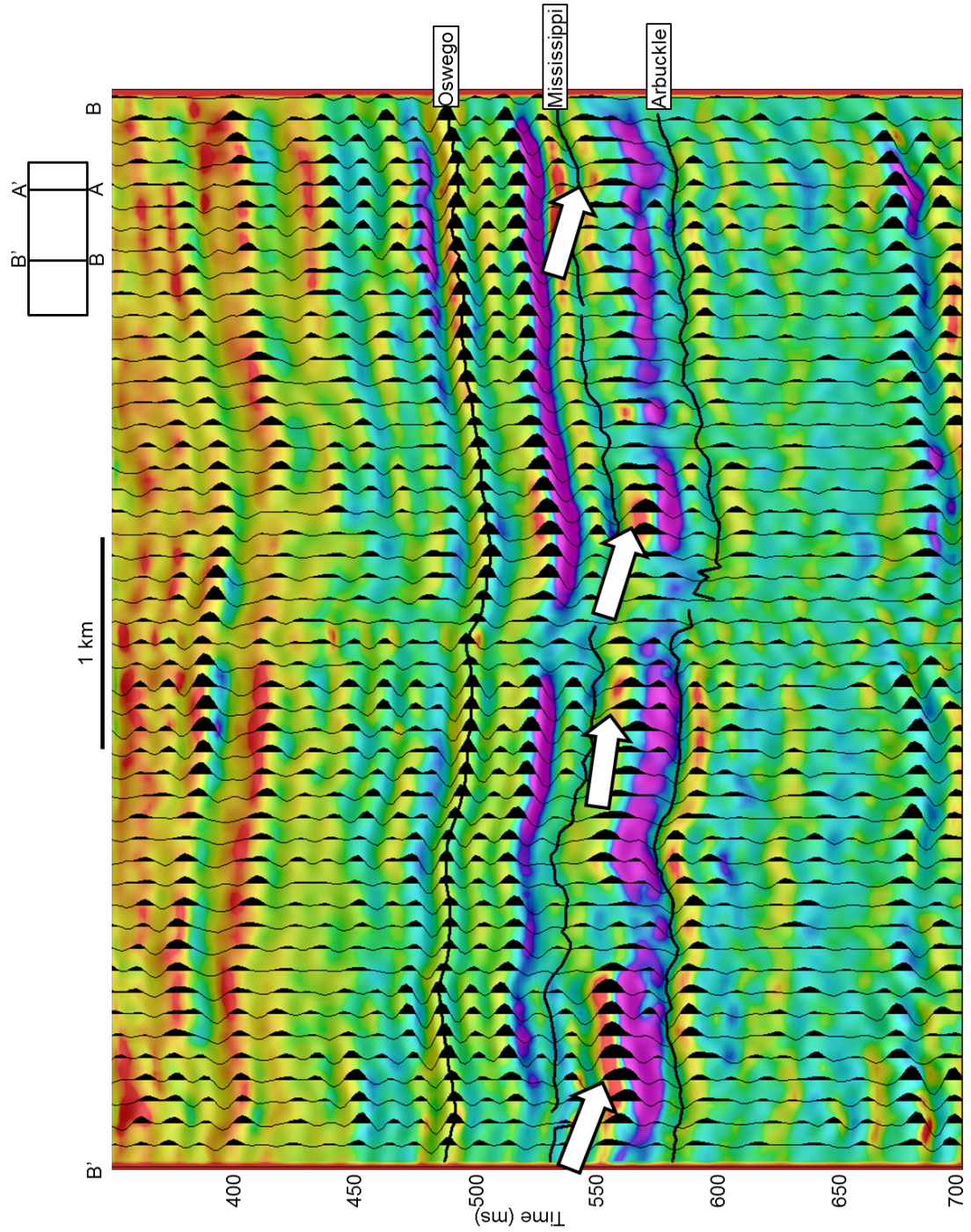
Figure 60: Vertical slice BB' through seismic amplitude corendered with $\lambda\rho$. Warm colors correspond with low $\lambda\rho$. Low values of $\lambda\rho$ indicate potential pockets of tripolite, denoted by white arrows.
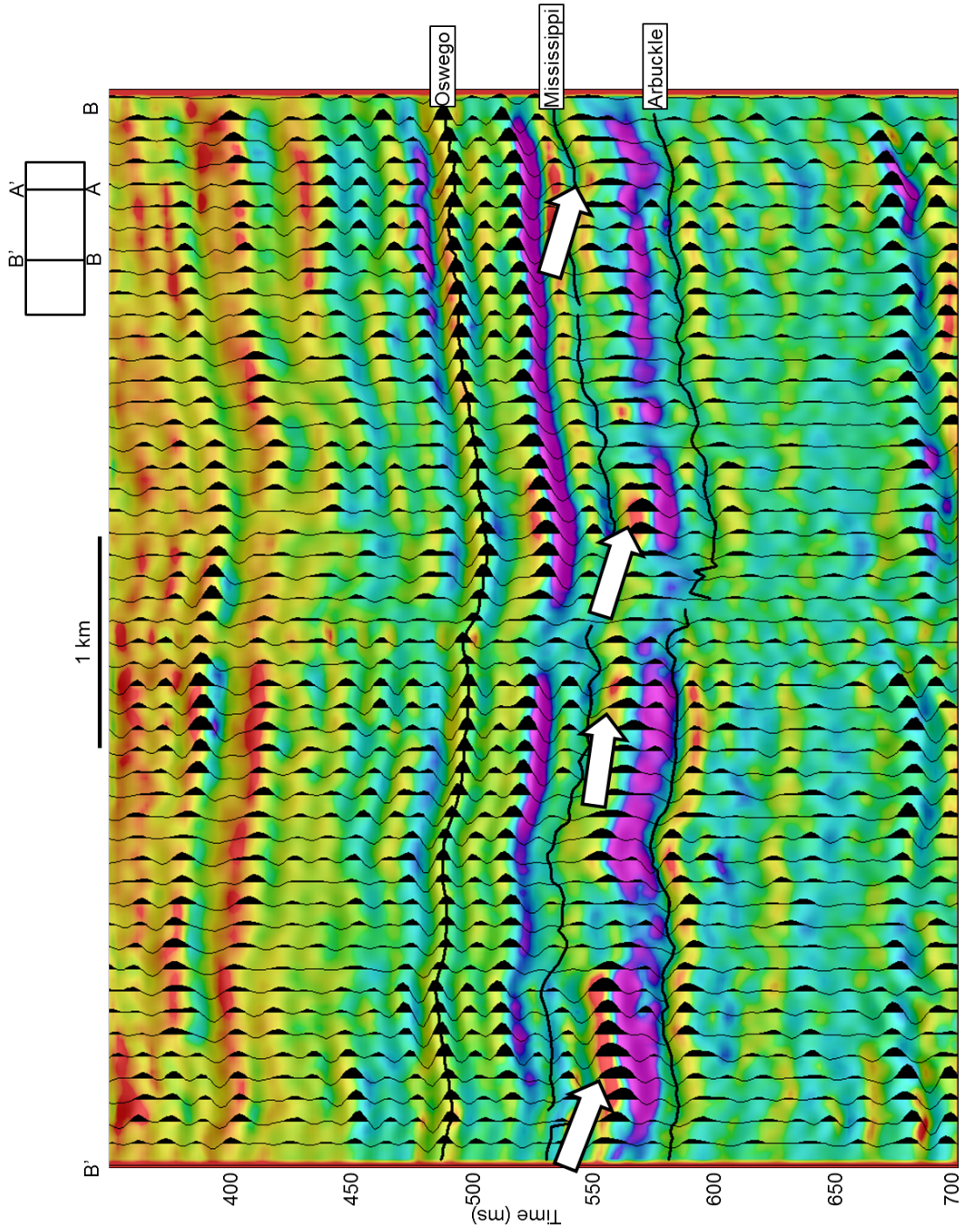
Figure 61: Vertical slice BB' through seismic amplitude corendered with $\mu\rho$. Warm colors correspond with $\mu\rho$. Low $\mu\rho$ indicates potential pockets of tripolite, denoted by white arrows.

97

Figure 62-66 show the inversion attributes extracted along the top of the Mississippian surface with a vertical seismic amplitude inline and crossline forming a chair back. Again, warm colors indicate low values while cool colors indicate high values.   As tripolite is a diagenetic product, it is laterally discontinuous, resulting in a high amount of lateral variability. Additionally, the tripolite is not only confined to the top of the Mississippian, but is found throughout the silicified limestone of "Osage A", which makes up the top of the Mississippian interval in Osage County (Matson, 2013). Because of this lateral and vertical variability, seismically mapping tripolite is challenging, yet with the aid of the inversion attributes, mapping the tripolite is possible.
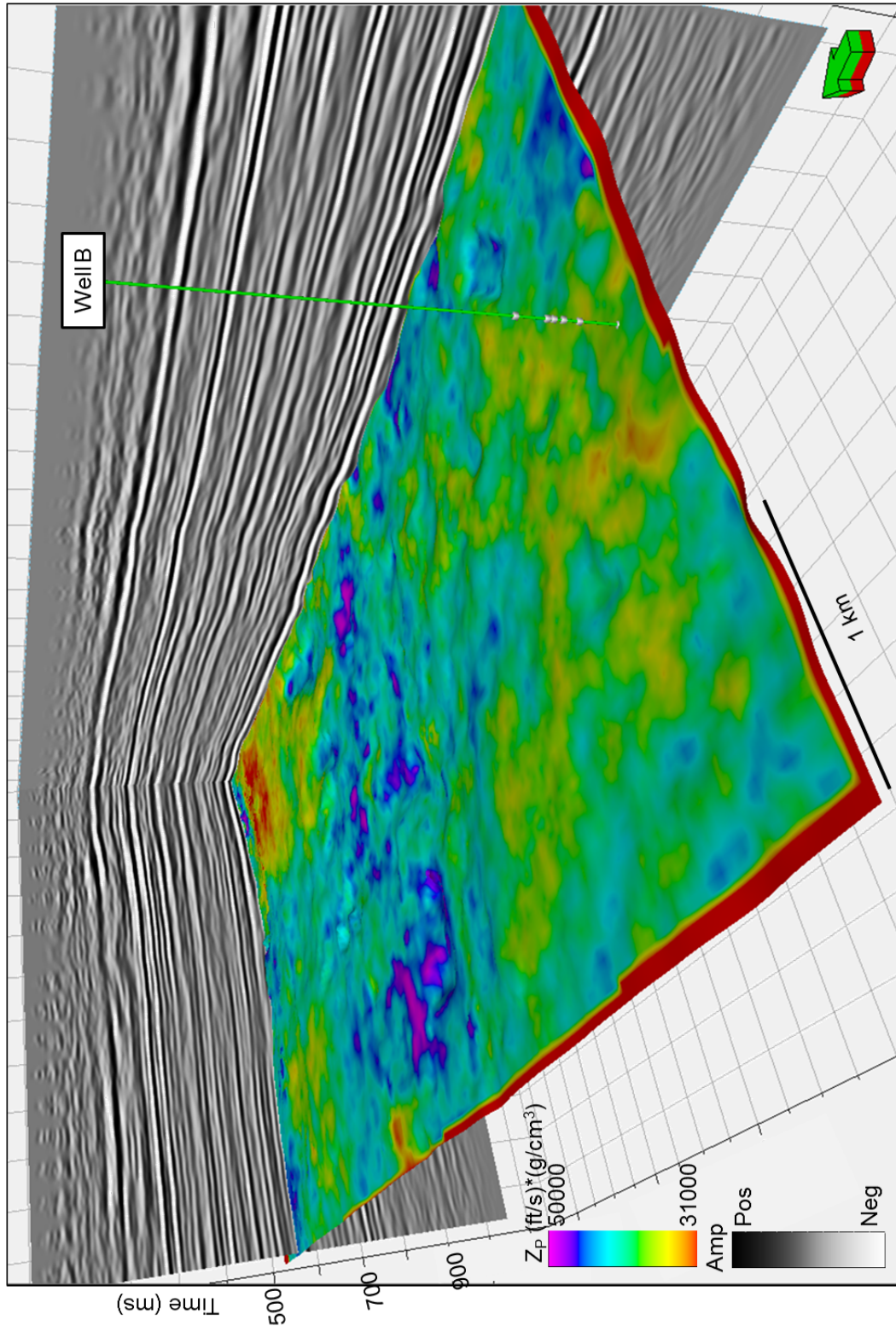
Figure 62: Z_P extracted on the top of the Mississippian horizon. Low Z_P corresponds with warm colors.
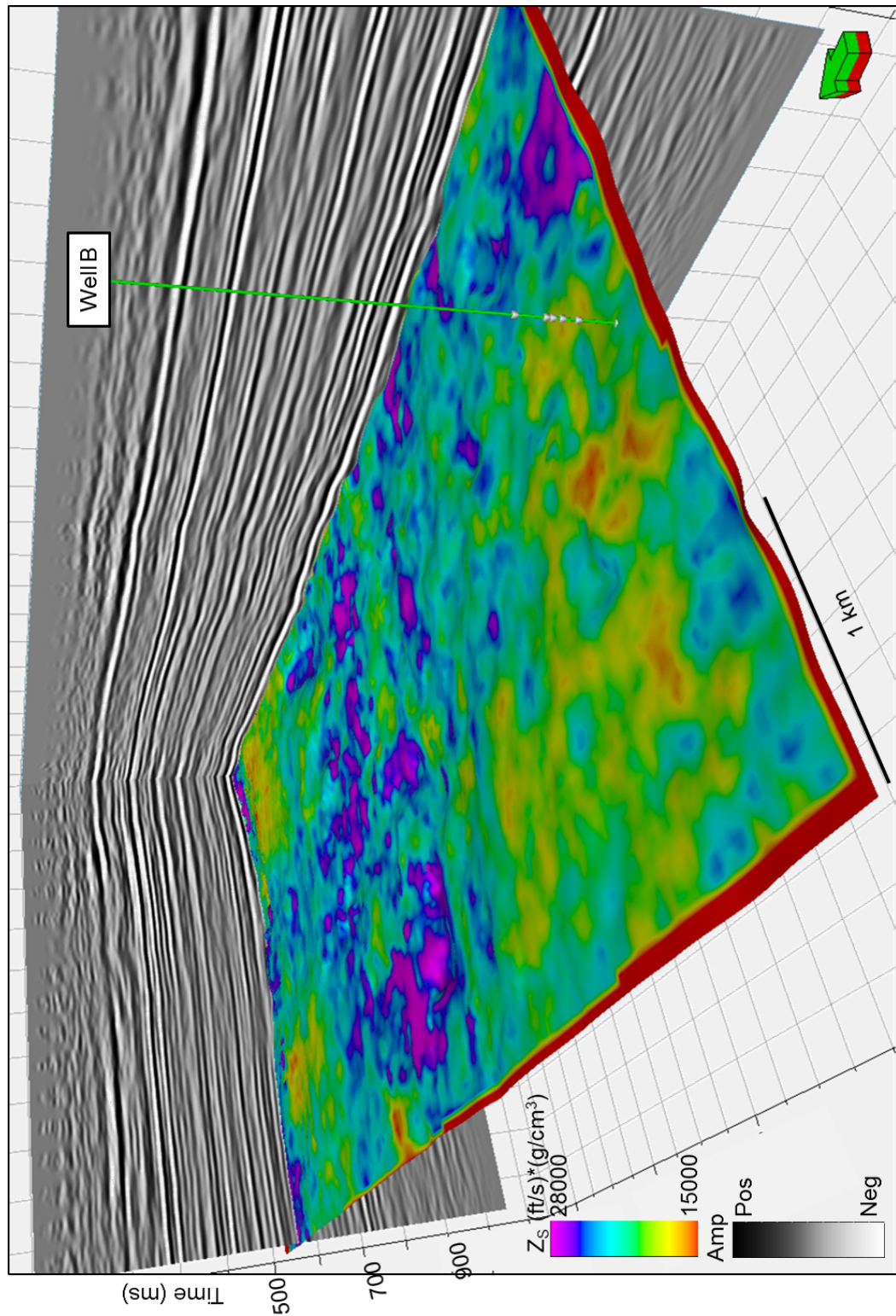
Figure 63: Z_S extracted on the top of the Mississippian horizon. Low values of Z_S correspond to warm colors. Because Z_S is not sensitive to pore fluid, it is a good lithology discriminator.
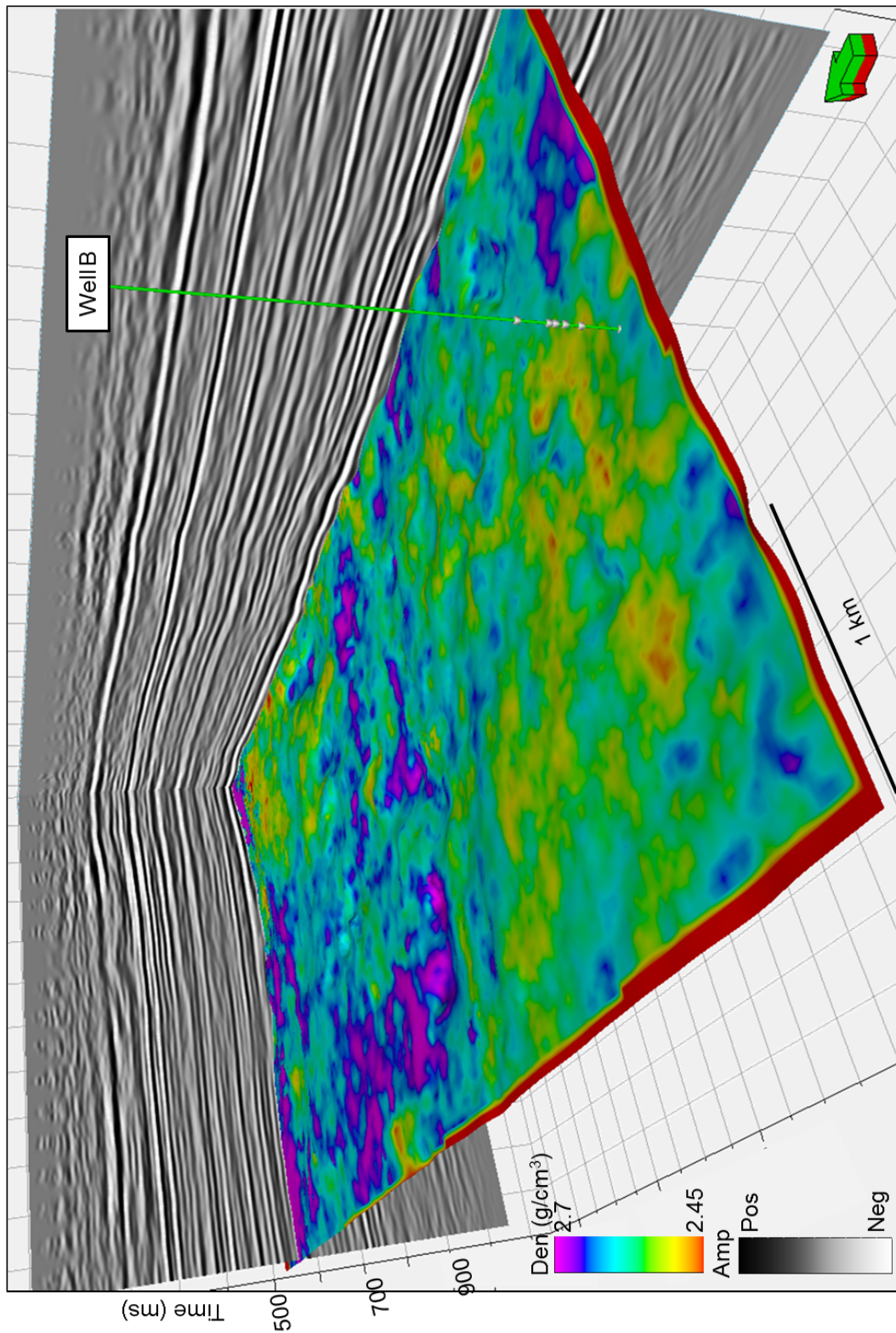
Figure 64: Density extracted on the top of the Mississippian horizon. Low density corresponds with warm colors. Pockets of lower density may indicate tripolite.

101
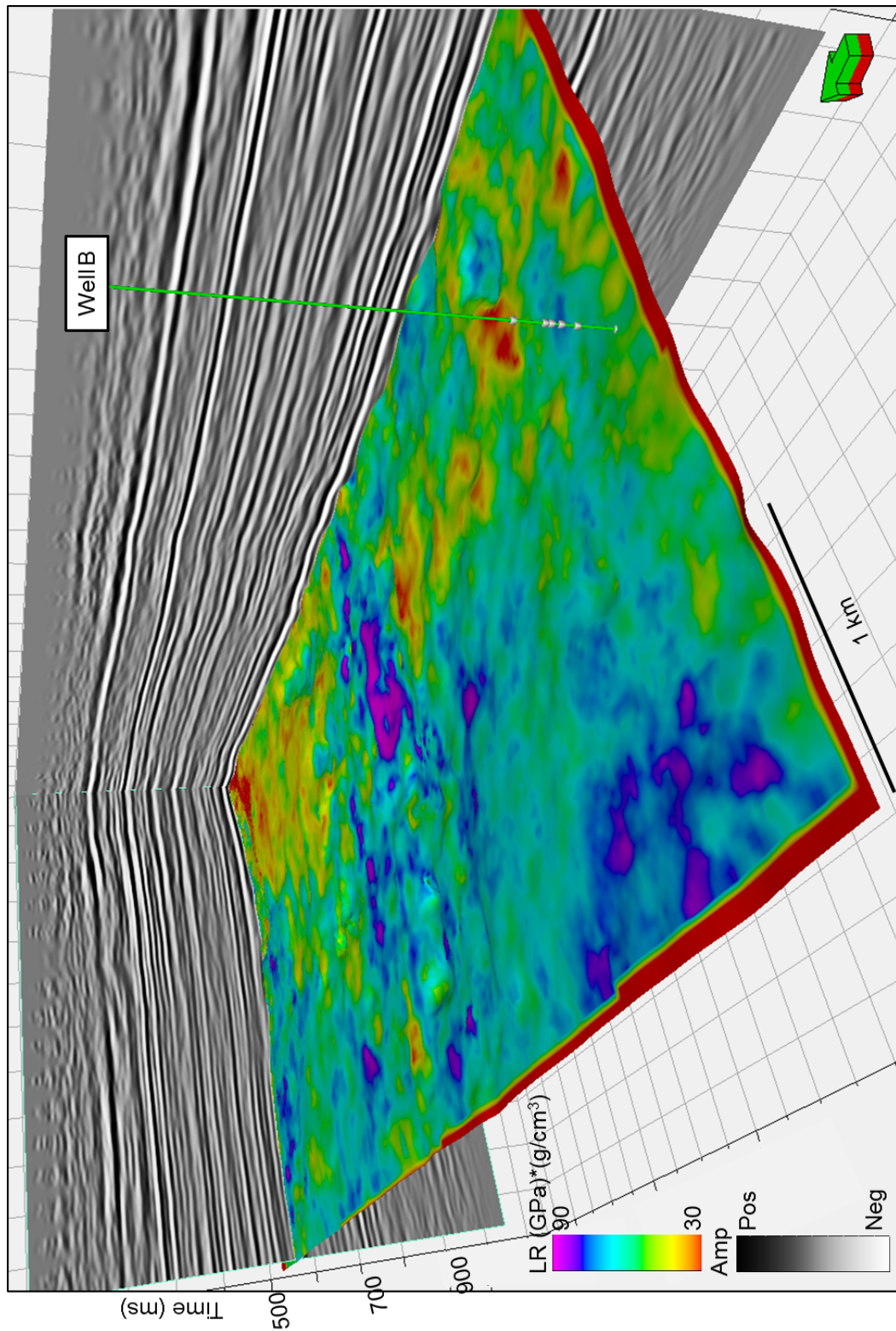
Figure 65: $\lambda\rho$ extracted on the top of the Mississippian horizon. Tripolite is indicated by low values of $\lambda\rho$, shown in warm colors.
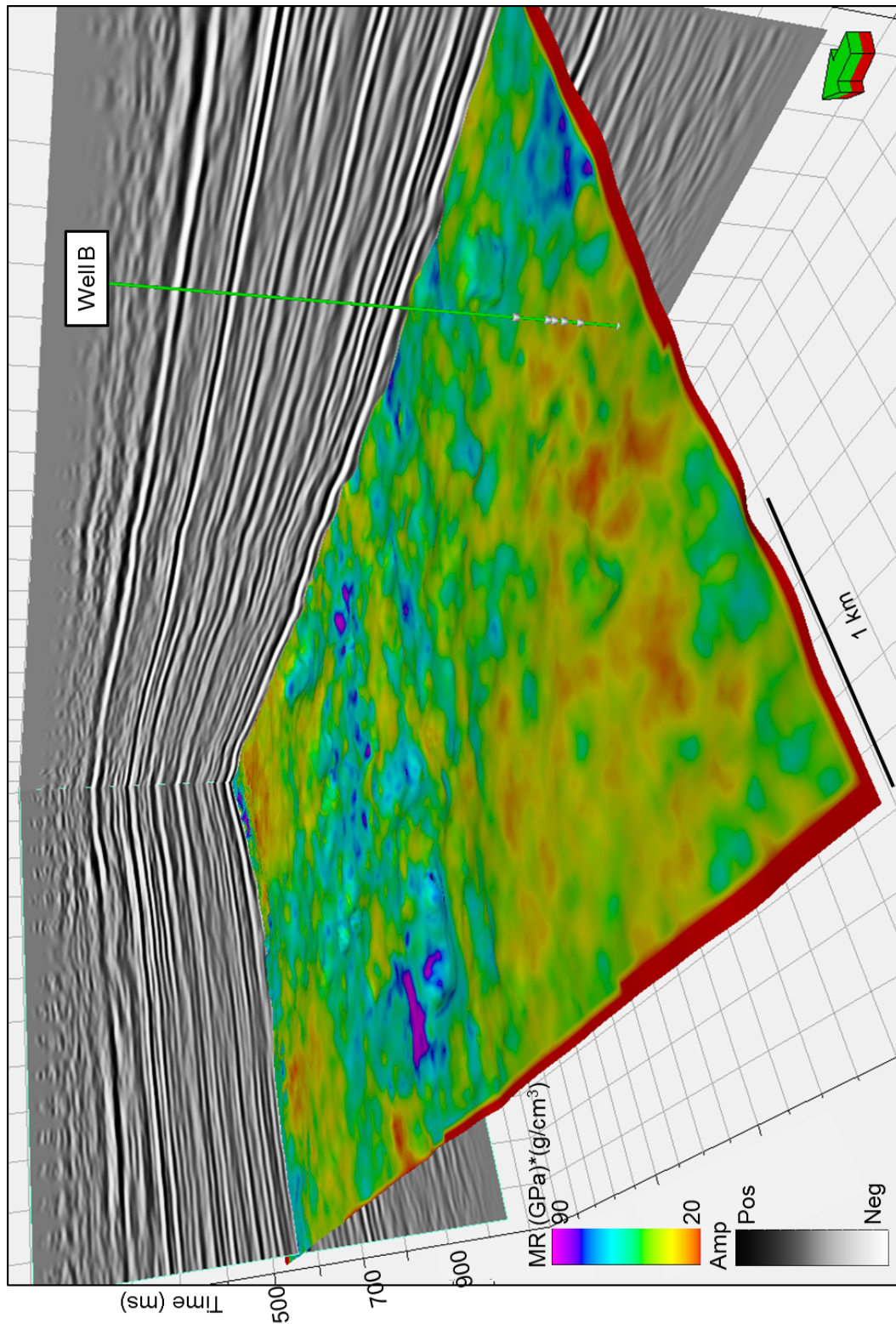
Figure 66: $\mu\rho$ extracted on top of the Mississippian horizon. Tripolite is indicated by low values of $\mu\rho$, shown in warm colors.

Figure 67 shows extracted geobodies after crossplotting the Z_P and Z_S inversion attribute volumes between the top of the Mississippian and Arbuckle, representing the entire Mississippian section. Using log crossplots as a guide, polygons can be picked that correspond with "Osage A" (yellow), "Osage B" (orange), and the St. Joe Limestone (red), and then 3D geobodies are extracted. The "Osage A" (yellow) geobody is laterally discontinuous and occurs almost entirely at the top of the Mississippian and represents tripolitic chert. The "Osage B" (orange) geobody is much more continuous and occurs mostly in the top half of the Mississippian. The St. Joe Limestone (red) geobody is largely continuous and occurs almost entirely at the bottom of the Mississippian. Figure 68 shows the geobodies extracted by crossplotting the V_P and density inversion attribute volumes and exhibits similar patterns.

Using the linear regression from the Z_P and PHIT crossplot in Figure 44, a total porosity attribute volume is created between the top of the Mississippian and Arbuckle. Figure 69 shows the geobodies extracted by crossplotting the total porosity and density attribute volumes. The yellow polygon and extracted geobody correspond with zones of high porosity and low density, both characteristic of tripolitic chert in "Osage A". The orange polygon and extracted geobody correspond with zones of low porosity and intermediate to high density, which is characteristic of the interbedded fractured limestone and chert of "Osage B". The red polygon and extracted geobody correspond with the very low porosity and high density St. Joe Limestone at the bottom of the Mississippian.
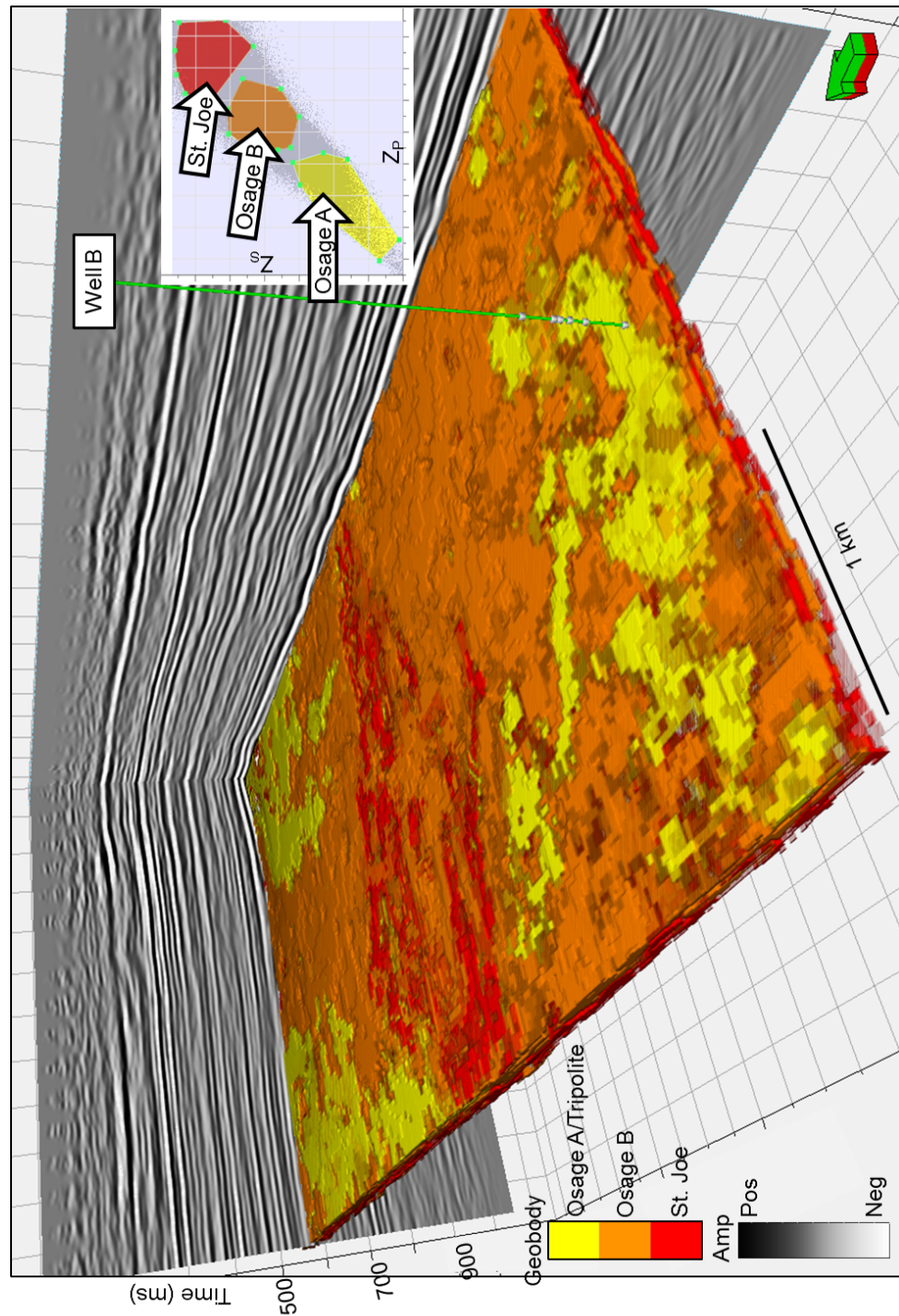
Figure 67: Geobodies extracted by crossplotting Z_P and Z_S attribute volumes between the top of the Mississippian and Arbuckle, using log crossplots as a guide for picking polygons. The "Osage A" (yellow) geobody corresponds with accumulations of tripolitic chert at the top of the Mississippian. The "Osage B" (orange) geobody corresponds with interbedded fractured tight limestone and chert, while the St. Joe Limestone (red) geobody corresponds with the chert-free limestone at the bottom of the Mississippian.

105
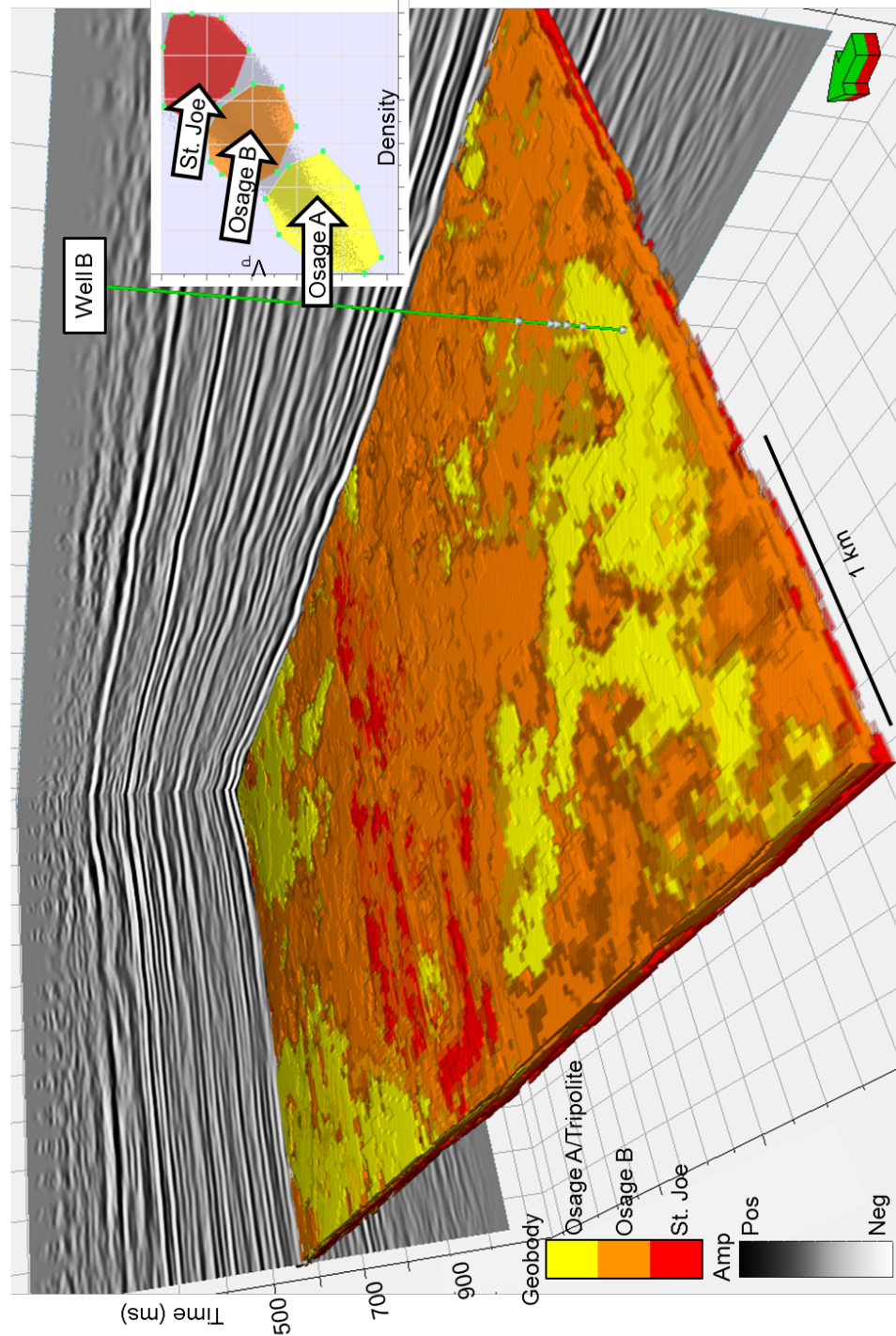
Figure 68: Geobodies extracted by crossplotting V_P and density inversion attribute volumes between the top of the Mississippian and Arbuckle, using log crossplotting as a guide for picking polygons. The "Osage A" (yellow) geobody corresponds with accumulations of tripolitic chert at the top of the Mississippian. The "Osage B" (orange) geobody corresponds with interbedded fractured tight limestone and chert, while the St. Joe Limestone (red) geobody corresponds with the chert-free limestone at the bottom of the Mississippian.
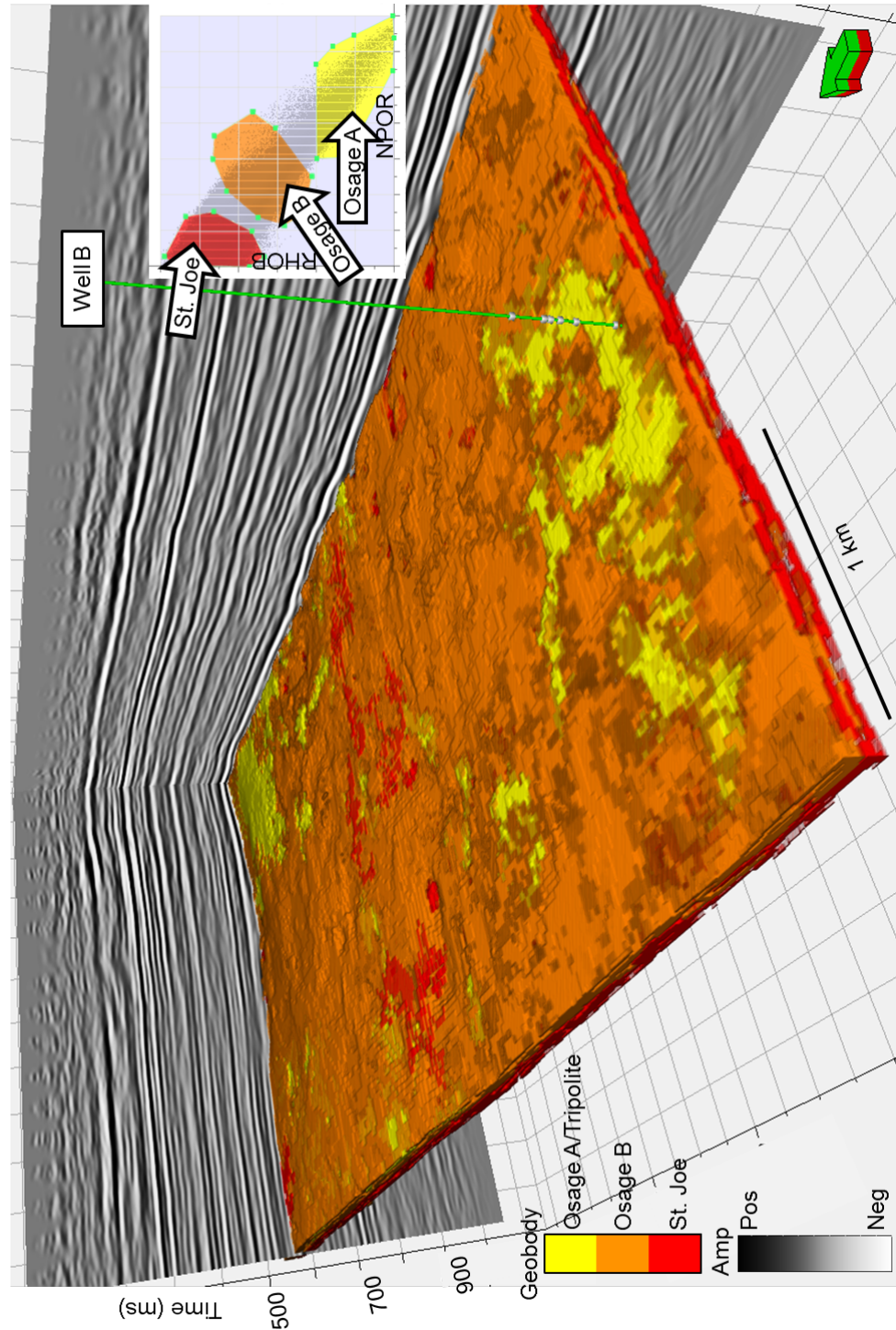
Figure 69: After creating a total porosity attribute volume using the linear regression from log crossplotting Z_P and total porosity, the total porosity attribute volume is crossplotted with the density attribute volume, and then geobodies are extracted. Accumulations of tripolitic chert are denoted by the yellow geobodies which correspond with zones of both low density and high porosity.

Figure 70 shows coherence extracted along the top of the Mississippian. Circular depressions along the top of the Mississippian are most likely karsts and may be filled with collapse breccias, which are an important part of Rogers' (2001) model for chert formation. Figure 71 shows coherence corendered with k_1 most-positive principal curvature, and Figure 72 shows coherence corendered with k_2 most-negative principal curvature. There appears to be several linear trends of karst development that may be associated with basement faulting as suggested by Elebiju et al. (2011).

Part of Rogers' (2001) model for tripolite deposition includes a detrital tripolitic chert facies, which should express as chaotic and lowly coherent on seismic. The lowly coherent zones seen in Figure 70-72 may correspond to detrital deposits of tripolite and collapse breccias, perhaps moved along fault zones detected by curvature and coherence. Zones that are highly coherent and correspond with paleohills observed on the TWT structure map of the Mississippian in Figure 51 are also likely accumulations of tripolitic chert. These zones are highlighted by the geobodies extracted in Figure 67-69 and the patterns observed in Figure 62-66. Conversely, tight limestone and chert seem to correspond with highly coherent areas which also reside in structural lows observed on the TWT structure map of the Mississippian in Figure 51.
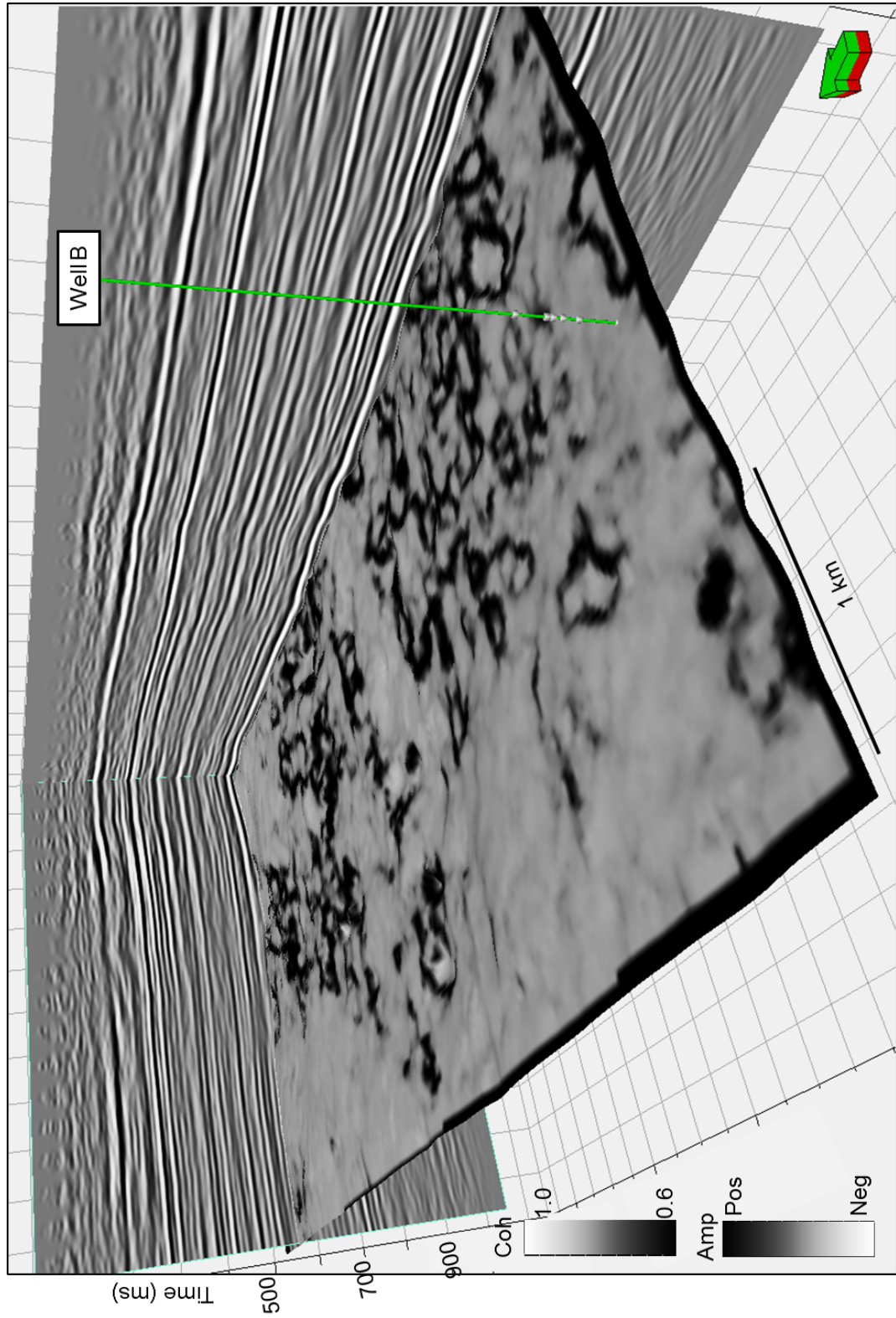
Figure 70: Coherence extracted along the Mississippian horizon. Circular feature along the surface are likely karst features, potentially filled with collapse breccias.

109
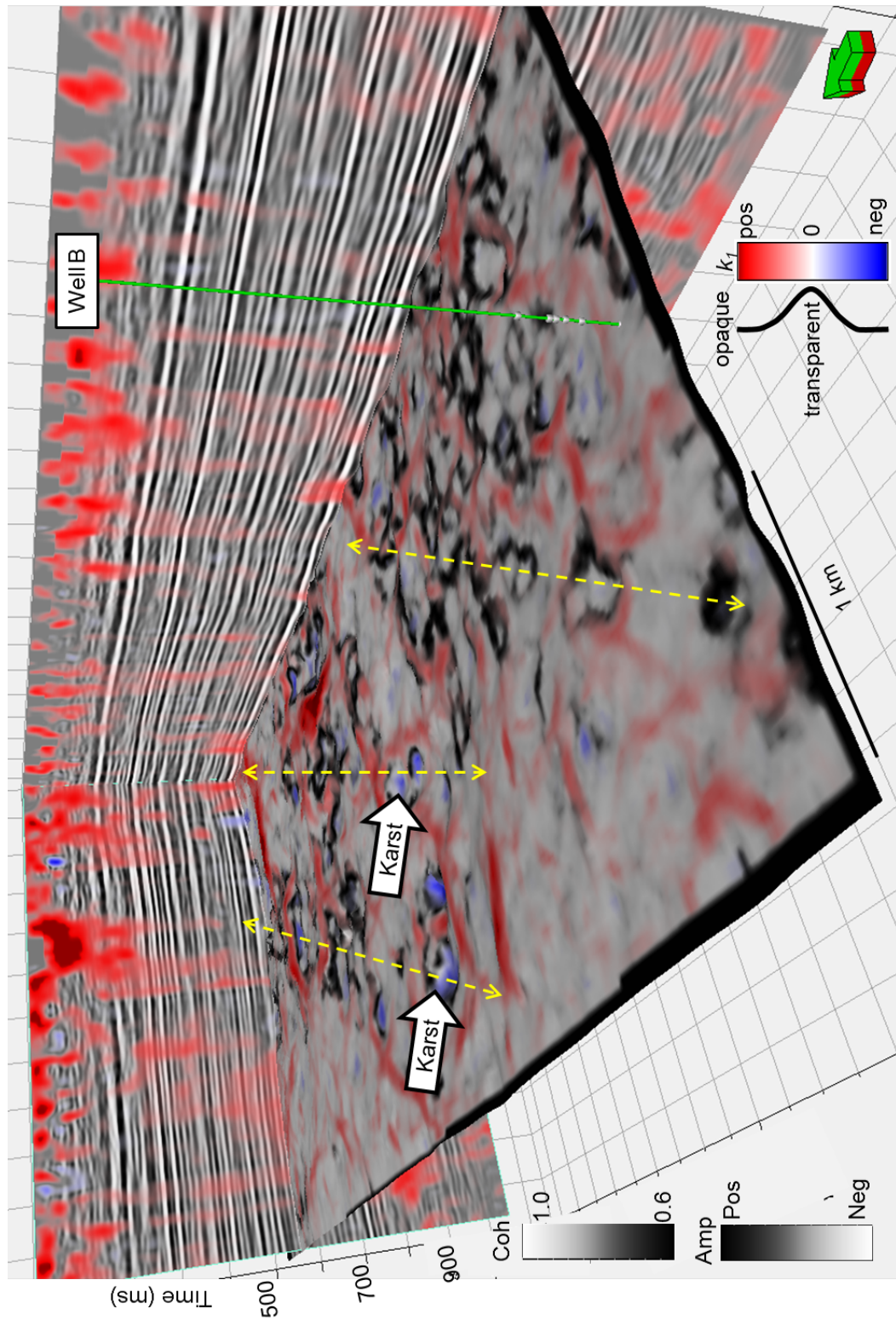
Figure 71: Coherence corendered with k_1 most-positive principal curvature. Curvature anomalies coinciding with coherence anomalies bolster my interpretation of karst features, and there appears to be several linear trends that may be associated with basement faulting.

110
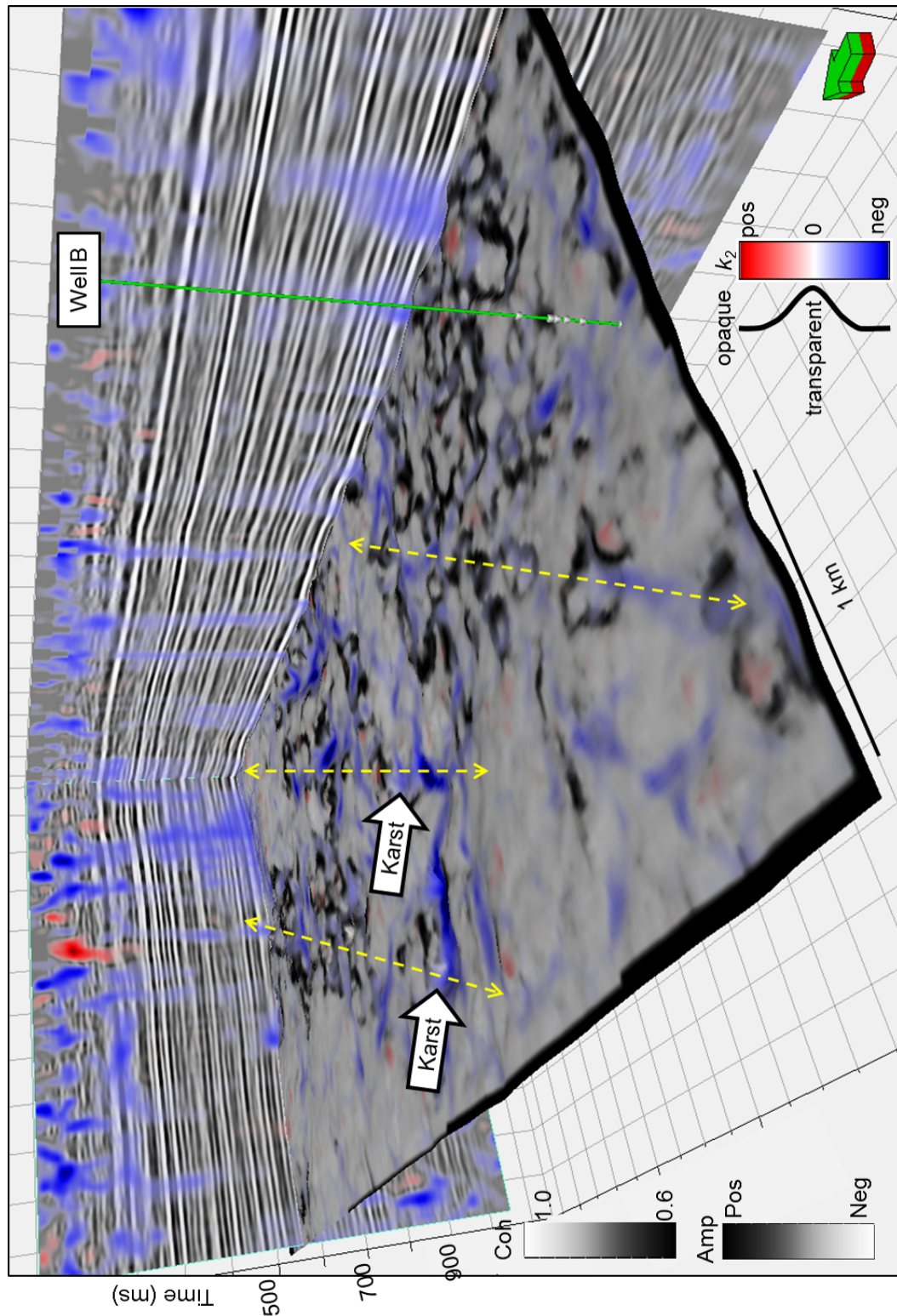
Figure 72: Coherence corendered with k_2 most-negative principal curvature along the top of the Mississippian. Curvature anomalies coinciding with circular coherence anomalies are likely karst features.

111

As previously mentioned, experiments by Staples (2011) and White (2013) suggest a relationship between fractures and curvature. Figure 73 shows an experiment in which a clay cake underwent plate bending, resulting in fracture formation along the hinge of the fold (Staples, 2011). The surface of the deformed clay cake was laser scanned and then its curvature was calculated, showing a relationship between fractures, strain, and curvature (Staples, 2011).

A 60 m section of a horizontal borehole image log from "Well B" is shown in Figure 74, both uninterpreted, above, and with interpreted natural fractures, below (White et al., 2012). Fracture density is then calculated using the interpreted natural fractures along the horizontal borehole image log (White et al., 2012). Expanding upon the relationship between curvature and fractures established by Staples (2011), White et al. (2012) show seismic amplitude corendered with curvature along a portion of vertical line BB' with fracture density along the horizontal borehole at "Well B", shown in Figure 75. White et al. (2012) observe a correlation between high fracture density, calculated from interpreted horizontal borehole image logs, and 3D structural curvature.

a)

b)
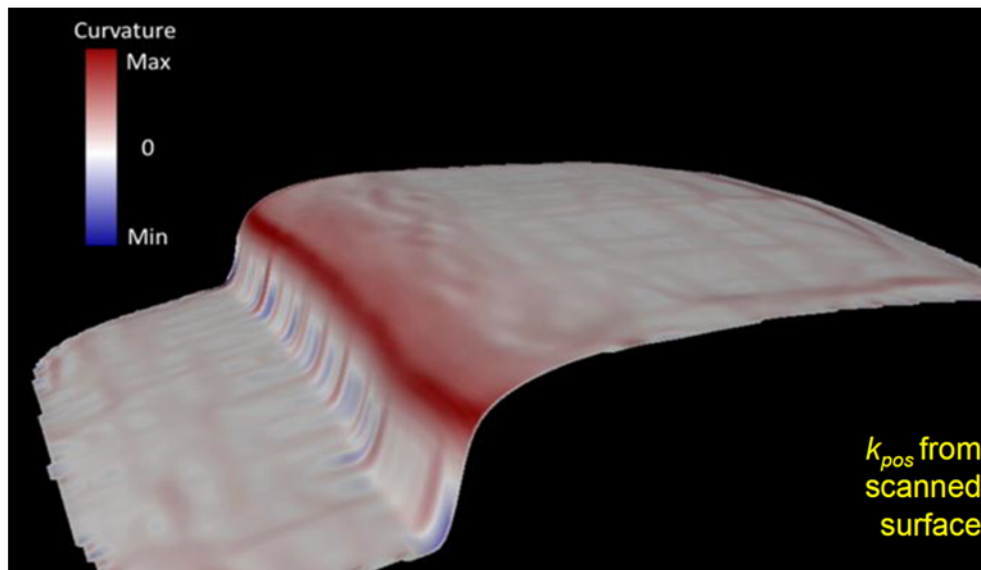
Figure 73: Plate bending experiment using a clay cake showing (a) fractures forming along the hinge of the fold, and (b) curvature anomalies corresponding with the zone of strain which resulted in fracture formation (Staples, 2011).
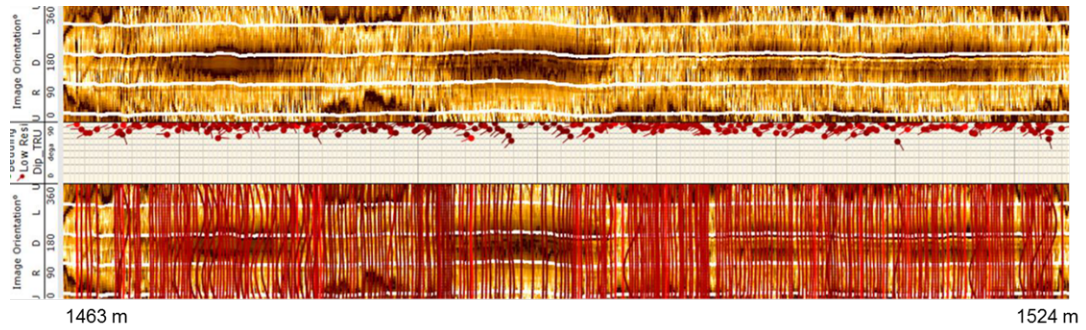
Figure 74: A 60 m section of a horizontal borehole image log from "Well B", both uninterpreted, above, and with interpreted natural fractures, below (White et al., 2012).
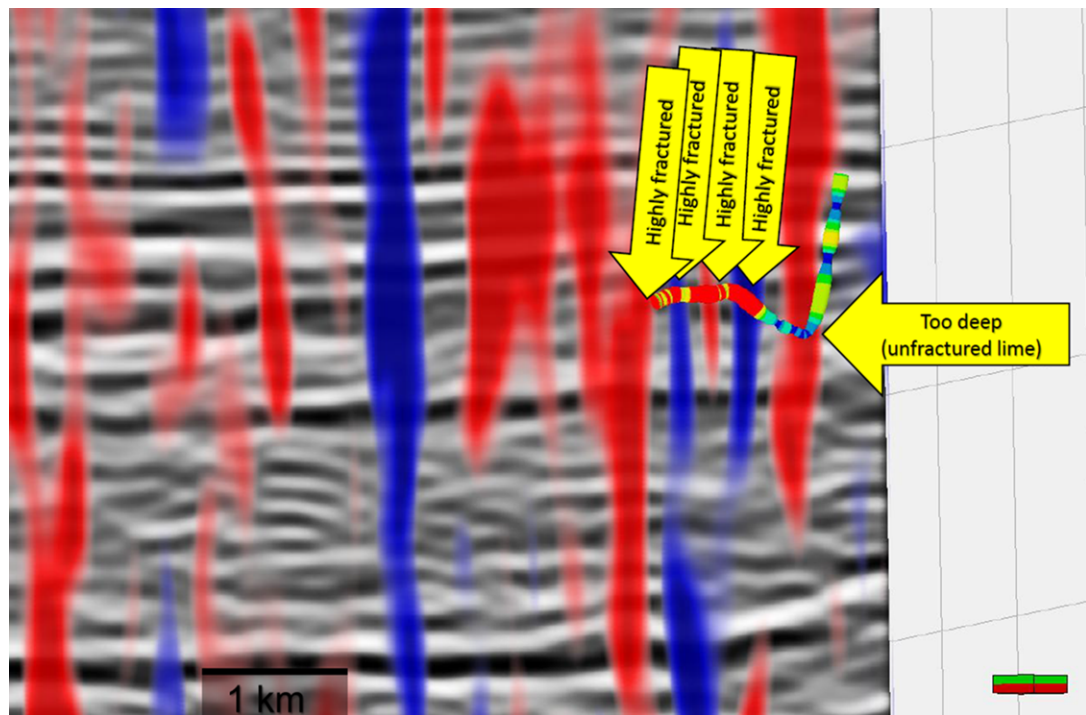
Figure 75: A portion of vertical line BB' showing seismic amplitude corendered with structural curvature, and the horizontal borehole at "Well B" with calculated fracture density from the interpreted natural fractures. A correlation between curvature and fracture density is observed (White et al., 2012).

Figure 76 shows Z_P extracted along the top of the Mississippian corendered with k_1 most positive principal curvature in grayscale. Figure 77 shows Z_P extracted along the top of the Mississippian corendered with k_2 most negative principal curvature in grayscale. Tripolitic chert "sweet spots" are defined as a convergence between low impedance values, which indicate zones of low density and high porosity, and intense curvature anomalies, which may indicate areas of high fracture density critical to producing from the tripolite. While k_1 and k_2 are sensitive to different features, both serve as a proxy to strain, and therefore both can be used as a proxy to zones of intense fracturing.
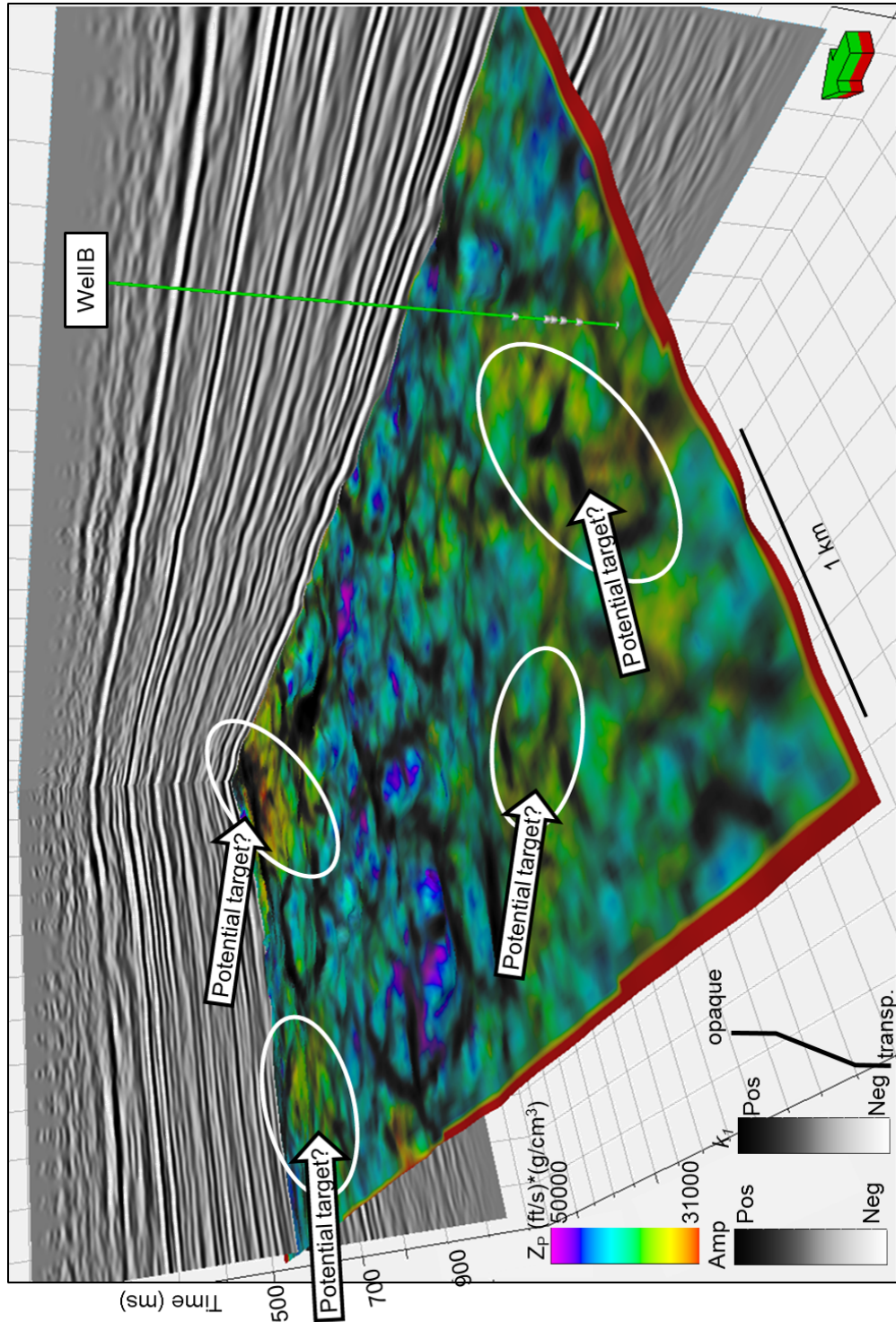
Figure 76: Z_P along the top of the Mississippian with k_1 most positive principal curvature corendered in grayscale. Tripolitic chert "sweet spots" are the convergence of curvature anomalies, indicative of strain and a proxy for fractures, and low values of impedance, indicative of a rock exhibiting high porosity and low density, which are both characteristics of tripolitic chert.
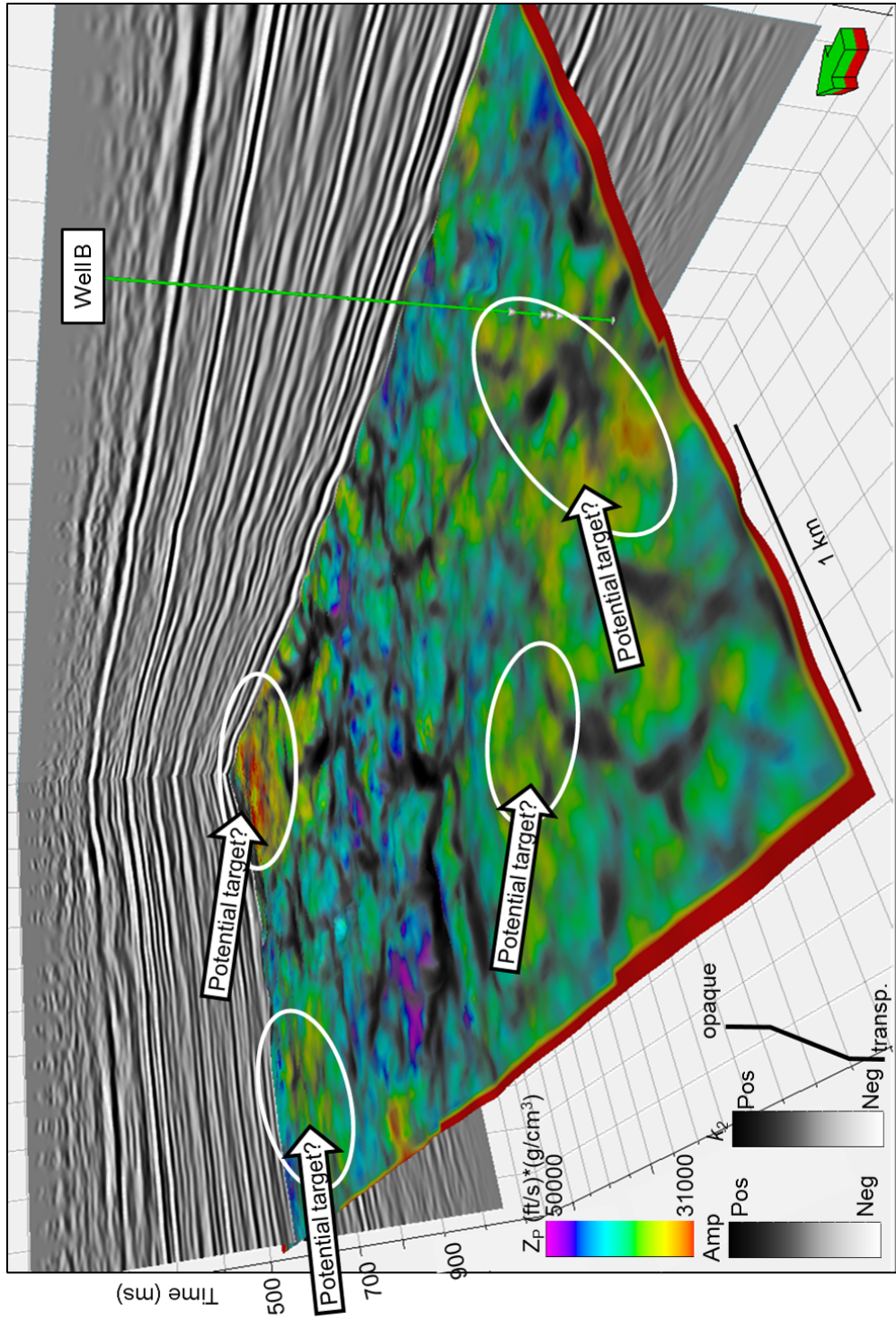
Figure 77: Z_P along the top of the Mississippian with k_2 most negative principal curvature corendered in grayscale. Tripolitic chert "sweet spots" are the convergence of curvature anomalies, indicative of strain and a proxy for fractures, and low values of impedance, indicative of a rock exhibiting high porosity and low density, which are both characteristics of tripolitic chert.

CHAPTER 5: CONCLUSIONS

Tripolitic chert is a complex reservoir rock, and its discontinuous lateral distribution makes it challenging to map. Characterized by low density and high porosity, it is very similar to unconsolidated sandstone. The fact that it coincides with nonporous chert and tight, highly fractured siliceous limestone adds to the reservoir complexity. It is a weathering, diagenetic product but does not have to occur at the top of the Mississippian. For these reasons, it is extremely beneficial to use seismic attributes calibrated to well control when mapping tripolitic chert.

I have shown that careful reprocessing of 3D prestack seismic data provides high quality data suitable for long-offset prestack inversion. By using surface consistent deconvolution, time-variant spectral whitening and scaling, structure-oriented filtering, and paying careful attention to velocity analysis and residual statics, I am able to resolve more reflectors with higher frequency. Realizing that operations such as FX deconvolution applied by the vendor can harm the data resolution, I have stayed away from such algorithms. The commercially-processed sub-700 ms basement appears very wormy. Careful reprocessing results in sub-basement structures that I interpret to be either layered volcanics or intrusives. Kirchhoff prestack time migration followed by velocity analysis, NMO, prestack structure-oriented filtering, and spectral whitening result in a properly imaged stack section and clean gathers with good offsets which can be used for prestack inversion.

Prestack inversion attributes applied to the long offset data provides an estimate of not only Z_P and Z_S, but also density, which is the single best discriminator of tripolite. Log crossplots provide an improved estimation and guide for crossplotting seismic inversion attribute volumes. The siliceous limestone, interbedded tight, fractured limestone and chert, and the tight St. Joe Limestone are also easily mapped. Geometric attributes such as coherence and curvature not only show faults and karsts, but are correlated to fractures seen in the horizontal image logs (White et al., 2012). Thus, an ideal target would be to drill horizontally in the thin bedded lime and chert perpendicular to folds ("fractures") that fall below the tripolite seen on the impedance inversion.

REFERENCES

Angelo, S.M., 2010, Integrated seismic texture segmentation and clustering analysis to improved delineation of reservoir geometry: Master's Thesis, University of Oklahoma, Norman, Oklahoma, 29 p.

Bass, N.W., 1942, Subsurface geology and oil and gas resources of Osage County, Oklahoma: USGS Bulletin 900-K, 343-393.

Blakey, R., 2011, Colorado Plateau stratigraphy and geology and global and regional paleogeography: Northern Arizona University of Geology, http://www2.nau.edu/rcb7/RCB.html, accessed 03/26/2012

Cary, P.W. and G.A. Lorentz, 1991, Four-component surface-consistent deconvolution: annual SEG expanded abstracts SP4.2.

Chopra, S. and K.J. Marfurt, 2007, Seismic attributes for prospect identification and reservoir characterization: Tulsa, Oklahoma, Society of Exploration Geophysicists, 464 p.

Dowdell, B.L., A. Roy, and K.J. Marfurt, 2012, An integrated study of a Mississippian tripolitic chert reservoir – Osage County, Oklahoma, U.S.A.: SEG Expanded Abstract.

Elebiju, O.O., S. Matson, G.R. Keller, and K.J. Marfurt, 2011, Integrated geophysical studies of the basement structures, the Mississippian chert, and the Arbuckle Group of Osage County region, Oklahoma: AAPG Bulletin, **95**, 371-393.

Farzaneh, S., 2012, An integrated paleomagnetic and diagenetic study of the Mississippian limestones in northern Oklahoma: Master's Thesis, University of Oklahoma, Norman, Oklahoma, 98 p.

Franseen, E.K., A.P. Byrnes, J.R. Cansler, D.M. Steinhauff, and T.R. Carr, 2004, The geology of Kansas – Arbuckle Group: Current Research in Earth Science, Kansas Geological Survey Bulletin, **250**, 43 p.

Goodway, B., T. Chen, and J. Downton, 1997, Improved AVO fluid detection and lithology discrimination using Lamé petrophysical parameters; "λρ", "μρ", & "λ/μ fluid stack", from P and S inversions: SEG Expanded Abstract.

Johnson, K.S., 2008, Geologic History of Oklahoma, Oklahoma Geological Survey.

Johnson, K.S., and B.J. Cardott, 1992, Geologic framework and hydrocarbon source rocks of Oklahoma, *in* K.S. Johnson and B.J. Cardott, eds., Source rocks in the southern Midcontinent, 1990 symposium: OGS Circular, **93**, p. 21-37.

Karr, B. and R.A. Hefner, 2010, Long sweep times increase the recoverable higher frequencies for Mid-continent seismic data: SEG 80th Annual Convention Expanded Abstract.

Matos, M.C., M. Yenugu, S.M. Angelo, and K.J. Marfurt, 2011, Integrated seismic texture segmentation and cluster analysis applied to channel delineation and chert reservoir characterization: Geophysics, **76**, P11-P21.

Nissen, S.E., T.R. Carr, and K.J. Marfurt, 2006, Using new 3-D seismic attributes to identify subtle fracture trends in Mid-Continent Mississippian carbonate reservoirs: Dickman Field, Kansas: Search and Discovery Article #40189.

Matson, S., 2013, Mississippi Lime: Kinematics of a play: AAPG Mississippian Lime Forum, Oklahoma City, OK.

Northcutt, R.A., K.S. Johnson, and G.C. Hinshaw, 2001, Geology and petroleum reservoirs in Silurian, Devonian, and Mississippian rocks in Oklahoma, *in* K.S. Johnson, ed., Silurian, Devonian, and Mississippian geology and petroleum in the southern Midcontinent, 1999 symposium: Oklahoma Geological Survey, Circular **105**, p. 1-15.

Oklahoma Geological Survey, Oklahoma counties reference map, available at web: http://ogs.ou.edu/pdf/counties.pdf ; accessed 10-19-2012.

Rogers, S.M., 1996, Depositional and diagenetic history of the Mississippian chat, north-central Oklahoma: Master's Thesis, University of Oklahoma, Norman, Oklahoma, 121 p.

Rogers, S.M., 2001, Deposition and diagenesis of Mississippian chat reservoirs, north-central Oklahoma: AAPG Bulletin, **85**, 115-129.

Roy, A., B.L. Dowdell, and K.J. Marfurt, 2012, Characterizing a Mississippian Tripolitic Chert reservoir using 3D unsupervised seismic facies analysis and well logs: an example from Osage County, Oklahoma: SEG Expanded Abstract.

Snyder, R., R. Carter, R. Haveman, D. Jacobs, and W. Spitzer, 2013, A case history of the East Hardy Unit Mississippian Highway 60 Trend, Osage

County, Oklahoma: AAPG Mississippian Lime Forum, Oklahoma City, OK.

Staples, E., 2011, Subsurface and experimental analysis of fractures and curvature: Master's Thesis, University of Oklahoma, Norman, Oklahoma, 100 p.

Thorman, C.H. and M.H. Hibpshman, 1979, Status of mineral resources information for the Osage Indian Reservation, Oklahoma: U.S. Geological Survey and Bureau of Mines, Administrative Report BIA-47, p. 1-60.

University of Texas Libraries, Perry-Castaneda Library map collection, USA outline map, available at web: http://www.lib.utexas.edu/maps/united_states/usa_blank.jpg ; accessed 10-19-2012.

Walton, R., 2011, Horizontal drilling breathes new life into Mississippi Lime oil region: TulsaWorld, http://www.tulsaworld.com/business/article.aspx?subjectid=49&articleid=20110924_49_e1_cutlin919814 , accessed 03-26-2012.

Watney, W.L., W.J. Guy, and A.P. Byrnes, 2001, Characterization of the Mississippian chat in south-central Kansas: AAPG Bulletin, **85**, 85-113.

White, H., 2013, Calibration of surface seismic attributes to natural fractures using horizontal image logs: Master's Thesis, University of Oklahoma, Norman, Oklahoma, In press.

White, H., B.L. Dowdell, K.J. Marfurt, and Z. Reches, 2012, Calibration of surface seismic attributes to natural fractures using horizontal image logs, Mississippian Lime, Osage County, Oklahoma: SEG Expanded Abstract.

Yenugu, M., K.J. Marfurt, and S. Matson, 2010, Seismic texture analysis for reservoir prediction and characterization: The Leading Edge, **29**, 1116-1121.

Yenugu, M., K.J. Marfurt, C. Wickstrom, and S. Matson, 2011, Correlation of AVO inversion methods with porosity seen on logs and cores: A case study for Mississippian chert reservoirs of Oklahoma, USA: SEG Expanded Abstract.

Yenugu, M., and K.J. Marfurt, 2011, Relation between seismic curvatures and fractures identified from image logs – application to the Mississippian reservoirs of Oklahoma, USA: SEG Expanded Abstract.

Zeller, D.E., 1968, The stratigraphic succession in Kansas: Kansas Geological Survey Bulletin, **189**, 81 p.

Zhao, M., 2011, Petrologic and petrophysical characteristics: Mississippian Chert, Oklahoma: Master's Thesis, Oklahoma State University, Stillwater, Oklahoma, 84 p.

APPENDIX A: 3D PRESTACK TIME PROCESSING

A large portion of my thesis work involved reprocessing a 3D land seismic survey. My dataset is a prestack time survey from the Midcontinent U.S.A. consisting of raw gathers with refraction and elevation statics applied. The purpose of this appendix is to document in detail how I reprocessed the data in hopes that it can be of some use to those who come after me. For my thesis, I used Landmark's ProMAX 3D software which has generously been provided to the University of Oklahoma for educational work. Any 3D seismic processing package can be used, however. I also use AASPI's prestack utilities for migration and other data conditioning steps. In addition to this appendix, I refer the reader to an accompanying slideshow that details each flow with parameterization as well as displays, which I include with this thesis as a DVD. If I do not explicitly mention changing a parameter throughout this appendix, it is then implied that I use the default setting.

The first step is to import the SEGY seismic data into ProMAX. My first flow is "01-import" which contains SEGY Input, Extract Database Files, and Disk Data Output. In the parameters for SEGY Input, I use the file browser to locate the SEGY file I want to import. Next, I set the sort order to SHOT and change the maximum number of traces per ensemble to 9999, indicating that this number is unknown. If I knew the exact number, I could set it here, but there is a risk that a certain ensemble will have more traces and this would result in a truncated ensemble. Next, I choose to remap the SEGY header values because I know that my trace headers do not conform to the SEGY

Revision 1.0 standard. The two headers I have to add are SOU_SLOC and SRF_SLOC, which are the source and receiver location numbers, respectively.

Once I have set the parameters for SEGY Input, I set up the parameters for Extract Database Files, which will begin building the ProMAX database from the trace headers. I set the data type to land, the source index type to FFID (Field File Identification Number), and the receiver index method to coordinates. As this extraction is prior to creating the geometry, I set the pre-geometry extraction check to yes. Finally, in Disk Data Output I create a name for the output dataset and set the trace sample format to 32 bit.

The next step after the SEGY file has been imported and written to disk in ProMAX's internal format is to create the geometry in the database. My next flow is "02-geometry" and consists of Disk Data Input, Trace Header Math, Database/Header Transfer, and 3D Land Geometry Spreadsheet. For Disk Data Input I select the file I just created in the previous import step. I use Trace Header Math to define the source and receiver line headers (S_LINE and R_LINE, respectively) from the source and receiver location numbers (SOU_SLOC and SRF_SLOC, respectively). Next, I transfer the newly created trace headers to the database using Database/Header Transfer, setting the direction of the transfer as loading from the trace header to the database. The 3D Land Geometry Spreadsheet does not have any parameterization.

A interactive menu appears as 3D Land Geometry Spreadsheet runs. The first step is to click Setup and a new menu appears. I set the midpoint assignment method to "Existing index number mappings in the TRC" meaning

that the trace database is used to assign midpoints. I set the nominal receiver and station interval to 220.0 and the nominal crossline separation to 660.0. I leave the nominal survey azimuth as it is. I set the source type to surface seismic source as the data was acquired using Vibroseis and the units to feet. Then I click ok to exit the setup.

Next, I click the Receivers menu in the 3D Land Geometry Spreadsheet. I see that the station, x, y, elevation, and line columns are all filled. Because the elevation statics are applied, I set the elevation to 1500 ft using the edit menu in the receiver spreadsheet. Then I exit the receiver spreadsheet and open the sources spreadsheet. Again, I set the elevations to 1500 ft. By clicking View > View All > Basemap, I can plot a map of all the sources and receivers. This is useful for determining how many lines are live for any given shot. For my survey, there are 10 live receiver lines per shot, and each receiver line has 52 active geophones for 520 traces per ensemble. I can also see that source line 513 was the overlap of the two patches, with some shots recorded in patch 1 and some recorded in patch 2. I close the Basemap view and exit the sources spreadsheet.

Next, I click on Bin which brings up the 3D Binning and QC menu. The first step is to assign the midpoints, so I click this option and click "OK". After assigning midpoints, I click Define Binning Grid and click "OK". This brings up XYgraph display. I click Display > Midpoint > Control Points > White. This plots all of the midpoints as white dots. Next, I click Grid > Display which brings up a small blue grid in the lower left hand corner. I then click Grid > Parameterize

which displays the grid parameters. I set the azimuth to 358.98 degrees. The cell size along azimuth (dy and dx) are equivalent to the midpoint binning grid size, which for this survey is 110 ft by 110 ft, which is what I enter for dy and dx. The number of cells along the azimuth (ny) is equivalent to the number of crosslines, which I know is 198 from a stacked version of the data. Similarly, the number of cells along the azimuth (nx) is the number of inline which I set to 402. Finally, I enter the X and Y origin coordinates, which are 2399729.25 and 667392.00, respectively. I click the green stoplight button which creates a grid matching these specifications and closes the window. I now see a blue grid that covers all of my midpoints. I use the zoom tool to check all four corners of the survey to ensure that the grid covers all the corners without any midpoints falling outside of the grid. I then use the zoom tool to check several locations inside of the grid to ensure that the midpoints fall within the bins and not along the bin lines themselves. With the binning grid satisfactorily defined, I click Grid > Save to and give the grid a name. Then I exit XYgraph.

With the midpoint grid defined, I click Bin midpoints in the 3D Binning and QC dialog. This brings up the 3D Land Midpoint Binning dialog. I click the "Load" button at the bottom and select the binning grid I defined in the previous step. This loads all my parameters into the menu and I click "Apply". After midpoint binning is complete, I click "Cancel" to close the dialog.

Back in the 3D Binning and QC menu, I select QC Bin Data, click the "QC Bin Space" button selecting my midpoint grid, and click "OK". The default QC type is Coordinate Space Fold which will display a fold map. The other

options are Line Space Fold, Spider, and Mid-Points. Once I am satisfied with the midpoint binning, I select Finalize Database and click "OK". Once the database is finalized, click "Cancel" to exit the 3D Binning and QC dialog.

I now click TraceQC which brings up a new spreadsheet. This spreadsheet should be entirely filled out with the exception of the FB Pick column. Under the view menu are more options to QC various geometries. I close the spreadsheet and click File > Exit to quit the 3D Land Geometry Spreadsheet. Geometry assignment is now complete, and the next step is to apply the geometry in the database to the trace headers of the dataset.

Before applying the geometry to the data, I first want to test for True Amplitude Recovery, define several time gates for Time-Variant Scaling, and decide how to define patch 1 and patch 2 for later phase matching. I create a flow for True Amplitude Recovery testing that consists of Disk Data Input, Parameter Test, True Amplitude Recovery, and Trace Display. I select the raw input dataset, sorting by Field File Identification Number (FFID) and Absolute value of Offset (AOFFSET). I set the sort order to "*:200-3000/" which means get all FFIDs and limit the AOFFSET from 200 to 3000 ft. I set Parameter Test to "2|4|6|8|10|12" for the various dB/sec corrections I wish to test. I then set Apply dB/sec correction to yes in the TAR parameters and enter 99999.0 for the correction constant to indicate I want to use values from Parameter Test. As I am testing six correction values, I set the number of ensembles per screen in Trace Display to six. I change the primary and secondary trace labels to match my sort order in Disk Data Input. I then execute the flow. Trace Display opens

and I see six panels in the window, each labeled by the dB/sec correction constant it uses. Each panel uses FFID 1 between 200 and 3000 ft AOFFSET. After inspecting each panel, I decide the most balanced panel is between 8 and 10 dB/sec correction, so I will use a value of 9.

Next, I want to define a series of time gates for Time-Variant Scaling (TVS). I build a flow consisting of Disk Data Input and Trace Display. Again, the sort order is FFID and AOFFSET, but now I have it set as "*:*" meaning all FFIDs and AOFFSETs are used. I only want one ensemble per screen, so I set this value to one and I execute the flow. In the Trace Display window, I click Picking > Miscellaneous Time Gates. I give the gate the name TVS-FFID and select AOFFSET for the secondary header key. I then proceed to pick four time gates with the top of the next gate overlapping the bottom of the previous gate. Once I have picked a layer, I use the right mouse button to project the picks and then select a new layer. Once I have finished picking the time gates I click File > Save Picks and then exit Trace Display.

Finally, before I apply the geometry I must decide how to delineate records in patch from those in patch 2. I open DBTools (Database Tools) and navigate to the SIN (Source Database) tab. Then I click View > 2D Matrix. This brings up a window with four selections – Horizontal, Vertical, Color, and Histogram. I select X coordinate for the horizontal axis and Y coordinate for the vertical. Then I choose S_LINE for both color and histogram. The resulting plot shows the source lines as laid out for the survey. I do the same for the SRF (Receivers Database), this time using receiver station (STATION) for color and

histogram. I now have two plots showing the geometry of the source and receiver lines.

There are six icons on the left hand side of the plot window. The third one down allows me to select sources or receivers using an arbitrary polygon. The fourth icon down tracks the values when I mouse over the plot and displays the values in the bottom portion of the window. I click the arbitrary selection tool in the sources plot window and select source line 513 which I earlier identified as the overlap between patch 1 and patch 2. I then click Project > SRF. This shows that all of the receivers record shots along source line 513. Next, I select source lines 514-526 which make up patch 2. Projecting the SIN selection onto the SRF plot, I see that receivers xxx1049-xxx1100 are active for source lines 514-526. I then select source lines 501-512 and project them onto the SRF plot. Receivers xxx1001-xxx1051 are active for source lines 501-512. This tells me that receivers xxx1049-xxx1051 overlap for patches 1 and 2. From this I determine that patch 1 is defined as source lines 501-513 and receivers xxx1001-xxx1051 while patch 2 is defined as source lines 513-526 and receivers xxx1049-xxx1100. This information will be used in the geometry application step.

Now that I have finished several intermediary steps, I am ready to apply the geometry to the trace headers of the ProMAX dataset. This allows the trace headers to be used to reference the database. The flow I build for "03-Geom-Apply" is as follows: Disk Data Input, Inline Geom Header Load, True Amplitude Recovery, Time-Variant Scaling, Database/Header Transfer, IF > Trace Header

Math > ENDIF, Database/Header Transfer, Trace Header Math, IF > Trace Header Math > ELSEIF > Trace Header Math > ENDIF, Database/Header Transfer, Disk Data Output. I select the raw dataset for Disk Data Input and set the trace read option to get all traces. I set the primary header for database matching in Inline Geom Header Load to FFID and all other options to No. I set True Amplitude Recovery to apply dB/sec correction with a constant value of 9. I use the gate I picked earlier for Time-Variant Scaling. I use the first Database/Header Transfer to load the TRC GEOMETRY AZIMUTH header from the database to the trace header as AZIM. I then set the IF statement to exclude values of AZIM between 0 and 179.999. I then use Trace Header Math to calculate azimuths beyond 180 as negative using the equation AZIM=AZIM-180. This sets the azimuth to range between +/- 180 instead of 0-360 degrees. I then load the TRC GEOMETRY AZIM header I created from the trace header to the database. I use another Trace Header Math to define receiver station numbers without the receiver line prefix. I create a new header I call R_STATN and set it equal to the modulo function of SRF_SLOC (Receiver Station Number with Receiver Line prefixed) and 10000. This gives values of 1001-1100.

Now I begin the process of defining the two patches. Using an IF statement, I include traces with a primary trace header of S_LINE and secondary trace header of the newly created R_STATN using an order of "501-513:1001-1051/". As I previously mentioned, this is how I will define patch 1. I then insert a Trace Header Math creating a new trace header I call survey and set the included traces to "survey=1". Next, I use ELSEIF and include traces

from primary trace header S_LINE and secondary trace header R_STATN with a sort order of "513-526:1049-1100/". Again, I follow this with a Trace Header Math but this time I use the equation "survey=2". I have now defined patches 1 and 2 based off source lines and receiver stations. I then use Database/Header Transfer in which I load from the trace header to the database, creating a new database entry in TRC TRCSTATS SURVEY using the trace header SURVEY I created. Finally, I use Disk Data Output to write the dataset with the geometry applied, setting the trace sample format to 32 bit. Once the flow is finished running, the job log should say that the geometry loaded in the trace headers matches the database and that trace numbers can be used to reference the database.

I now want to use DBTools to QC my definition of patch 1 and patch 2. I open DBTools selecting TRC and click View > 2D Matrix. I select CMP X for the horizontal axis, CMP Y for the vertical axis, and SURVEY for the color and histogram. The resulting plot shows the two patches split in the middle of the survey along the horizontal direction, just as I wanted. In the histogram, I can click on either vertical bar, one of which is at 1 and the other at 2, which allows me to select all CMPs falling in either patch 1 or patch 2. I click on the bar for patch 1. Then I use DBTools to plot source lines and receiver stations just as I did earlier. Using the selection tool in the SURVEY plot, I select all of patch 1 and project onto both the SIN and SRF plots. I see that patch 1 is exactly as I defined it. I then click the vertical bar for patch 2 in the SURVEY histogram and then use the selection tool to select all of patch 2. I project the selection onto

the SIN and SRF plots, and again patch 2 is exactly as I defined it. This will be important later when I want to phase match patch 1 to patch 2.

At this point, it is a good idea to examine the spectral content of my data. I build a flow I call "view-spectra" which consists of Disk Data Input, Bandpass Filter, and Interactive Spectral Analysis. I input my dataset with geometry applied, sorting by SOU_SLOC and AOFFSET. I pick a single source station of 5051076 and get all offsets. I turn off the bandpass filter by right clicking it with the mouse. In the parameters for Interactive Spectral Analysis I set the data display to ensembles, and set the primary and secondary trace header labels to match the sort order in Disk Data Input. I then execute the flow.

The Interactive Spectral Analysis window opens, and there are four panels. The upper left panel is the ensemble which in this case is a shot gather. The lower left panel is an F-X plot. The upper right panel is the frequency plot while the lower right panel shows the phase. I see that my raw gathers with geometry applied has a frequency range of about 15-110 Hz with a notch at about 42 Hz and a drop of -10 dB starting at 50 Hz up to 110 Hz. After 110 Hz the frequency sharply rolls off. The default view for the frequency is in dB power. It is also useful to examine the percent power, which can be selected by clicking View > Power Spectrum. I exit the viewer and turn the bandpass filter on by right clicking it. I begin by investigating the low frequencies. I set the bandpass filter as an Ormsby zero phase frequency filter with corners of 0-2-22-24 Hz. Executing the flow brings the interactive viewer back up. I notice that in the selected frequency range, most of the data is

ground roll with only a small amount of actual data. I then set the bandpass filter to 20-24-110-120 Hz. Even with such a severe low cut there is still considerable ground roll leaking into the data. With this in my, I design a bandpass of 10-20-90-120 Hz. This allows me to retain some of the low frequency data, but with a gradual ramp from 10 to 18 Hz, minimizing some of the ground roll. Although the data was recorded at a 2.0 ms sample interval which translates to a Nyquist frequency of 250 Hz, there appears to be no frequency content beyond 120 Hz.

Next, I build a flow to calculate some trace statistics in order to perform some trace edits, called "04-trace-statistics". The flow is simple and consists of Disk Data Input and Trace Statistics. I read in the data with geometry applied and set the trace read option to get all traces. For the types of trace statistics to compute, I select TRCAMP, SPIKES, FRQ_PK, FRQ_DV, and ADECAY. TRCAMP is the average trace energy. SPIKES is a measure of the spikiness of the data, defined as the maximum amplitude divided by the average amplitude. FRQ_PK measure the peak frequency of the data while FRQ_DV measures the statistical deviation of the frequency. ADECAY is a measure of the estimated energy decay rate of the data. I chose YES to get the analysis gate from the database and see that I need to pick one. I fire up a trace display using FFID and AOFFSET and select Picking > Pick Miscellaneous Time Gates. I call it TRCSTATS and select AOFFSET as the secondary key. I pick the top of the gate slightly above the first breaks, following the contour of the first breaks, project it by right clicking the mouse and then create a new layer. The second

134

layer I pick across the bottom of the data as a flat layer. I then save the picks and exit the trace display. I can now select the time gate table I just picked and then execute the flow.

While I wait for the trace statistics to run, I decide to pick a top mute. I want to use about four or five shot gathers to check for spatial variability. I use DBTools and create a 2D matrix plot of the source index numbers by x and y coordinates. I use the mouse tracker to pick out five locations, one in the mid-section of each corner and one in the center of the survey. I take note of the source numbers for a view shots flow. This flow consists of Disk Data Input and Trace Display. I set the primary trace header key to Live Source Number (SIN) and the secondary trace header key to Recording Channel Number (CHAN). My sort order list is "5051305, 5041061, 5151199, 5201341, 5211079:*/" which is the five shots I selected an all channels for each shot.

In the trace display window, I click Picking > Pick Top Mute. I call the mute table "Top Mute" and set the secondary key to AOFFSET, even though I used recording channels in the sort order. I see ten records, one for each cable that is live for the shot. A flag identifies the receiver cable that is collocated with the shot for that particular record. I put a pick at the top of the cone for this cable, and make another pick at the base of the cone on one side. I then right click the mouse and click project, which projects this pick for the entire shot across all cables. If the geometry is properly applied, the project pick will follow the contour of each record within the shot. Pleased with the pick, I save it and click the arrow to go to the next shot to check how the project pick holds up.

Once I am satisfied that the pick does well for shots in different parts of the survey, I save once more and exit. Back in the flow parameters, I change the secondary trace header key from CHAN to AOFFSET and restart the flow. I then click Picking > Pick Top Mute and select the mute I just picked. This is another way to QC the top mute pick. I am pleased with it, so I can now move on.

By now, my Trace Statistics flow is complete. I open DBTools to examine the output. First, I will look at the average trace energy, TRCAMP. I select the TRC order and click View > 2D Matrix. I choose TRC for the horizontal axis and TRCAMP01 for vertical axis, color, and histogram. Using the histogram, I can see the distribution of my data and click and drag the mouse to select a desired range. The plot will change according to the histogram selection. This allows me to pick a range that contains most of the data except outliers, giving a smooth, squared appearance to the plot. I take note of the limits I choose. I do this also for the remaining four statistics I calculated.

Next, I create a flow called "04b-trace-editing". The flow begins as Disk Data Input, Database/Header Transfer, and Trace Display. However, I will add several Trace Kill/Reverses in a minute to see the effect of trace editing. I select the raw data with geometry applied and sort by CMP bin number and AOFFSET. I choose a single CMP for the moment at a location in which I know the fold is high (this can easily be done using DBTools) and all the offsets for that CMP. Therefore, my sort order list looks like "73804:*/". Next, I need to

transfer the trace statistics I calculated from the database to the trace headers. I set the number of parameters to five, and begin selecting the database statistics. For example, the first database parameter is "TRC TRCSTATS FRQ_DV01" and the first header entry is "FRQ_DV01". I do this for the remaining four statistics. I set the primary and secondary trace header labels in Trace Display to match my sort order of CMP bin number and AOFFSET. Then I execute the flow. This will simply transfer the statistics and display the CMP gather without any edits applied.

I minimize the trace display so I can compare subsequent edited displays with the unedited gather. After the Database/Header Transfer, I insert a Trace Kill/Reverse. I set it to Kill and select SPIKINESS as the primary edit list header word. From the DBTools 2D Matrix plot, I decide to kill traces that have a range above 100 for SPIKINESS, so I set the edit list as 101-9999. I then execute the flow. The changes are not drastic but that is OK. I do not want to over-edit the traces. I simply want to eliminate the spikiest traces. I can use DBTools to view the effect of eliminating traces with spikiness over 100. If I want to be more heavy handed, I could set the Trace Kill/Reverse to kill traces with spikiness over 50-60.

Although I have calculated five trace statistics, I will only use two to three for performing trace edits. Now that I have a handle on what I want to use for editing spikiness, I add a second Trace Kill/Reverse and this time I set it to kill based on TRCAMP, the average trace energy. Using DBTools, I decide to kill traces from 0-0.09 and 1.69-99999. This statistic has more of a Gaussian

distribution and I am cutting off the fringes. Again, I view the result in using the trace display and the result is not drastic, but there are places where careful inspection shows improvement. If I wanted a more drastic result, I would choose to kill from 0-0.6 and 1.6-99999.

The final trace statistic I decide to use for editing is FRQ_DV, the statistical deviation of the frequency. This statistic is very Gaussian in distribution and again I kill the fringes. I set the edit list as "0-1.4, 10.6-99999/", killing the fringes where there is little data. This kills several traces overwhelming dominated by groundroll. I finish the flow by turning off the trace display and adding a Disk Data Output at the end. I give the output dataset a filename of "geom-apply-trc-ed" and set the trace sample format to 32 bit. I change the sort list in Disk Data Input to include all the CMPs and then I execute the flow.

Before I proceed any further, I want to QC the refraction statics previously applied to the raw data. I use a Trace Display flow, sorting by SIN and CHAN, using SIN 5071060. In the display, I use the DX/DT tool to measure the approximate velocity of the first breaks, which is around 11,200 ft/sec for this shot. I close the display and build a flow called "05-qc-previous-refr-statics". The flow contains Add Flow Comment (sources), Disk Data Input, Automatic Gain Control (AGC), Linear Moveout Correction, CMP/Ensemble Stack, Trace Display, Add Flow Comment (receivers), Disk Data Input, Automatic Gain Control, Linear Moveout Correction (LMO), CMP/Ensemble Stack, and Trace Display. The idea behind this flow is create an ensemble

138

stack along a source line and along a receiver line, applying a linear moveout correction using the first break velocity, and if the first breaks are flat and smooth, the refraction statics are properly applied. Stacking along the source line gives us the refractors. This method was suggested to me after discussing various methods to check previously applied refraction statics with my colleague Oswaldo Davogustto.

The first half of the flow is for the source line ensemble stack. I read in the dataset with geometry applied after the trace edits, setting the primary sort key to SOURCE and the secondary sort key to S_LINE. I get all the shots (*) for S_LINE 504. Next, I apply AGC, keeping the default parameters. I then apply an LMO correction using the velocity I estimated from the first breaks in the trace display window. It is a forward correction. I set the primary header key to SOURCE and the secondary header key to AOFFSET. The format for the velocity parameter list is SOURCE:OFFSET:VELOCITY. Therefore, my parameter list is "5071060:0:11200/", meaning I choose SOURCE 5071060 at 0 ft AOFFSET (or the nearest offset to 0 ft) and a first break velocity of 11,200 ft/sec. Next, I use CMP/Ensemble stack, setting the sort order to SHOT and indicating that NMO is not applied. Then I use trace display to view the ensemble stack along the source line.

The second half of the flow is identical to the first half, except changing source-specific parameters to receiver-specific parameters, e.g., SOURCE header key becomes Receiver Index Number, and CMP/Ensemble Stack is in Receiver sort order. I do not, however; change the parameters for LMO. Both

139

stack are flat and smooth so I can conclude that the previously applied refraction statics are sufficient.

Next, I build a flow called "06-prelim-decon". I use this flow to create a deconvolved dataset before phase matching patch 1 and patch 2. The flow consists of Disk Data Input, Trace Muting, Spiking/Predictive Decon, Air Blast Attenuation, AGC, Bandpass Filter, and Disk Data Output. I read in the geometry-applied trace-edited dataset with the trace read option set to get all traces as it is already in CMP order. Next, I use Trace Muting to apply the top mute I picked several steps back. I set Spiking/Predictive Decon to Zero phase spiking deconvolution with a 120 ms operator length and 0.1% additive white noise. I select the deconvolution gate I picked earlier. For Air Blast Attenuation, I set the velocity to be attenuated as 1100 ft/sec starting at 0.0 ms at zero offset. When testing this parameter it is handy to first set it to mute, switching to attenuation after determining the correct parameters. Here I have set it to attenuation. I keep the default parameters for AGC. I set Bandpass Filter as an Ormsby bandpass zero phase frequency filter with corners of 10-20-90-120 Hz. I then write out the dataset as "prelim-decon" with a 32 bit trace sample format.

Once is complete, I view the output deconvolved dataset using a flow called "view-CMP". This flow consists of Disk Data Input and Trace Display. Disk Data Input is set to read "prelim-decon". The primary sort key is CMP bin number and the secondary sort key is AOFFSET. I pick a single CMP in the center of a high-fold zone for the sort list, which in this case is "71208:*/". The

default display window size is too large for viewing CMP gathers, so I shrink the window horizontally until I am pleased with the view. I can see events fairly well down to almost 800 ms. The deconvolution has also done a good job of handling groundroll. Later, I will use surface-consistent spiking deconvolution on the geometry-applied trace-edited dataset after I have phase matched patch 1 and patch 2.

I also want to have an idea of what the deconvolution has done to the spectral content of my data, so I exit the viewer and return to my "view-spectra" flow. I turn off the bandpass filter, switching Disk Data Input to read "prelim-decon". I keep the sort order at SOU_SLOC and AOFFSET so I can get a better view of the data. I see that frequencies still lie mostly between 15-110 Hz. However, thanks to the deconvolution operation, the spectra are considerably flatter. There is still a noticeable notch at 40 Hz, but it is not as drastic as I observed with the raw data.

A handy flow to go ahead and build is "header-value-range-scan", which scans all the trace headers for an input dataset and displays the minimum and maximum values for each trace header encountered in the job run log. The flow consists of Disk Data Input and Header Value Range Scan. I choose "prelim-decon" and leave the trace read option as get all traces. I select to process only the trace headers. Header Value Range Scan is parameterless. I open the job run log and select the option to monitor. I will keep this log open as I will need to reference it momentarily.

Now that I have a deconvolved dataset, I am ready to begin velocity analysis and calculating residual statics. I build a flow called "07-brute-stack". The flow consists of 3D Supergather Formation, AGC, Bandpass Filter, Velocity Analysis Precompute, Disk Data Output, Disk Data Input, Velocity Analysis, Volume Viewer, Add Flow Comment (separator between velocity analysis and residual statics calculation), Disk Data Input, NMO Correction, Bandpass Filter, Disk Data Output, 2D/3D Max. Power Autostatics, Disk Data Input, Apply Residual Statics, Stack 3D, Time-Variant Scaling, and Disk Data Output. I begin with 3D Supergather Formation through the first Disk Data Output. I turn off everything else in the flow by highlight each process and right clicking.

For the brute stack, I wish to use a single point for velocity analysis. Using DBTools, I create a 2D matrix plot of CMP fold to get an idea of where to pick a point. Typically, a point in the center is ideal, however; because the center of my survey is the edge of two patches, fold is very low in the center. I then choose a point slightly off center in patch 1 at inline 186 and crossline 148. I close DBTools and return to the brute stack flow and begin parameterizing 3D Supergather Formation. I select to use "prelim-decon" and presort in memory. My maximum CMP fold is 186, and location selection is by grid. I set the minimum and maximum center inline number to 186 and keep the inline increment at 10, which will have no effect in this 1 point analysis. I combine 3 inlines. Then, I set the minimum and maximum crossline number to 148, with the increment kept at 15. I combine 3 crosslines. I keep the default AGC parameters. I use the same parameters for Bandpass filter as in previous flows

– Ormsby bandpass zero phase frequency filter with corners of 10-20-90-120 Hz.

Next, I parameterize Velocity Analysis Precompute. As I am combining 3 inlines and 3 crosslines for supergathers, I set the number of CMPs to sum into a gather as 9. The next parameter I set is the absolute offset of the first bin center. I refer to the job run log from Header Value Range Scan and see the value for this is 55.0. I enter 220.0 as the bin size for vertically summing offsets, which is the receiver group spacing. The maximum offset is read in from the database, and I choose to use this value. I set the minimum semblance analysis velocity to 5000.0 ft/sec and the maximum to 25000 ft/sec. I then change the number of semblance calculations to 101. I set the number of stack velocity functions to 19 to give me more velocity functions to test, and the number of CMPs per stack strip to 9 to equal the number of CMPs summed into a supergather. I change the method of computing velocity functions to percentage and set the percent maximum at 30.0. As this is the first round of velocity analysis, I do not have a previous table I can use as a guide function, so I set the option to "No" and enter 5000.0 and 25000.0 ft/sec for the minimum and maximum guide values. I keep the NMO stretch mute at 30.0% and do not choose to apply a long offset correction. As I already applied my top mute to my deconvolved data, I keep the option as "NONE". Finally, I output the precomputed data using Disk Data Output, saving it as "brute-velo-pc" using a 32 bit trace sample format. I click execute and let the first part of the flow run.

Once the precomputed dataset is written, I turn off the first part of flow and turn on the first Disk Data Input and Velocity Analysis. I select "brute-velo-pc" as the input dataset, change the trace read option to sort and select Supergather Bin Number (SG_CMP) as the primary trace header key. In Velocity Analysis, I click the button next to the velocity table selection. I then create a new table to store my picks and call it "velo-brute". Instead of getting the guide function from an existing table, I use the same parameters I used in the precompute stage. I also turn off the stretch mute for NMO by setting it to 0.0 as I like to first pick velocities without any stretch muting. The target zone is shallow at about 580 ms, so turning off the stretch mute gives me a better indication of whether I am under or over correcting for hyperbolic movement. After I have picked the velocities, I go back and set the stretch mute at 30% and check the corrected gathers in the interactive velocity analysis display. Once I have set these parameters, I click execute. This brings up the velocity analysis window. The display can be adjusted either within the window or by setting the option to set visible items to "Yes" in the parameters. I like to turn off the semblance contours and the guide function and turn on NMO animation, the dynamic stack, the interval velocity function, and the velocity color background. I have set the brute stack velocity analysis to use a single location. Once I have finished picking the velocities for this supergather, I click File > Save Picks.

Leaving the velocity analysis window open, I return to the parameters and turn off Disk Data Input and Velocity Analysis and turn on Volume Viewer/Editor. I set the input volume as "velo-brute", the table in which my

current pick is saved. I leave all the other parameters as they are and click execute. After a moment the Volume Viewer Cross-Section and Map windows appear. I see a nicely stratified velocity field in the cross section. If I click the bottom button in each window, the analysis location is displayed in the map and cross-section views. I will use the Volume Viewer/Editor more extensively later in my processing flows. However, for now I simply close the viewer and the velocity analysis window.

With velocity analysis for the brute stack completed, I turn off Volume Viewer/Editor and turn on Disk Data Input to the Disk Data Output before 2D/3D Max. Power Autostatics. For the Disk Data Input I select "pelim-decon". I then set up NMO Correction to use "velo-brute" as the velocity parameter file, leaving the 30.0% stretch mute on. I set Bandpass Filter as an Ormsby bandpass zero phase frequency filter with corners of 10-20-90-120 Hz. I then set Disk Data Output to create a new dataset called "brute-nmo" with a 32 bit trace sample format. I turn off the processes I just ran and turn the remaining processes in the flow on.

I need to pick an Autostatics horizon before I can continue parameterizing 2D/3D Max. Power Autostatics. I build a new flow called "pick-ahz" which contains Disk Data Input, Stack 3D, Inline Sort, and Trace Display. I select "brute-nmo" as the input volume to Disk Data Input and set the trace read option to sort. I set the primary header key as ILINE_NO and the secondary header key to XLINE_NO. I need the first and last inlines and all crosslines to define a horizon that spans the volume. Therefore, my sort order list is

"1,402:*/". I do not change any parameters for Stack 3D. I set the primary sort key for Inline Sort to ILINE_NO and the secondary sort key to XLINE_NO. I also change the maximum number of traces from 186, the CMP maximum fold, to 198, the number of crosslines within an inline. I then set the trace labels in Trace Display as ILINE_NO for the primary label and XLINE_NO for the secondary label. Even though I am only inputting data from the first and last inlines, Stack 3D will also create all the inlines in between so I set the ensemble increment to 401 so I can skip immediately to the last inline. I then execute the flow.

Once the trace display appears, I see the first inline and 198 crosslines. The stack section does not look like much right now, but that is fine. This is, after all, a brute stack, and the analysis location was far away from the first inline. I click Picking > Pick Autostatics Horizons. A menu pops up asking me to name the horizon. I name it and click OK. Another window appears with two options. The first is smash and the second is gate width. I set the smash to 9 to match the number of CMPs I combine in supergather formation and set the width to 1000. Now I am able to pick the horizon. I make the first pick at ILINE_NO 1 and XLINE_NO 1 at 1000 ms. My next pick is at ILINE_NO 1 and XLINE_NO 198 at 1000 ms. I then click to go to the next ensemble which is the final inline. I make a third pick at ILINE_NO 402 and XLINE_NO 1 at 1000 ms and a fourth pick at ILINE_NO 402 and XLINE_NO 198. I then right click with the mouse and click Project. I then click File > Save Picks and exit the trace display. I now continue to parameterizing 2D/3D Max. Power Autostatics.

The next step is to parameterize 2D/3D Max. Power Autostatics. I select "brute-nmo" as the input trace data file. I select my newly created Autostatics horizon file. I change the number of iterations to 6 and the minimum number of live samples in a gate to 30.0%. I set the maximum statics allows to 12.0, 16.0, 20.0, 24.0, 28.0, and 32.0. Because I have selected to have 6 iterations, I have to have 6 different values here, as well. I then set the correlation reject percent to 30.0%. I set the final minimum static to -32.0 and the final maximum static to 32.0 to match the final value in my list above. For the first run I keep the Run ID at 0000. Next, I use Disk Data Input to read "brute-nmo". I add Apply Residual Statics, keeping the default parameters. As I run more iterations of Max. Power Autostatics, I will change the Run ID, and I will have to change the naming mode to reflect this. Next I use Stack 3D, keeping the default parameters. Next, I use Time-Variant Scaling using the gates I picked earlier. Finally, I output the stacked data as "stack-brute" with a 32 bit trace sample format. Running 2D/3D Max. Power Autostatics takes time, so now I wait.

Once the flow is finished, I can view the residual statics using DBTools. First, I will view the residual statics applied to the sources. I create a 2D Matrix plot using the SIN database. I choose X coordinate for the horizontal axis and Y coordinate for the vertical axis. I then select SPWR0000 for both color and histogram and click OK. I see that after the first run of residual statics, the majority of the corrections to the sources are within +/- 2.0 ms. Ideally, I want the solution to converge to 0.0 ms, but if I can within less than +/- 1.0 ms I will be satisfied. I do the same for the receiver statics using the SRF database, this

time selecting RPWR0000 for color and histogram. Again, my residual static corrections for the receivers are mostly between +/- 2.0 ms.

Next, I wish to view the NMO corrected CMP gathers. I open my "view-CMP" flow and select "brute-nmo" as the input volume. I then execute and the trace display window appears. I can see some strong, flat events between 300 and 800 ms, with groundroll and noise overpowering whatever signal may be present below 1000 ms. I also want to view the stack, so I create a new flow called "view-stack" consisting of Disk Data Input and Trace Display. I read in "stack-brute", setting the trace read option to sort. I set the primary key to ILINE_NO and the secondary key to XLINE_NO. My sort list is "20-380(10):*/", meaning I want inlines 20 through 380 incremented by 10 and all crosslines. The stack appears in the trace display window and I can move through. Already I am able to see events resolving, and as I move closer to areas of better fold, the stack section improves.

Now that I have made a brute stack, I will continue velocity analysis with an 80x80 grid, followed by a 40x40, 20x20, and finally a 10x10 grid. Each flow will be close to identical to the flows I used creating the brute stack. However, I will split the velocity analysis and residual statics calculation into two separate flows for convenience. The major changes are to the inline and crossline increments in 3D Supergather Formation, and changing the tables for storing velocity picks, and the addition of Apply Residual Statics from previous runs. I will detail this for the 80x80 velocity analysis and residual statics flows.

I make a new flow called "08-velo-80x80". The flow consists of 3D Supergather Formation, Apply Residual Statics, Air Blast Attenuation, Automatic Gain Control, Bandpass Filter, Velocity Analysis Precompute, Disk Data Output, Disk Data Input, Velocity Analysis, and Volume Viewer/Editor. I begin with with the last three turned off and everything else turned on. I select "prelim-decon" as the input dataset for 3D Supergather Formation. I set the minimum center inline to 40 and the maximum center inline to 400, with an increment of 80. I then set the minimum center crossline to 40 and the maximum center crossline to 198 with an increment of 80. This 80x80 inline-crossline increment is why I call this "velo-80x80". I still combine 3 inlines and 3 crosslines for a supergather smash of 9 CMPs. I keep the defaults for Apply Residual Statics so it grabs the first Run ID of 0000. I use Air Blast Attenuation with the same parameters I have used in previous flows. I use AGC with the default parameters, as they give desirable results. I set Bandpass Filter with the same parameters I have been using. The parameters for Velocity Analysis Precompute are identical to the parameters in the "07-brute-stack" flow, with the exception that I choose to get the guide function from an existing parameter table and select "velo-brute". I then create a new output dataset in Disk Data Output called "velo-80x80-pc" with a 32 bit trace sample format. I then run the flow.

Once the precompute step is complete, I turn off everything in the flow and then turn on Disk Data Input and Velocity Analysis. I set Disk Data Input to read in "velo-80x80-pc" with the trace read option set to sort and a primary

header key of SG_CMP. The parameters for Velocity Analysis are identical to those found in the "07-brute-stack" flow, except I have changed the table to store picks to a newly created "velo-80x80" and I use "velo-brute" as the guide function.

I execute the flow and the velocity analysis window appears. I begin picking points for the first analysis location. Once I have picked points for the first location, I save the picks, keeping the velocity analysis window open. I then return to the flow editor and turn off Disk Data Input and Velocity Analysis and turn on Volume Viewer/Editor. I pick "velo-80x80" for the input volume. I then select "Yes" to display poststack seismic data, picking "stack-brute". Then I run the flow. The Volume Viewer Cross-Section and Map windows appear. Clicking the bottom button displays the analysis locations in the Volume Viewer. I continue picking velocities in the analysis window and using the volume viewer to QC the velocity field. I want the velocity field to look smooth and layered, without any strange closures. Once I am done picking velocities, I click File > Save Picks and exit the flow. Each time I advance to the next CMP, the picks save auotmatically, but it never hurts to save the picks manually.

Next, I create a flow called "08b-residual-statics-80x80". The flow here is identical to the residual statics portion of "07-brute-stack", except I have added an Apply Residual Statics after the initial Disk Data Input. The full flow is as follows: Disk Data Input, Apply Residual Statics, Air Blast Attenuation, AGC, Bandpass Filter, NMO Correction, Disk Data Output, 2D/3D Max. Power Autostatics, Disk Data Input, Apply Residual Statics, Stack 3D, Time-Variant

Scaling, and Disk Data Output. I keep everything through 2D/3D Max. Power Autostatics on and turn off everything else.

I set Disk Data Input to read "prelim-decon". I keep the default settings for Apply Residual Statics. I use the same parameters I have been using for Air Blast Attenuation, AGC, and Bandpass Filter. I set NMO Correction to use "velo-80x80" for the velocity parameter file. I then write out the NMO corrected gathers using Disk Data Output as "nmo-80x80". I then select "nmo-80x80" as the trace data file for 2D/3D Max. Power Autostatics. I select my same Autostatics horizon file as before. I keep all the other parameters the same as in the "07-brute-stack" flow, except I change Run ID to 0001. If Run ID is not changed, it will overwrite the previous residual statics calculation, which I wish to keep. I then run the flow, which takes some time.

Once 2D/3D Max. Power Autostatics is completed, I decide to use DBTools to view the source and receiver residual statics. This time I will select SPWR0001 in the SIN database and RPWR0001 in the SRF database. My source residuals are now mostly between +/- 1.0 ms, which is below the seismic sample interval of 2.0 ms. The receiver residuals are also mostly between +/- 1.0 ms.

Using my "view-CMP" flow, I also want to look at the NMO corrected gathers after the 80x80 velocity analysis. I read in "nmo-80x80" using Disk Data Input. I can see more flattened events between 200 and 900 ms, almost down to 1000 ms. Groundroll and noise are still present below 1000 ms, but less prevalent.

Once the flow has completed, I turn off everything that is on, and turn on the Disk Data Input after Autostatics to the final Disk Data Output. I select "nmo-80x80" as the input dataset to Disk Data Input. I then change the database entry naming mode for Apply Residual Statics to "No". I click on the button next to source residual statics and select "SIN STATICS SPWR0001", and for the receiver residual statics, I select "SRF STATICS RPWP0001". I then use Stack 3D with the default settings, followed by Time-Variant Scaling using my time gates I picked. I then output the stack using Disk Data Output, naming the dataset "stack-80x80" and use a 32 bit trace sample format. Then I run the flow.

Once the flow has completed, I use my "view-stack" flow to examine the stack after 80x80 velocity analysis. I read in "stack-80x80" sorting by ILINE_NO and XLINE_NO. I continue to use my "20-380(10):*/" sort order list to get inlines 20-380 incremented by 10 and every crossline. The stack looks much better now. I see more events that are continuous and in areas of higher fold I am beginning to really resolve some finer details. I am also beginning to resolve some structure in the basement sub-1000 ms, which is quite exciting.

Now that I have completed two rounds of velocity analysis, I decide to phase match patch 1 to patch 2. I build a new flow called "09-phase-matching". There are three sections to this flow and I begin each one with an Add Flow Comment to delineate one from the next. The first section of the flow is as follows: Add Flow Comment, Disk Data Input, Apply Residual Statics, Apply Residual Statics, Air Blast Attenuation, AGC, Bandpass Filter, NMO Correction,

Stack 3D, Time Variant Scaling, and Disk Data Output. I begin by reading in "prelim-decon" in Disk Data Input. The sort order uses three header keys. The primary header key is CMP bin number, the secondary header key is AOFFSET, and the tertiary header key is SURVEY. The sort list is "*:*:1/", indicating that I am getting all CMPs and AOFFSETs for patch number 1. I then use two Apply Residual Statics to apply both the statics after the brute velocity analysis (Run ID 0000) and the 80x80 (Run ID 0001) velocity analysis. Air Blast Attenuation, AGC, and Bandpass Filter all use the same parameters as in previous flows. NMO Correction uses "velo-80x80". Stack 3D uses the default parameters, and I use my time gate file for Time Variant Scaling. I write out the data as "stack-surv-1" with a 32 bit trace sample format. The second section of the flow is identical to the first section, with the exception that the sort list in Disk Data Input is "*:*:2/" to get all CMPs and AOFFSETs for patch 2 and the output is "stack-surv-2".

The final section of this flow consists of Disk Data Input, Disk Data Input, Derive Match Filter. The First Disk Data Input reads in "stack-surv-2" while the second Disk Data Input reads in "stack-surv-1". Derive Match Filter is set to use an L2 Norm filter. The match filter length is set to 400 ms, and the analysis window starts at 200 ms and ends at 700 ms. The entire flow can be ran at once. I choose to read in "stack-surv-2" first because patch 2 has a more even fold distribution than patch 1. While the flow runs, I monitor the job run log. Once the process is over, the match filter prints to the log a time shift, a phase shift, amplitude gain, and the correlation coefficient. To phase match patch 1 to

patch 2, it must be rotated -50.47 degrees with no time shift. The correlation coefficient is 48.2%.

Next, I want to examine "stack-surv-1" and "stack-surv-2". I open my "view-stack" flow and read in "stack-surv-1" first. I can see that the patch has been properly defined and that only traces from patch 1 are present in this part of the survey. I have the same observation for "stack-surv-2". Next, I want to compare the full stack before and after I apply the phase rotation to patch 1. I build a new flow called "09b-phase-stack". The flow consists of Disk Data Input, Apply Residual Statics, Apply Residual Statics, IF, Phase Rotation, ENDIF, Air Blast Attenuation, AGC, Bandpass Filter, NMO Correction, Stack 3D, Time Variant Scaling, and Disk Data Output. I read in "prelim-decon", getting all traces. I then apply both passes of residual statics. I set the IF statement to include traces from primary header key SURVEY and specify 1 in the trace list. In Phase Rotation, I set the rotation angle to -50.47 and then use ENDIF to denote the end of the conditional statement. Air Blast Attenuation, AGC, and Bandpass Filter use the same parameters from previous flows. NMO Correction uses "velo-80x80" and Stack 3D uses the default parameters. Time Variant Scaling uses my picked time gates, and I write out the data as "stack-80x80-phase-rot".

Now that I have created a stack with the phase rotation applied to patch 1, I want to compare the stack before and after the phase rotation. I create a flow called "compare-inlines". The flow contains Disk Data Input, Disk Data Insert, Inline Sort, and Trace Display. I read in "stack-80x80" using Disk Data

154

Input, sorting by ILINE_NO and XLINE_NO and I set the sort list to get only one inline, "360:*/". I read in "stack-80x80-phase-rot" using Disk Data Insert, setting it to insert after the previous traces. I set the sort and sort list to be the same as in Disk Data Input. I then use Inline Sort, setting the primary header key to ILINE_NO, the secondary header key to SEQ_NO, and the tertiary header key to XLINE_NO. This allows me to separate the traces from the two datasets. I then use Trace Display, setting the labels to ILINE_NO and XLINE_NO. I then execute the flow.

Once the display window appears, I first see the inline from the stack prior to any phase rotation. I then click the next button to go to the inline from the stack after phase rotating patch 1. I can use the animate tool, which is the fifth button down on the left. This brings up a dialog window to control animation between the two stack images. I set it to manual and use the button that has two arrows pointing away from each other and a dot in the center. This allows me to toggle between the two images. I see that after phase matching patch 1 to patch 2, the reflectors are much better aligned and the "tear" or seam between the two patches is much less prevalent. I then exit the display.

Now, I am almost ready to use surface consistent deconvolution on my geometry-applied trace-edited data. However, I first want to test a few more noise attenuation processes. I build a new flow called "10a-noise-attenuation". The flow is as follows: Disk Data Input, Apply Residual Statics, Apply Residual Statics, Trace Muting, Air Blast Attenuation, Time Variant Spectral Whitening, Time Variant Scaling, and Trace Display. I read in "prelim-decon" and set the

155

sort order to CMP bin number and AOFFSET. I set the sort order list to get a subset of the CMPs and a all of their AOFFSETs (71180-71220:*/). As before, I apply both passes of residual statics. I already know the effect of using my top mute in Trace Muting and the effect of Air Blast Attenuation. I then set up Time Variant Spectral Whitening (TVSW) to balance between frequencies 10,18,110, and 120. I use my picked time gates for Time Variant Scaling (TV Scaling). When the display window appears, I can see that the combination of TVSW and TV Scaling has significantly improved the signal-to-noise ratio (SNR) of my data. I am now able to see events all the way down to almost 1200 ms at CMP 71208.

Now that I have tested some noise attenuation parameters, I am ready to create a flow called "10b-scdecon". The flow consists of Disk Data Input, IF, Phase Rotation, ENDIF, Trace Muting, Surface Consistent Deconvolution, Air Blast Attenuation, Time Variant Spectral Whitening, Time Variant Scaling, Bandpass Filter, and Disk Data Output. I elect not to apply residual statics in the flow and instead will apply them individually in the proceeding flows. I read in "geom-apply-trc-ed" with the read option set to get all traces. I set up IF > Phase Rotation > ENDIF exactly the same as in "09b-phase-stack". The noise attenuation parameters are set up exactly the same as in "10a-noise-attenuation", and the Bandpass Filter at the end uses the same parameters from previous flows. Disk Data Output creates a dataset called "scdecon-5-gs-iters".

Surface Consistent Deconvolution reads in the starting and ending CMPs from the database. As my dataset is 17 GB in disk space, I decide to set the process to use the disk version as opposed to the memory version. I select my "decon" time gate I picked earlier. I set the type of deconvolution as spiking. I use the default settings for the components of spectral decomposition (SHOT, RCVR, OFFSET, CMP) and for the spectral decompositions used in the application of the deconvolution (SHOT, RCVR). I decide to limit the offsets used to calculate the deconvolution operator as the documentation suggests this may lead to a better operator. I set the minimum offset to 500 ft and the maximum offset to 3500 ft. I use a 120 ms operator length with 0.1% additive white noise. I then change the number of Gauss-Siedel iterations from the default 3 to 5. The documentation notes that Cary and Lorentz (1991) recommend using 5 Gauss-Siedel iterations during the spectral decomposition phase. Once I am done parameterizing the flow, I execute and let it run. This flow takes a while to run.

Once the flow is finished, I open my "view-CMP" flow and read in "scdecon-5gs-iters". The combination of noise attenuation and surface consistent deconvolution (SC decon) has dramatically improved the SNR of the data. I can now see hints of events even below 1200 ms, especially at near and far offsets. I exit the viewer and open the flow "view-spectra" to examine how the noise attenuation processes and SC decon have affected the data's spectra. Between frequencies of about 15 to 110 Hz, the spectrum is now very flat, and the notch that was very noticeable at 40 Hz is much less apparent.

The spectral content of the data appears to be nicely whitened and flat throughout 15-110 Hz.

Now that I have phase matched the two patches, applied surface-consistent deconvolution and noise attenuated the data, I continue with velocity analysis on a 40x40 inline-crossline increment grid. The flow for "velo-40x40" is identical to the flow for "velo-80x80", with a few exceptions. I have added a second Apply Residual Statics after the first one to apply SPWR0001 and RPWR0001 after the 80x80 calculation. I change 3D Supergather Formation from an 80x80 grid to a 40x40 grid, leaving the minimum and maximum center inline and crossline the same. I change the velocity guide function from "velo-brute" to "velo-80x80" in Velocity Analysis Precompute, and name the output "velo-40x40-pc". I run 3D Supergather Formation through Disk Data Output. Once this is finished, I turn them off and turn on Disk Data Input and Velocity Analysis. I create a new table to store velocity picks called "velo-40x40" and change the guide function to "velo-80x80". For my first pass, I decide to turn off the NMO stretch mute by setting the maximum stretch percentage to 0.0, indicating to ProMAX that I do not want any stretch muting. I run the flow and the interactive velocity analysis window appears.

I begin picking velocities, first using the semblance panel as a guide and then fine tuning my picks using the constant velocity function stacks. Once I have picked a few CMPs and saved the picks to "velo-40x40", I return to the flow editor, leaving velocity analysis open. I turn off Disk Data Input and Velocity Analysis and turn on Volume Viewer/Editor. I switch the input volume

158

to "velo-40x40" and choose to display "stack-80x80" as the postack data. I run the flow, and the Volume Viewer Cross-Section and Map windows appear. I can click the lower button on the left hand side and I will see where the analysis points reside. I continue picking velocities in the interactive picking window, using the button that looks like a bow and arrow to send my picks to the volume viewer. I use the viewer to QC my picks, looking for places where my picks may be creating a non-realistic velocity field. Once I am finished, I save my picks one final time and exit both the volume viewer and the velocity analysis window. I can now go back and set an NMO stretch mute at 30% to check how the gathers look with a stretch mute.

Now that the 40x40 velocity analysis is complete, it is time to calculate a new set of residual statics, so I create a flow called "11b-residual-statics-40x40". The flow is identical to my previous residual statics flow with a few exceptions. I am now inputting "scdecon-5g-iters" instead of "prelim-decon". I add a second Apply Residual Statics to apply SPWR0001 and RPWR0001. I switch NMO correction to use "velo-40x40" and I write out "nmo-40x40" with Disk Data Output. I switch 2D/3D Max. Power Autostatics to read in "nmo-40x40" and I change the Run ID to 0002. I then run the flow from the beginning through Autostatics. Before continuing, I use DBTools to examine SPWR0002 and RPWR0002, plotting both by X and Y coordinates just as before. The residual statics for the sources are mostly between +/- 1.0 ms, as are the residual statics for the receivers. I also open my "view-CMP" flow and read in

"nmo-40x40" to view with Trace Display. Again, I see flat events from about 200ms down to almost 1200ms with some hints of other events even lower.

Once this is complete, I turn off the first half of the flow and turn on the second half, beginning with the Disk Data Input after Autostatics. I input "nmo-40x40" and change Apply Residual Statics to apply SPWR0002 and RPWR0002. I make no changes to Stack 3D or Time-Variant Scaling from the flow "08b-residual-statics-80x80". I run the flow and wait for it to finish. Once it is done, I open my "view-stack" flow and read in "stack-40x40" and display using the sort list "20-380(10):*/" to get inlines 20-380 incremented by 10 with all crosslines. The stack is now beginning to look very nice. I am really beginning to resolve the events in the zone of interest between 500-700ms nicely and the basement structure is becoming apparent. I could still do better with my velocity picks in the shallow 100-250 ms range, but picking good velocities at shallow times can be very challenging. It looks like I may be picking a little fast, but it is hard to tell.

Although I am very pleased with the amount of noise reduction I have been apply to attain, I am still struggling with some groundroll and other types of noise. To clean up the gathers further, I am going to write out my "scdecon" with all residual statics and NMO correction applied without a stretch mute as a SEGY file. This SEGY file is then passed through a prestack structure-oriented filter that searches along dip using coherency to filter out problem areas. I build a flow called "11c-NMO-gathers-out" containing Disk Data Input, Apply Residual Statics, Apply Residual Statics, Apply Residual Statics, NMO Correction, Trace

Display, and SEGY Output. I first test with a single CMP and turn on Trace Display and turning off SEGY Output. I apply SPWR0000, RPWR0000, SPWR0001, RPWR0001, SPWR0002, and RPWR0002 using the three Apply Residual Statics. I set the stretch mute percentage to 0.0 in NMO correction and use "velo-40x40" as the velocity parameter file. I run the flow and the CMP I selected appears in the display window. Happy with the output, I return to the flow editor, change the read option to get all trace, turn off Trace Display, and turn on SEGY Output. I set SEGY Output to save to disk and use the file browser to navigate to where I want to output the SEGY file and name it "prs-nmo-no-mute.sgy". I then edit the EBCDIC header to contain information about the processing history and pertinent header locations such as the CMP x and y coordinates and the inline and crossline numbers. I then execute the flow.

Once the prestack structure-oriented filter is completed, I must reimport the data to ProMAX. I build a flow called "11d-import-of-sof-gathers+rnmo". The flow consists of SEGY Input, Inline Geom Header Load, Spike & Noise Burst Edit, Inline Sort, Trace Header Math, NMO Correction, Header Values, and Disk Data Output. I set SEGY Input to read in a file saved to disk and use the file browser to navigate to and select the file I want to read. I set the sort order to CMP and the maximum number of traces per ensemble to 186, the maximum CMP fold. I do not need to overwrite any trace headers. I set Inline Geom Header Load to match using valid trace numbers. I set Spike & Noise Burst Edit to edit automatically spikes, using a spike detection threshold of 10 times greater than surrounding samples with an operator length of 100 ms. I do

not edit automatically noise bursts. I set the primary sort key for Inline Sort to CMP bin number and the secondary key to AOFFSET. I set the maximum number of traces per ensemble to 186. I use Trace Header Math to create the header equation "NMO_APLD=1" to indicate that the incoming data has already been NMO corrected. If this flag is not set, the reverse NMO correction will fail. I set the direction for NMO correction to inverse and the stretch mute at 0.0. I select "velo-40x40" as the velocity parameter file. I want to check that the headers have been properly preserved, so I used Header Values and dump "CMP, CMP_X, CMP_Y, ILINE_NO, XLINE_NO", listing only the last trace in the ensemble. I use Disk Data Output to create "scdecon-pssof" and set the trace sample format as 32 bit. I then run the flow.

I now have two more passes of velocity analysis and residual statics before I write out my final gathers for prestack time migration. I build a flow called "12-velo-20x20" which will use a 20x20 inline-crossline increment grid. I set the increment in 3D Supergather Formation to 20 for both inline and crossline and change the minimum center inline and crossline from 40 to 20. I select "scdecon-pssof" as the input dataset for creating supergathers. I applied the residual statics already when I wrote the data out as a SEGY, so I will not apply them again. I then use AGC and Bandpass Filter, using the same parameters I have previously. I change the velocity guide function to "velo-40x40" in Velocity Analysis Precompute and set the maximum NMO stretch mute percentage to 0.0. I then execute the flow.

I turn off 3D Supergather Formation through Disk Data Output and turn on Disk Data Input and Velocity Analysis. I read in "velo-20x20-pc" using Disk Data Input. I create "velo-20x20" as the table to store velocity picks in Velocity Analysis. I change the guide function to "velo-40x40" and set the maximum NMO stretch mute percentage to 0.0. I then run the flow. The picking window appears and I begin picking velocities, saving as I go. After I have picked a few velocities, I minimize the window and return to the flow editor. I turn off Disk Data Input and Velocity Analysis and turn on Volume Viewer/Editor. I set "velo-20x20" as the input volume and "stack-40x40" as the displayed poststack seismic data. I then execute the flow and the Volume Viewer Cross-Section and Map windows appear. I then continue picking velocities as before, QC'ing picks with the viewer as I go. Once I am done, I save my picks and exit. I may choose to rerun Velocity Analysis with a 30% stretch mute to see how the gathers look with a stretch mute applied.

I now build a flow called "12b-residual-statics-20x20". The flow consists of Disk Data Input, AGC, Bandpass Filter, NMO Correction, Disk Data Output, 2D/3D Max. Power Autostatics, Disk Data Input, Apply Residual Statics, Stack 3D, Time-Variant Scaling, and Disk Data Output. I turn off the second Disk Data Input to the end of the flow. I read in "scdecon-pssof" using Disk Data Input, followed by AGC and Bandpass Filter. I set NMO Correction to use "velo-20x20" as the velocity parameter file. I then use Disk Data Output to create "nmo-20x20". I then select "nmo-20x20" for 2D/3D Max. Power Autostatics and I change the run ID to 0003. I then execute the flow. Once the

flow has finished, I check SPWR0003 and RPWR0003 using DBTools. I open my "view-CMP" flow and view the "nmo-20x20" gathers.

Next, I turn off the first half of the "12b-residual-statics-20x20" flow and turn on the second Disk Data Input to the end. I read "nmo-20x20" with Disk Data Input. I then select "SPWR0003 and RPWR0003" in Apply Residual Statics. I stack using Stack 3D and then use Time-Variant Scaling. Then I create "stack-20x20" using Disk Data Output. Once the flow has finished, I view the stack using my "view-stack" flow.

I build the final velocity analysis flow, which I call "velo-10x10". The flow is identical to "velo-20x20", except I insert an Apply Residual Statics after 3D Supergather Formation. I change the minimum center inline and crossline number to 10 and the inline and crossline increment to 10. I also change the maximum center inline to 390 and the maximum center crossline to 190. I apply SPWR0003 and RPWR0003 using Apply Residual Statics. I AGC and use Bandpass Filter. I select "velo-20x20" as the velocity guide function for Velocity Analysis Precompute. I set the maximum NMO stretch mute percentage to 0.0 to turn it off. I then create "velo-10x10-pc" with Disk Data Output and run the first part of the flow.

Once the first part has finished, I turn off 3D Supergather Formation through Disk Data Output and turn on Disk Data Input and Velocity Analysis. I read "velo-10x10-pc" using Disk Data Input. I then create "velo-10x10" to store my velocity picks in Velocity Analysis. I change the guide function to "velo-20x20" and set the stretch mute to 0.0. I then run the flow and the velocity

analysis window appears. I begin picking velocities, saving as I go. The 10x10 grid will take some time. I am picking inlines 10 to 390, incremented by 10, and crosslines 10 to 190, incremented by 10. This translates to picking 741 CMPs. Once I have picked a few CMPs, I return to the flow editor and turn off Disk Data Input and Velocity Analysis and turn on Volume Viewer/Editor. I select "velo-10x10" as the input volume and use "stack-20x20" as the poststack seismic data. I then run the flow and the Volume Viewer Cross-Section and Map window appear. I continue picking velocities and QC the picks using the volume viewer windows. Once I have finished picking, I save the picks and exit.

Next, I build the final residual statics flow called "13b-residual-statics-10x10". The flow is identical to "12b-residual-statics-20x20" except I insert an Apply Residual Statics after the first Disk Data Input. I read in "scdecon-pssof" and apply SPWR0003 and RPWR0003 using Apply Residual Statics. I use AGC and Bandpass Filter with the same parameters I have previously. I then select "velo-10x10" as the velocity parameter file for NMO Correction. I write out "nmo-10x10" using Disk Data Input. I then read in "nmo-10x10" for 2D/3D Max. Power Autostatics and change the Run ID to 0004. I then run the flow. Once it is finished, I use DBTools to examine SPWR0004 and RPWR0004. I then use my "view-CMP" flow to inspect the "nmo-10x10" gathers.

I then turn off the first half of the flow and turn on everything from the second Disk Data Input to the end. I select "nmo-10x10" for Disk Data Input. I apply SPWR0004 and RPWR0004 using Apply Residual Statics. Next, I use Stack 3D and Time Variant Scaling with the same parameters I have previously.

I then create "stack-10x10" with Disk Data Output and select 32 bit for the trace sample format. I then execute the flow. Once it is finished, I use my "view-stack" flow to display "stack-10x10".

I am now ready to write out the final CMP gathers for prestack time migration. I build a flow called "14-final-gathers-out" consisting of Disk Data Input, Apply Residual Statics, Apply Residual Statics, True Amplitude Recovery, TV Spectral Whitening, Time-Variant Scaling, Bandpass Filter, and SEGY Output. I select "scdecon-pssof" in Disk Data Input and set the trace read option to get all traces. I apply SPWR0003, RPWR0003, SPWR0004, and RPWR0004 using the two Apply Residual Statics. I set True Amplitude Recovery to apply a spherical divergence correction using a 1/distance basis and select "velo-10x10" as the input velocity parameter file. I do not apply any other corrections. I then reapply TV Spectral Whitening and specify 10, 18,110, and 120 Hz for spectral balancing. I then use Time-Variant Scaling, followed by a final Bandpass Filter, both using parameters I have selected in previous flows. I then set SEGY Output to save to disk and use the file browser to navigate to where I want to output the file, also giving the output file a name. I edit the EBCDIC to reflect pertinent information about the output SEGY file. For example, I include the processing history, the range of CMP numbers, inline and crossline numbers, the CMP bin size, the CMP X and Y coordinate origin, the azimuth, and byte locations for important trace headers. I then execute the flow.

The final step is to output my "velo-10x10" velocity file as a SEGY. However, I want to interpolate the grid to a 1x1 inline-crossline increment so I can use it for prestack time migration. I create a flow called "14b-final-velocity-out" and it consists of Volume Viewer/Editor, Trace-Vel Table Transfer, and SEGY Output. I turn off Trace-Vel Table Transfer and SEGY Output, leaving only Volume Viewer/Editor on. I select "velo-10x10" as the input volume and "stack-10x10" as the poststack seismic data. I then execute the flow.

Once the viewer windows appear, I first click File > Save Active Volume To and call the volume "velo-10x10-interp". Next, I click Edit > Grid/Smooth Volume. I set the increments for inlines and crosslines to both be one and set the time increment to 30 ms. I then set the minimum and maximum inline and crossline values and the minimum and maximum time. I then click "Apply", and after a few moments, the volume is now re-gridded at a 1x1 inline-crossline increment and 30 ms time increment. Next, I set the smoothing parameters for both inline and crossline to three to match my supergather smash. I click "Apply" and then I click "OK". Once this is finished, I click File > Save Active Volume and then I exit. I can then check the table "velo-10x10-interp", which now contains picks at every CMP and every 30 ms.

I turn off Volume Viewer/Editor and turn on Trace-Vel Table Transfer and SEGY Output. I set the transfer direction to transfer a velocity table to trace data, and then I select to read an RMS parameter file. I select "velo-10x10-interp". I set the start time to 0.0 ms, the sample interval to 2.0 ms to match my seismic data, and the maximum time to 2000.0 ms. I then set SEGY Output to

save a disk image and use the file browser to navigate to where I want to save the file, giving it a name as well. I then edit the EBCDIC header in a similar fashion as before, but this indicating that the file is an RMS stacking velocity field interpolated for every CMP. I then execute the flow, and now I am done with ProMAX until I want to do residual velocity analysis after prestack time migration.